Hydrolysis of particulate organic matter originated from municipal wastewater treated under aerobic and anaerobic conditions

Zur Erlangung des akademischen Grades einer

DOKTORIN DER INGENIEURWISSENSCHAFTEN (Dr.-Ing.)

von der KIT - Fakultät für Chemieingenieurwesen und Verfahrenstechnik des

Karlsruher Instituts für Technologie (KIT)

genehmigte

DISSERTATION

von

M.Sc. Alondra Paulette Alvarado Munguía

aus Tepic, Mexiko

Tag der mündlichen Prüfung: 12.11.2021

Erstgutachter: Prof. Dr. Harald Horn

Zweitgutachter: Prof. Dr. Tobias Morck

Contents

Abstract

The hydrolysis of particulate organic matter (POM) originated from municipal wastewater is considered a limiting factor in biological systems. The mechanics and limiting factors involved in the hydrolysis process are not well understood. Therefore, the goal of this work was to characterize the hydrolysis products formed during the hydrolysis of POM originated from municipal wastewater under aerobic and anaerobic conditions. The biodegradability of the hydrolysis products was determined based on the nominal molecular weight (MW) and UV response by using the size exclusion chromatography coupled with online carbon and UV (254 nm) detection (SEC-OCD-UV) method together with standard sum parameters.

The experimental set-up used in the aerobic experiments allowed a parallel observation of the formation and utilization of the hydrolyzed POM. The chromatographic results showed accumulation of the high molecular weight (HMW) organic products (nominal MW > 20.000 g/mol) within the first three days indicating that bacteria needed this time to grow and develop the necessary enzymes to degrade the HMW organic products, which were mostly depleted after 13 d. The volatile suspended solids (VSS) removal after 13 d was around 70 %.

The chromatographic results of the anaerobic hydrolysis experiments showed accumulation of the low MW organic products (nominal MW: 150 - 1550 g/mol) within the first 2 and 4 d at pH 7 ± 0.2 and pH 6 ± 0.2, respectively. It was determined that changes of pH (i.e., 7 and 6) did not affect the hydrolysis rate but the kind of volatile fatty acids (VFA) produced and their further utilization rate. The VSS removal after 24 d was around 60 %.

The bacteria growth dynamics and the extracellular polymeric substances (EPS) formation were visualized under aerobic and anaerobic conditions by using confocal laser scanning microscopy images. The findings of this work significantly extended the fundamental understanding of the aerobic and anaerobic hydrolysis of POM. The SEC-OCD-UV effectively characterized the hydrolysis products providing detailed insight into the hydrolysis process.

Kurzzusammenfassung

Die Hydrolyse von partikulären organischen Substanzen (POM) aus kommunalem Abwasser gilt als limitierender Faktor in biologischen Systemen. Die Mechanik und die limitierenden Faktoren des Hydrolyseprozesses sind nicht hinreichend bekannt. Ziel dieser Arbeit war es, die Produkte zu charakterisieren, die bei der Hydrolyse von POM aus kommunalem Abwasser unter aeroben und anaeroben Bedingungen entstehen. Die biologische Abbaubarkeit der Hydrolyseprodukte wurde, basierend auf dem nominalen Molekulargewicht (MW) und der UV-Absorption, unter Verwendung der Größenausschlusschromatographie, gekoppelt mit der kontinuierlichen Detektion von gelöstem organischen Kohlenstoff (DOC) und UV-Absorption- (254 nm) (SEC-OCD-UV), bestimmt.

Unter aeroben Bedingungen konnte die Bildung und der Abbau von hydrolysierter POM gleichzeitig beobachtet werden. Das Chromatogramm zeigte zudem eine Akkumulation von organischen Produkten mit hohem Molekulargewicht (HMW) (nominelles MW > 20.000 g/mol) innerhalb der ersten drei Tage. Dies deutet darauf hin, dass Bakterien diese Zeit zum Wachstum und zur Entwicklung der notwendigen Enzyme für den Abbau der organischen HMW-Produkte benötigen, die größtenteils nach 13 Tagen abgebaut waren. Der Abbau der organischen Trockensubstanz (VSS) betrug nach 13 Tagen etwa 70 %.

Unter anaeroben Bedingungen, hingegen, akkumulierten organische Produkte mit niedrigem Molekulargewicht (nominelles MW: 150 – 1550 g/mol) innerhalb von zwei Tagen bei pH 7 ± 0,2 und innerhalb von vier Tagen bei pH 6 ± 0,2. Es wurde festgestellt, dass pH-Änderungen (d. h. 6 und 7) nicht die Hydrolysegeschwindigkeit beeinflussten, sondern die Art der produzierten flüchtigen Fettsäuren (VFA) und deren Abbaugeschwindigkeit. Der VSS-Abbau betrug nach 24 Tagen etwa 60 %.

Die Wachstumsdynamik der Bakterien und die Bildung extrazellulärer polymerer Substanzen (EPS) wurde unter aeroben und anaeroben Bedingungen mit Hilfe der konfokalen Laserscanning-Mikroskopie visualisiert.

Die Ergebnisse dieser Arbeit haben das grundlegende Verständnis der aeroben und anaeroben Hydrolyse von POM stark verbessert. Mittels der verwendeten Chromatographie-Methode konnten Hydrolyseprodukte erfolgreich charakterisiertund detaillierte Einblicke in den Hydrolyseprozess gewonnen werden.

Figures

Tables

Acknowledgments

The Ph.D. has been a whole journey, where I gained not only a Ph.D. but new relationships and a new way of seeing life. I had the luck to work with people with bast knowledge in their areas and learned something from them.

I want to thank CONACYT - Consejo Nacional de Ciencia y Technología de México and DAAD - Deutscher Akademischer Austauschdienst for the provided scholarship during my Ph.D. work.

Professor Harald Horn, thank you for giving me the opportunity to do my Ph.D. work under your guidance, for giving me the freedom to conduct my analysis in the way that I thought better and for all the dedication you put in my work and my formation as a researcher. The idea of this project was yours and I am thankful that I was part of it. When I arrived to Germany, you gave me an overview on the Germans ways and that helped me to adapt in an easier way. You always push me to learn German, thing that I am still doing. I value your advice and I respect you as my supervisor.

Frau Abbt-Braun, I am so thankful to you, all those meetings where you explained me about chromatography or some other area of your expertise, your continuous efforts in trying to improve my writing (I hope that I´ve improved a bit). I appreciate your encouragement when my scholarship was over to continue giving my best. Thank you very much for reading and correcting my thesis work.

Professor Tobias Morck, thank you for accepting to be the second reviewer of this work and for giving me comments to improve the thesis. I thank as well to the members of the thesis examination committee.

Stephanie West, thanks to you I know how to write decent reports. Thank you for introducing me to the AMPTS II and for discussing the experiments with me. You were always concerned that I had all the material needed to work, so, thank you.

Mathias Weber, besides measuring my samples, which were the highlight of my work, we discussed many times the chromatographic results, the “issues” with the column, the DOC/dTN results. You also helped me with the Huber software and Origin. Your cooperation and your responsibility were exceptional. I even have the impression that we synchronized

our holidays to be sure that we could finish a whole experiment. I know that more than once you worked extra-time to finish some measurements, and for that I am deeply thankful to you.

Ulrich Reichert and Rafael Peschke, thank you so much for collecting my wastewater, I know that bringing tons of wastewater and going twice to the WWTP is not the funnest thing ever, but you did it for a long time, so, thank you very much!

Reihnard Sembritzki and Axel Heidt, thank you very much for measuring my samples!

Luisa Gierl, you introduced me to the CLSM, every time that I had a doubt, I knew I could count on you, so thank you very much!

Michael Wagner, thank you because you also gave me a second introduction to the CLSM and the Jimage software to count the pixels of the images.

Sylvia Heck and Frau Schäfer, every time I had an administrative question, I never doubt to run and ask you, thank you for all the years of support.

I want to thank specially to my family in Mexico, quiero agradecer especialmente a mi familia en México: Beatriz, Alejandra, Aline, Sergio y Gustavo, muchísimas gracias, pues aún en la distancia solo recibí de ustedes amor y apoyo incondicional.

Fabian Brunner, I have no words to express my gratitude to you, you supported me like no other, you were there with me all these years, at my highest moments celebrating with me and also at my lowest moments offering me encouragement to continue. Work related, I am thankful to you for introducing me to the aerobic experiments and for discussing the results of those experiments with me.

Finally, I would like to thank all my friends, colleagues, students, and previous professors who offered me support, advice, comments, and/or suggestions to improve the quality of this work. Thank you Jobin George, Jana Jenkins, Zacharias Heck, Damare Valenzuela, Rowayda Ali, Ewa Borowska, Nico Seeleib and the DOC Labor Dr. Huber, Marc Tuczinski, Jueying Qian, Elham Fatoorehchi, Florian Blauert, Philip Brown, Enrique Samaniego, Fernando Olvera, Sonia Flores, Jorge Calderón, Fernanda Pérez, Penélope Moctezuma, Jinpeng Liu, Mathias Kieslich, Alexander Timm, Florencia Saravia, Birgit Gordalla, Florian Ranzinger, Oscar Delgado, Michael Sturm, Dominic Breitkopf and Ali Sayegh.

Alondra Alvarado

List of Abbreviations

AA	Amino acids
AAL	Aleuria aurantia lectin
ADM1	Anaerobic digestion model 1
AMPTS II	Automated methane potential test system
ANS	Anaerobic sludge
ARB	Antibiotic resistant bacteria
ARG	Antibiotic resistance genes
AS	Activated sludge
ASM	Activated sludge model
ATU	Allylthiourea
BOD	Biochemical oxygen demand, mg/L O_2
CAS	Conventional activated sludge
cDOC	Chromatographable dissolved organic carbon, mg/L C
CHONS	Carbon, Hydrogen, Oxygen, Nitrogen, Sulfur
CLSM	Confocal laser scanning microscopy
COD	Chemical oxygen demand, mg/L O_2
D.F.	Dilution factor
DO	Dissolved oxygen, mg/L O_2
DOC	Dissolved organic carbon, mg/L C
DOM	Dissolved organic matter
dTN	Dissolved total nitrogen, mg/L N

EAWAG	Swiss Federal Institute for Aquatic Science and Technology
ECs	Emerging contaminants
EPS	Extracellular polymeric substances
FITC	Fluorescein isothiocyanate
F1	fraction 1, corresponding to the nominal molecular weight of calibration standard used in the range of 20,000 - $2 \cdot 10^6$ g/mol, mg/L
F2	fraction 2, corresponding to the nominal molecular weight of calibration standard used in the range of 1550 - 20,000 g/mol, mg/L
F3	fraction 3, corresponding to the nominal molecular weight of calibration standard used in the range of 100 - 1550 g/mol, mg/L
F4	fraction 4, corresponding to the nominal molecular weight of calibration standard used in the range < 100 g/mol, mg/L
$F1_{UV}$	UV-absorbing fraction F1
$F2_{UV}$	UV-absorbing fraction F2
$F3_{UV}$	UV-absorbing fraction F3
$F4_{UV}$	UV-absorbing fraction F4
HMW	High molecular weight
Hbu	Butyric acid
Hpr	Propionic acid
Hva	Valeric acid
IC	Ion chromatography
iTSS	Inorganic total suspended solids, g/L
IAWPRC	International Association on Water Pollution Research and Control

k_{CH4}	kinetic constant of methane formation, 1/d
k_{hyd_anaer}	Anaerobic hydrolysis constant of POM degradation, 1/d
$k_{hyd\_anaer\ II}$	Degradation kinetic constant of $sCOD_{F3}$, 1/d
K_{hyd_aer}	Aerobic hydrolysis constant of POM degradation, 1/d
LCFA	Long chain fatty acids
MF	Microfiltration
MLSS	Mixed liquor suspended solids
MS	Monosaccharides
MW	Molecular weight
NA	Nucleic acid
NH_4^+ - N	Ammonium nitrogen, mg/L
NO_3^- - N	nitrate nitrogen, mg/L
NO_2^- - N	nitrite nitrogen, mg/L
OUR	Oxygen utilization rate, mg/L · d O_2
PO_4^{3-} - P	Phosphate phosphorus, mg/L
POM	Particulate organic matter
p.s.	Particle size, µm
sCOD	Soluble chemical oxygen demand, mg/L
SEC	Size exclusion chromatography
SEC-OCD-UV	Size exclusion chromatography with online detection of dissolved organic carbon and UV-absorption
SMPs	Soluble microbial products

SRT	Sludge retention time, d
SUVA	Specific UV-absorbance, L/mg · m
SWW	Settled wastewater
T	Temperature, °C
TSS	Total suspended solids, g/L
UF	Ultrafiltration
UV	Ultra violet absorbance at wavelength of $\lambda = 254$ nm
UVD	Ultra violet absorbance detection at a wavelength of $\lambda = 254$ nm
υ	Stoichiometric factor
VFA	Volatile fatty acids, mg/L
VS	Volatile solids, g/L
VSS	Volatile suspended solids, g/L
WWTP	Wastewater treatment plant
X_c	Composite particle organic matter, g/L

Chapter 1: Introduction

1.1 The path of the particulate organic matter along the municipal wastewater treatment line

Wastewater is subject of interest due to its implications to social health and environmental protection. Therefore, the central objective in wastewater treatment has been the removal of contaminants from the water. The composition of municipal wastewater varies depending on region, climate, and habits of the population. Consequently, the exact composition of municipal wastewater is unknown. Nevertheless, the wastewater quality can be evaluated by using physical, chemical, and biological parameters, which might differ between countries, e.g., in the USA, the influent total suspended solids (TSS) in a wastewater treatment plant (WWTP) is in the range of 60 - 150 g/capita · d, while in Germany is 82 - 96 g/capita · d (Metcalf and Eddy, 2014).

Pollutants in municipal wastewater are present in suspended or dissolved form depending on their size (von Sperling, 2007). Suspended solids (particulate matter) are solids retained onto the surface of a filter paper (0.45 µm); from these, around 60 % are settleable solids (settling within one hour), whereas the solids passing through the filter paper are called dissolved solids (von Sperling and Lemos Chernicharo, 2005). Moreover, organic matter, based on its particle size, can be further divided into four additional fractions: 1) settleable: > 100 µm, 2) supra colloidal: 1 - 100 µm, 3) colloidal: 0.08 - 1 µm and soluble: < 0.08 µm (Sophonsiri and Morgenroth, 2004).

In addition to the size, wastewater constituents can also be classified based on their biodegradability (Henze et al., 1987; Kommedal, 2003). Solids can be recognized as organic when they volatilize after ignition at 550 °C (volatile solids: VS). Typically, the influent content of volatile suspended solids (VSS) compared to TSS in municipal raw wastewater is around 80 %. The remaining 20 % non-volatile influent suspended solids corresponds to the inorganic total suspended solids (iTSS), which can be calculated by the difference in influent wastewater concentrations of TSS and VSS (Metcalf and Eddy, 2014). Friedrich (2016) indicated that non-biodegradable organic matter is aggregated to the VSS in the mixed liquor suspended solids (MLSS). According to Ramdani et al. (2012), the percentage of influent non-biodegradable particulate organic matter adding to the MLSS is of 25 % or more of the VSS depending on the characteristics of the wastewater and the sludge retention time (SRT).

Henze et al. (1987) fractionated the chemical oxygen demand (COD) in municipal wastewater according to its biodegradability as shown in Fig. 1-1. On the one side, the biodegradable organic matter was divided into two fractions: easily biodegradable and slowly biodegradable organic matter, which is present in soluble and particulate form, respectively (Fig. 1-1). Although, slowly biodegradable matter might be found in soluble form. The easily (soluble) biodegradable matter consists of simple molecules that may be taken directly by heterotrophic bacteria to be used for biomass growth (Henze et al., 1987; Henze and Mladenovski, 1991). The slowly (particulate) biodegradable organic matter must be first converted to easily (soluble) biodegradable organic matter through a process called hydrolysis (see Chapter 1.2). On the other side, non-biodegradable organic matter (inert matter) remains unchanged during the biological treatment. The soluble non-biodegradable organic matter leaves the WWTP with the final effluent, while the particulate non-biodegradable organic matter is incorporated into the MLSS (von Sperling, 2007).

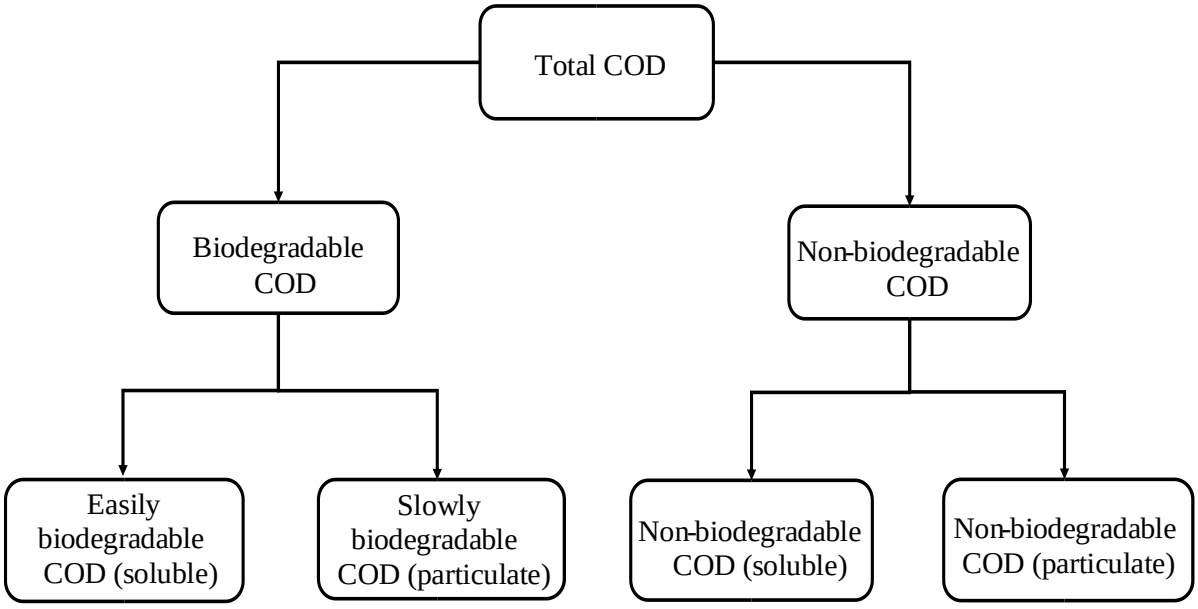

Fig. 1-1: Fractionation of COD in municipal wastewater. Adapted from Metcalf and Eddy, 2014.

In a conventional WWTP (Fig. 1-2), 50 - 70 % of the total influent organic matter is in particulate form (Derlon et al., 2016; Ødegaard, 1999; Wagner et al., 2015). Furthermore, particulate organic matter (POM) is the main component of carbon source (Liu et al., 2016; Zheng et al., 2013). The organic matter in wastewater contains 40 - 60 % of proteins, 25 - 50 % of carbohydrates and 8 - 12 % of oils and fats (Metcalf and Eddy, 2014). Butler et al. (1995) and Friedler and Butler (1996) found through data analysis that 40 % of the total pollution load generated in households originates from blackwater, i.e., the toilet. The latter was confirmed by

Ruiken et al. (2013) who found through sieving that around 35 % of the suspended solids in raw wastewater originate from toilet paper. The degradation of organic matter starts at the sewage system and reaches its maximum at the WWTP (Ødegaard, 1999; von Sperling, 2007). According to Metcalf and Eddy (2014), the wastewater treatment within a conventional WWTP is divided into preliminary, primary and secondary treatment (Fig. 1-2).

The preliminary treatment consists of screens and a grit chamber (Fig. 1-2a). Coarse screens remove particles larger than 6 mm and fine screens remove particles between 6 - 0.5 mm (e.g., small rags, paper, plastic material of various types, razor blades, grit, undecomposed food waste and feces). Depending on the screens design, up to 10 % of biochemical oxygen demand (BOD) is removed (Lackner, 2015). The grit chamber removes mainly inert material (iTSS) from the wastewater flow and retains more than 90 % of particles with a size of 210 to 150 µm depending on the design and the grit characteristics. When fine sand is present, the retention can decrease until less than 60 % (Metcalf and Eddy, 2014). Grit consists of inorganic material (e.g., sand, gravel, and other heavy materials). It includes organic material such as eggshells, bone chips, seeds, and coffee grounds. Screenings and grit are typically disposed either to a landfill (VS < 5 %) or are incinerated with the solids.

The effluent of the preliminary treatment is directed to the primary sedimentation tank where readily settleable solids and floating material are removed through sedimentation. 50 - 70 % of TSS and 25 - 35 % of BOD are removed depending on the design, temperature, and retention time, which typically varies from 1.5 - 2.5 h.

After the primary treatment, the wastewater is conducted into the biological or secondary treatment (Fig. 1-2a). There, ideally the biodegradable fraction of the POM is degraded. However, only a certain amount of the POM is totally degraded. The rest is only partially degraded (Henze and Mladenovski, 1991; Levine et al., 1991). Non-biodegradable particles could either be integrated into the activated sludge or/and could continue to the secondary sedimentation (Fig. 1-2a). Depending on the characteristics of the non-biodegradable particles at the secondary sedimentation, the POM could be captured as scum, which is considered as waste and therefore conducted into the anaerobic digester, (Fig. 1-2b) or could settle down to be returned into the aeration tank where their forward degradation is expected (Fig. 1-2a). The environmental factors and physical characteristics of the activated sludge contribute to the settling capacity of the sludge (Samer, 2015). According to Maximova and Dahl (2006), the activated sludge flocs formation within a clarifier determines the biomass settling capacity and

thus, its separation from the treated wastewater and MLSS concentration in sludge return flows. Hayet et al. (2010) found that in addition of the biomass concentration and the volume index, an increase in the temperature, i.e., 21 °C to 40 °C, increases the settling velocity of the sludge. The same author noticed an increase of the bacterial growth rate and the number of biologic flocs when the temperature was increased.

In relation to the treatment of the solids fraction, when the activated sludge accumulates exceeding the recommended limit, the excess sludge is removed from the tank as waste activated sludge/surplus sludge and is conducted into the thickener (Fig. 1-2b). Afterwards, both, the thickening effluent and the sludge produced during the primary treatment are combined and the flow is conducted into an anaerobic digester (Fig. 1-2b). The effluent of the anaerobic digester is dewatered (Fig. 1-2b). The biosolids are typically incinerated, while the liquid from the thickening and dewatering processes are normally led to the influent of the primary sedimentation (Fig. 1-2) or activated sludge tanks.

Depending on the final purpose of the treated wastewater, the effluent of the secondary treatment could be further treated, disinfected, and discharged into the water bodies' receptors. At this point, ideally, only "clean and safe for the environment" water is present. However, the effluent from conventional secondary treatment contains varying amounts of residual contaminants. Already in 1991, Levine et al., reported the persistence of particulate material with a size between 1 to 10 µm. Rogowska et al. (2019) discussed the effluents of WWTPs as a major source of pollutants, being conventional WWTPs "incapable of eliminating many compounds found in wastewater". Recently, Rodriguez-Mozaz et al. (2020) monitored final effluents from European WWTPs. The authors associated higher antibiotics consumption rates with higher concentrations at the WWTPs effluents. According to Luo et al. (2014), the discharge of treated effluent from WWTPs to surface water is a significant source for the introduction of micropollutants. Likewise, Petrie et al. (2014) indicated that emerging contaminants (ECs) such as pharmaceuticals and/or personal care products are originated from the discharge of WWTPs effluents. The presence of ECs could cause ecological impacts to biota in the environment (e.g., endocrine disruption). Brown (2019) found that the abundance in rivers of antibiotic resistant bacteria (ARB) and antibiotic resistance genes (ARG) are related to sanitary sewage overflows and to the discharges of WWTPs effluents. The author resolved that within the WWTP, antibiotics are partially reduced via retention in sludge or by degradation. Additionally, Proia et al. (2018) noted that urban rivers receive both antibiotics and antibiotic resistant fecal bacteria from WWTPs effluents. The same authors stated that a

continuous release of low levels of antibiotics into rivers could contribute to the spread of resistance in aquatic environments. Droppo et al. (2009) studied waterborne pathogens within river sediment (flocculated particles). The authors stated that "the lack of understanding around pathogen/sediment associations may lead to an inaccurate estimate of public health risk".

Due to the impact of the WWTPs discharges on the water bodies receptors, "many of the processes classified as tertiary or advance treatment will be considered conventional within the next 10 to 20 years" (Metcalf and Eddy, 2014). In addition to the need of a further treatment of the secondary effluent, it is of vital importance to optimize the conventional wastewater treatment. An et al. (2016) stated that due to the "huge amount of wastewater treated by activated sludge process worldwide, even a little improvement in the existing technology will have profound impact on the global economy and environment". Therefore, it is necessary a deeper understanding of the involved mechanisms in the biodegradation of organic matter during the biological treatment.

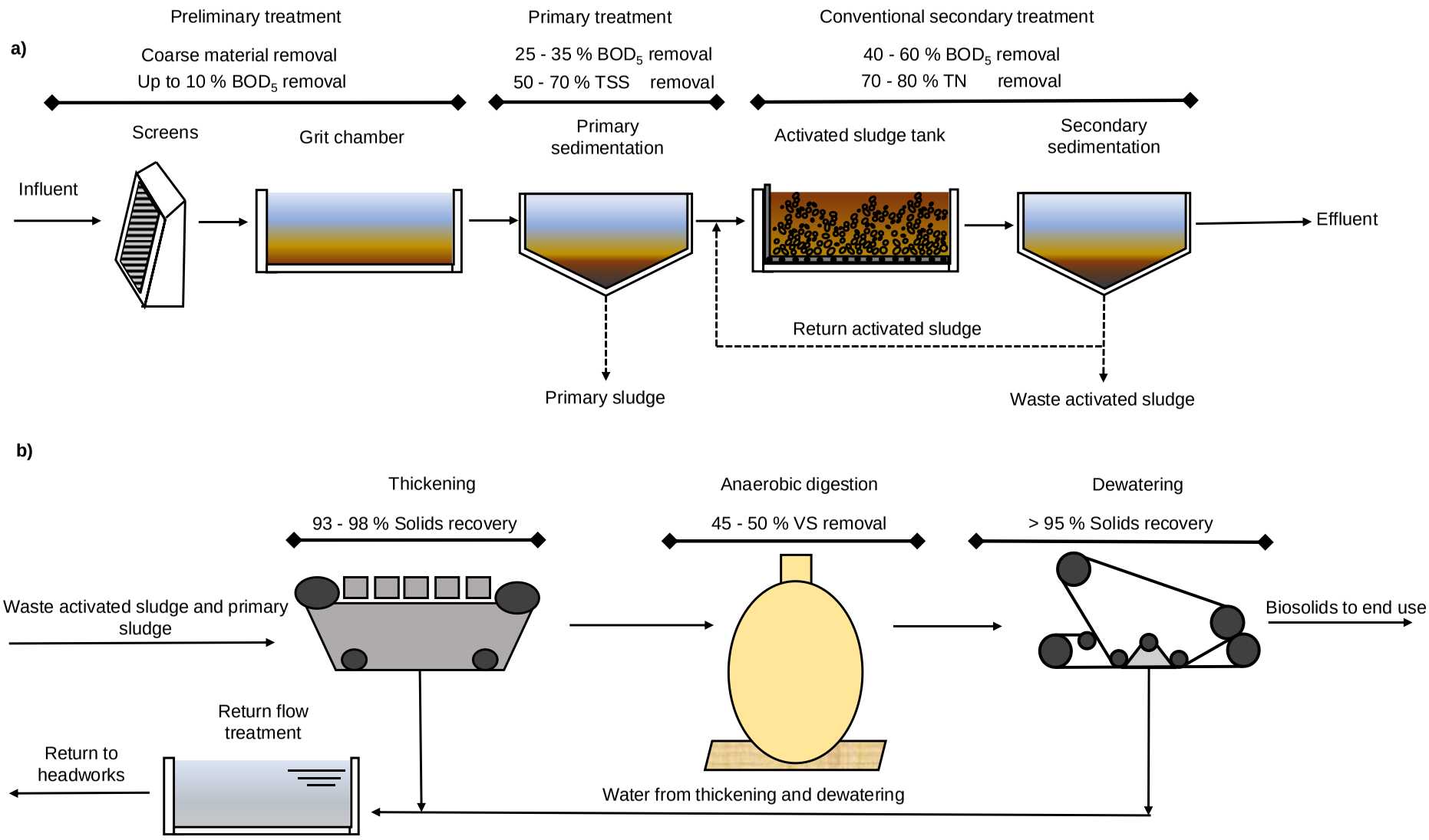

Fig. 1-2: Flow diagrams of a) conventional wastewater treatment plant and b) anaerobic treatment of sludge from primary sedimentation and excess biological sludge. Adapted flow diagrams and percentages from Metcalf and Eddy, 2014.

1.2 Biodegradation of particulate organic matter in a municipal wastewater treatment plant

In municipal wastewater treatment, organic matter is classified into easily biodegradable and slowly biodegradable organic matter (see Fig. 1-1, Chapter 1.1). POM has been recognized as slowly biodegradable organic matter (Batstone et al., 2002; Henze et al., 1987; Pavlostathis and Giraldo-Gomez, 1991; Vavilin et al., 2008). The biochemical transformation of organic matter (substrate decomposition and biomass growth) occurs simultaneously in a series of intermediate reactions catalyzed by specific enzymes (von Sperling, 2007). The responsible enzymes for biodegradation of organic matter are lyases and hydrolases. However, lyases reactions are few in comparison with the hydrolytic reactions (Morgenroth et al., 2002).

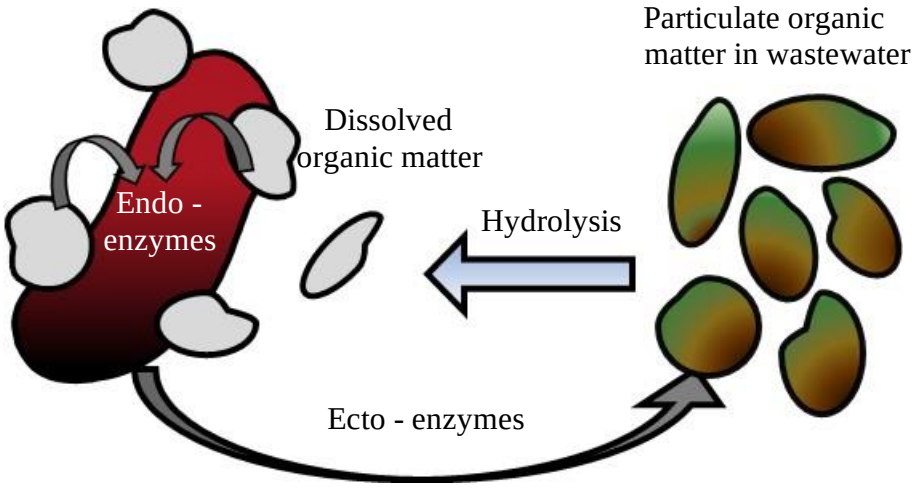

Fig. 1-3: (Right): particulate organic matter (size: 10 - 500 µm) hydrolyzed into dissolved organic matter and (left): assimilation of dissolved organic matter by bacteria (size: 1 µm). Adapted from von Sperling, 2007.

Hydrolysis is the process in which a polymer is broken down into products with a molecular weight (MW) lower than the initial polymer. During the break down of the covalent bonds of the initial polymer, water is consumed (Bajpai, 2017; Kommedal, 2003). Hydrolysis is catalyzed by hydrolytic ecto-enzymes (extracellular enzymes) produced by bacteria (Fig. 1-3). These enzymes are responsible for hydrolysis reactions outside the cell, in the liquid (Chróst, 1991; Li and Chróst, 2006; von Sperling, 2007). It is assumed that molecules larger than 1000 g/mol cannot diffuse into the cell wall (Chróst, 1991; Confer and Logan, 1997; Morgenroth et al., 2002). Therefore, the POM must be hydrolyzed until its products are sufficiently reduced for assimilation by bacteria with the aid of endo-enzymes (Fig. 1-3)

(Confer and Logan, 1998, 1997; von Sperling, 2007; Xia et al., 2008). The hydrolysis products (smaller fragments of the initial polymer) have a larger surface area available for the attack and further breaking down of the substrate by the microorganisms.

There have been continuous efforts to describe through mathematical models the hydrolysis of POM. Up today, there has not been an agreement on which is the best model because the existing models were developed for specific experimental conditions (Morgenroth et al., 2002). Nevertheless, together with the development of models, there has also been an attempt to simplify them to promote their use. Hydrolysis is often referred as a surface-limited process, which follows a first-order kinetics reaction model (Batstone et al., 2002; Confer and Logan, 1997; Eastman and Ferguson, 1981; Goel et al., 1998; Kappeler and Gujer, 1992; Vavilin et al., 2008, 1996). The assumption is that the POM degradation depends on the initial concentration of the particles, which are degraded at a constant rate. Hydrolysis of POM is considered the rate-limiting factor for the biomass growth because the hydrolysis rate of the POM is significantly lower than the utilization rate of the easily biodegradable organic matter (Batstone et al., 2002; Eastman and Ferguson, 1981; Henze et al., 1987; Koch et al., 2009).

A relationship between the size of a particle and the reaction rate has been found; the smaller the size of the particle the higher the rate of hydrolysis (Dimock and Morgenroth, 2006; Eastman and Ferguson, 1981; Kapoor et al., 2019; Levine et al., 1991; Sophonsiri and Morgenroth, 2004). Hydrolysis reactions do not involve energy utilization, therefore, there is no utilization of electron acceptor (Henze et al., 1987). Even though, the hydrolysis rate is affected by the electron acceptor conditions; aerobic conditions produce higher hydrolysis rates than anoxic or anaerobic conditions (Goel et al., 1998, 1997; Henze et al., 1987; Henze and Mladenovski, 1991). It seems that the electron acceptor affects not the specific activity of hydrolytic enzymes but the synthesis rate (Kommedal, 2003). Additionally, the amount of hydrolytic bacteria seems to be of special importance in the hydrolysis process (Goel et al., 1998; Vavilin et al., 2008). The conventional activated sludge (CAS) systems work under the premise that the necessary amount of active hydrolytic bacteria is ensured in the activated sludge tank.

By using confocal laser scanning microscopy (CLSM), Behle (2011) visualized the bacteria association to the particulate material originated from raw municipal wastewater (Fig. 1- 4). The author divided the particles into six particle size fractions shown in Table 1-1. Behle identified the presence of bacteria (*intestinal enterococci*) in all the particle size fractions.

Moreover, the author identified in fraction 1 that cellulose material had more occurrence of bacteria than fruit shell material (Fig. 1-4a-b) suggesting an influence of the material on the bacteria-particle association. In addition, when the particle size was reduced, starting on fraction 2, the bacteria density started to increase, and agglomerates of bacteria were distinguished (Fig. 1-4c-d). The CLSM-images showed the highest bacteria density in fraction 3 and fraction 4 (Fig. 1-4e-f). However, in fraction 5, only some bacteria agglomerates were observed onto the surface of a single particle (Fig. 1-4g); most of the spread bacteria were related to freely suspended bacteria. The author explained the reduction of the bacteria density with the filter pore size and its particle retention capacity. In fraction 6, the smallest particle size fraction, only freely suspended bacteria were observed onto the filter surface (Fig. 1-4h).

Table 1-1: Fractionation of raw wastewater particles according to their size and bacteria density in the fractions. Adapted from Behle, 2011.

Particle fractions	**Particle size [µm]**	**Intestinal enterococci / 100 mL**
1	> 4,000	> 1 x 10^4
2	1,000 - 500	≈ 1 x 10^4
3	500 - 180	≈ 1 x 10^4
4	180 - 63	≈ 1 x 10^5
5	63 - 12	≈ 1 x 10^5
6	12 - 5	≈ 1 x 10^5

The findings of Behle (2011) are noteworthy because based on imaging techniques bacteria was found to be cell-associated and furthermore, the highest bacteria density found corresponded to the same particle size range of most of the POM reaching the secondary treatment in a conventional WWTP (see Chapter 1.1). Likewise, Walters et al. (2014a) studied the influence of particle-association and TSS by using UV for the inactivation of bacteria in a river. The authors showed that the smaller the size of the particle the higher is the bacteria association.

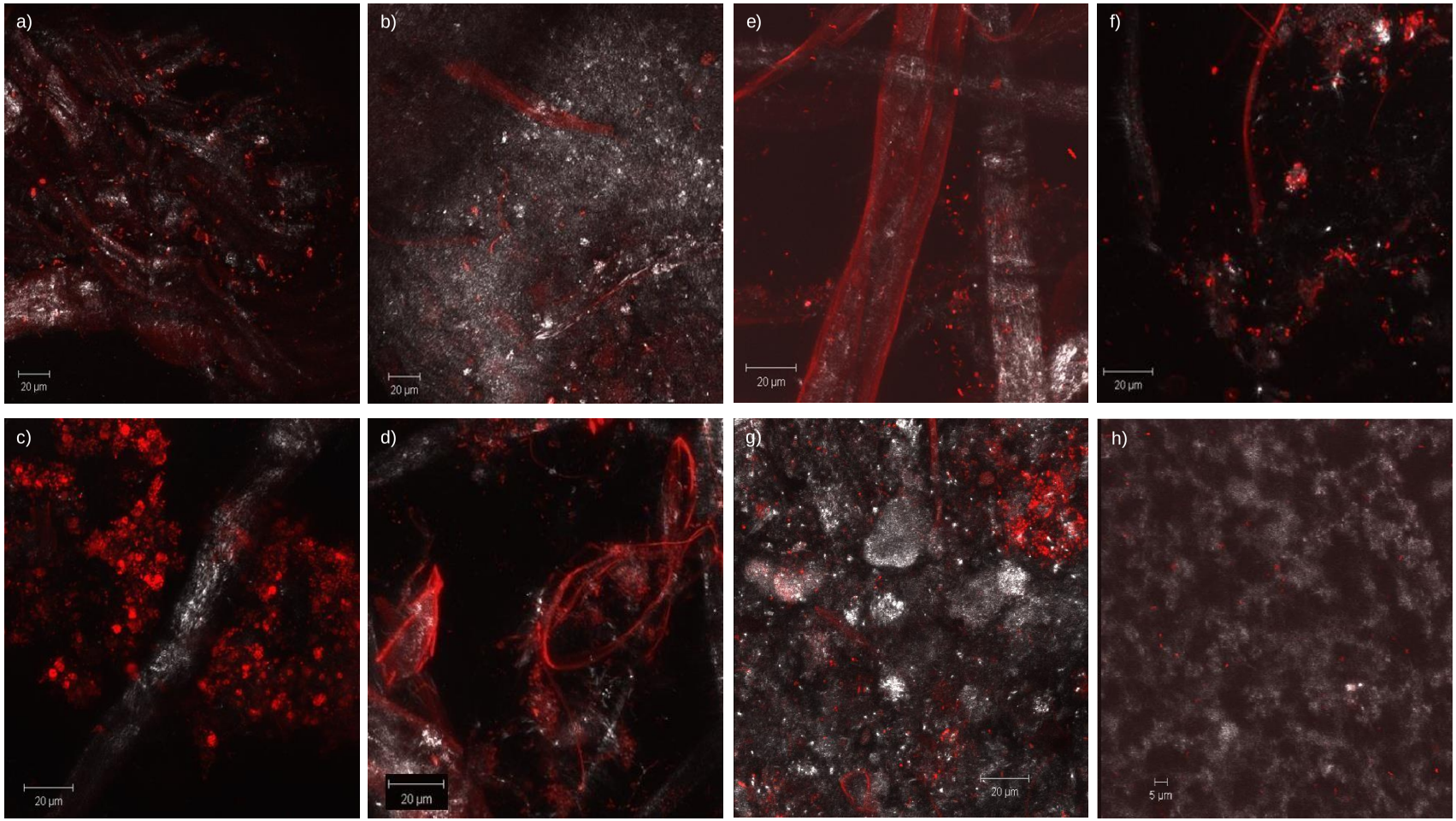

Fig. 1-4: CLSM-images of single particle fractions from raw wastewater; a) rest of cellulose and b) fruit shell out of a particle fraction with a particle size: > 4 mm; (c-d) particle size: 1,000 - 500 µm; e) particle size: 500 - 180 µm; f) particle size: 180 - 63 µm; g) particle size: 63 - 12 µm and h) particle size: 12 - 5 µm. All samples were marked with Syto 9 to visualize bacteria: red color. Reflection: white/grey color. Size bar: (a-g) 20 µm and (h) 5 µm. Taken from Behle (2011).

Li and Chróst (2006) reported that activated sludge flocs retain and accumulate a large number of enzymes. The authors determined that 97 % of the enzyme activity was cell-associated. Likewise, Chróst (1991), Confer and Logan (1998), and Goel et al. (1997) conclude that the hydrolysis process is mainly cell-associated. Bacteria associate with particulate material to gain protection against predation, to shield themselves from UV light rays and to obtain nutrients from the particles (Droppo et al., 2009; Walters et al., 2014a; Walters et al., 2014b).

Since enzymes are found to be cell-associated, it has been assumed that an increase in the biomass concentration will produce an increase in the hydrolysis rate (Goel et al., 1998) even when not all the biomass is active (Argaman, 1995; Henze et al., 1987; Henze and Mladenovski, 1991). However, San Pedro et al. (1994) stated that "biomass has no significant effect on the hydrolysis rate". The latter was supported by Benneouala et al. (2017), who showed that the pre-existing microorganisms associated to the POM have a major influence in the hydrolysis process. It seems that once there is more available surface by reason of hydrolysis, the amount of activated sludge becomes more relevant.

In addition to hydrolysis reactions, microorganisms such as rotifers and protozoa contribute in a small percentage to the degradation of POM. Rotifers capture bacteria and POM by using their cilia and pulling the captured food into their opening mouth (Salt, 1987); the presence of rotifers at the effluent of the secondary treatment indicates a highly efficient aerobic biological process (Metcalf and Eddy, 2014) because rotifers predominate a system with low organic level of unstabilized BOD (Stover and Campana, 2003).

Protozoa degrades bacteria as well as POM and depending on its feeding mode, protozoa can be classified into three groups, i.e. flagellated, free-swimming ciliated and stalked ciliated protozoa (Stover and Campana, 2003; von Sperling, 2007). Flagellated protozoa competes with bacteria for the assimilation of dissolved organic matter (DOM) (von Sperling, 2007); free-swimming ciliated protozoa degrade POM by phagocytosis (Friedrich, 2016; Kommedal, 2003; Metcalf and Eddy, 2014; Yang et al., 2017) and stalked ciliated protozoa predate bacteria by using their cilia to attach themselves to solid particles and feed on the bacteria available at the floc (Stover and Campana, 2003; von Sperling, 2007).

Viruses have been also found to contribute to the sludge mineralization process (Hao et al., 2011). Viruses are obligate intracellular infectious agents, which only multiply within a host cell. Bacteriophages are viruses that infect bacteria and are common constituents found in wastewater (Metcalf and Eddy, 2014). Viruses infect around 20 % of marine heterotrophic

bacteria (Hao et al., 2011; Suttle, 1994). According to Chen et al. (2019), virus impact microbial dynamics, metabolism, and community composition. Virus transform the microbial biomass into DOM by destroying host cells (cell lysis) and releasing the cytoplasmic compounds into the extracellular space (Wilhelm and Suttle, 1999).

It has been observed that the sludge retention time (SRT) has an impact on the degradation of micropollutants such as bisphenol-A, ibuprofen, bezafibrate and natural estrogens (Clara et al., 2005). The same authors found the longer the SRT the higher the removal of contaminants. Hatoum et al. (2019) stated that an increase of SRT caused an improvement of removal of the highly and moderate biodegradable compounds. Li et al. (2019) found a linear degradation of toilet paper fibers with the SRT. The latter is of special importance due to more than 50 % of the toilet paper fibers reach the secondary treatment in the WWTPs (Li et al., 2019).

1.3 Microbial growth in a batch reactor

According to Chróst (1991), heterotrophic bacteria are outstanding producers of hydrolytic enzymes and microbial growth depends on the products of the ecto-enzymatic reactions (Chapter 1.2). A biological process in a batch reactor commonly follows four microbial growth phases: lag phase, exponential growth phase, stationary phase, and death phase as shown in Fig. 1-5. During the lag phase, microorganisms adapt to the environment and there is no significant increase of biomass. The duration of the lag phase depends on the inoculum, the content of the wastewater and the microorganisms´ concentration. The lag phase is followed by the exponential growth phase, where microorganisms reproduce at their maximum rate and there is no nutrients or substrate limitation. Gradually, as the nutrients and/or substrate are depleted, the stationary phase is reached. The stationary phase is characterized by an equilibrium between growth and death of the cells. Inhibitory products of metabolism may be produced during this time. Lastly, during the death phase, the biomass decreases due to starvation. An approximate constant fraction of the remaining biomass is lost each day (Chisti, 2014; Metcalf and Eddy, 2014; von Sperling, 2007).

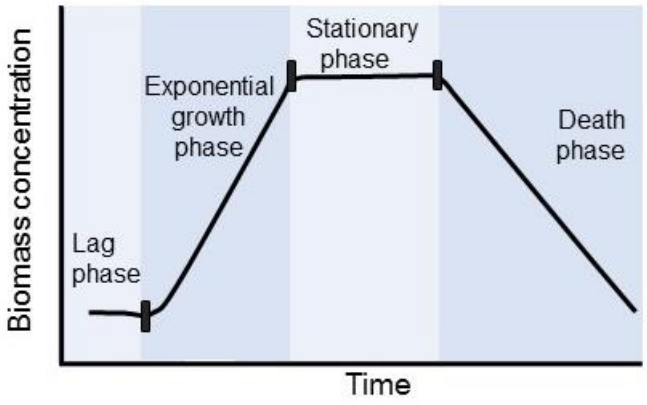

Fig. 1-5: Microbial growth pattern in a batch reactor. Adapted from von Sperling (2007).

Environmental conditions may have a significant effect on the microbial growth and the performance of the treatment (Leitão et al., 2006; Samer, 2015). According to von Sperling (2007), the effect varies depending on the microorganism; heterotrophic bacteria implicated in the stabilization of organic matter have higher tolerance to environmental changes than autotrophic bacteria implicated in the nitrification process. In biological systems, higher temperatures favor chemical conversion processes (von Sperling et al., 2020). Bacteria is classified into three groups: psychrophilic, mesophilic and thermophilic as shown in Table 1-2. Depending on the region and season, conventional WWTPs (Fig 1-2 in Chapter 1.1) operate within the mesophilic and thermophilic range (Wang et al., 2019; Ward et al., 2008).

Table 1-2: Temperature ranges for microbial growth. Adapted from von Sperling, 2007.

Range	**Temperature range [°C]**	**Optimal temperature range [°C]**
Psychrophilic	10 - 30	12 - 18
Mesophilic	20 - 50	25 - 40
Thermophilic	35 - 75	55 - 65

1.4 Methods to study hydrolysis of particulate organic matter from municipal wastewater

As discussed in Chapter 1.2, hydrolysis is the main pathway of biodegradation of POM. According to Morgenroth et al. (2002), hydrolysis of POM can be studied by four experimental methods: enzymatic activity, mass balances for bulk organic parameters, respiration rates and measurement of specific hydrolytic intermediates. The reader must be aware that the hydrolysis rate could differ depending on the selected method (Goel et al., 1998).

1.4.1 Enzymatic activity

As biodegradation of particulate matter is dominated by enzymatic reactions, a direct way to estimate hydrolysis is by measuring the enzyme activity. In the enzyme activity method, a specific substrate is degraded by a specific enzyme. Considering the diverse composition of the wastewater particles (see Chapter 1.1) and their corresponding enzymes, the applicability of this method is reduced (Morgenroth et al., 2002). Even though, the activity of activated sludge has been determined by measuring specific enzymes relevant for either hydrolysis or the metabolism of the substrate (Boczar et al., 1992; Confer and Logan, 1998; Goel et al., 1997; Nybroe et al., 1992). Besides the determination of microbial activity in wastewater (Nybroe et al., 1992), enzyme activity measurements have been also used to identify the location of the hydrolytic bacteria (Chróst, 1991; Confer and Logan, 1998; Li and Chróst, 2006) (see cell-association in Chapter 1.2).

1.4.2 Mass balance of bulk parameters

Mass balance of bulk organic parameters such as BOD, COD or VSS is a common method to study the hydrolysis process in wastewater treatment (Metcalf and Eddy, 2014). The mass balance is based on the law of conservation of mass, i.e., in an isolated system mass is neither created nor destroyed by chemical reactions or physical transformations (Felder and Rousseau, 2004). Equation (1-1) describes the general equation of the mass balance in a defined system.

$$\text{Accumulation} = \text{Input} - \text{Output} + \text{generation} - \text{decay} \qquad (1\text{-}1)$$

In wastewater treatment, steady-state equations are often used to simplify the calculations (von Sperling, 2007). At steady-state conditions, there is no accumulation within the system and there are no changes across time (Felder and Rousseau, 2004). Argaman (1995) proposed a model to study hydrolysis of POM by using a mass balance under steady-state conditions. The author measured the biomass (VSS) and the BOD to indicate the solubilization of POM. Argaman indicated the dependency of the hydrolysis rate to the biomass activity and the SRT.

The task group of the International Association on Water Pollution Research and Control (IAWPRC) presented mathematical models (ASM1, ASM2, ASM3) describing the CAS system by using mass balance equations for the main processes involved in the system with their corresponding stoichiometric coefficients and kinetic reactions (Henze et al., 1987).

Kappeler and Gujer (1992) characterized wastewater by using the ASM1 to estimate kinetic parameters of heterotrophic biomass under aerobic conditions. The authors determine hydrolysis of particulate (slowly) biodegradable substrate by applying a first order kinetics reaction and concluded that hydrolysis depends to some extent on the biomass concentration. In addition, the authors found that both the particulate organic matter and the hydrolysis constant impact the oxygen respiration only if growth depends on the hydrolyzed substrate.

1.4.3. Respiration rates measurements

Respiration rates are commonly used to study hydrolysis through the observation of the simultaneous production and utilization of biomass (Benneouala et al., 2017; Friedrich, 2016; Henze and Mladenovski, 1991; Lamarre et al., 2010; Li, Wu et al., 2019; Ramdani et al., 2012). Respiration is related to oxidation-reduction reactions. Therefore, respiration involves the utilization of electron acceptor (aerobic: oxygen, anoxic: nitrate, anaerobic: sulphate or carbon dioxide). Organic matter (electron donor) is oxidized to end products to obtain energy for cell maintenance and synthesis of new cells (1-2). Simultaneously, organic matter is converted to new cell tissue (biomass growth) (1-3). Once the organic matter is depleted, the new cells are used to obtain energy for cell maintenance (endogenous respiration) (1-4) (Metcalf and Eddy, 2014; von Sperling, 2007). These processes can be expressed in the following chemical reactions:

Energy reaction (oxidation)

$$CHONS + O_2 + \text{bacteria} \rightarrow CO_2 + H_2O + NH_3 + \text{other end products} + \text{energy} \quad (1\text{-}2)$$

Synthesis reaction

$$CHONS + O_2 + \text{bacteria} + \text{energy} \rightarrow \underset{\text{New cell tissue (biomass)}}{C_5H_7NO_2} \quad (1\text{-}3)$$

Endogenous respiration

$$C_5H_7NO_2 + 5\ O_2 \rightarrow 5\ CO_2 + NH_3 + 2\ H_2O \quad (1\text{-}4)$$

The standard methods (APHA et al., 2005) stablished the respirometric method 5210 D to determine the BOD, which represents the oxygen needed by the microorganisms to oxidize the organic matter (1-2 to 1-4). The WTW manual (Bridié, 1969) points out that the determination of BOD can be accomplished either directly by measuring the oxygen consumption or indirectly (Fig. 1-6) by measuring the carbon dioxide produced (i.e., the oxidized-end product of the organic matter). The respirometer, Oxitop Control OC 110, measures the pressure changes

produced by the fixation of carbon dioxide as shown in reaction (1-5) and provides a continuous signal of BOD (accumulated BOD) for the duration of an experiment.

$2\ NaOH + CO_2 \rightarrow Na_2CO_3 + H_2O$ (1-5)

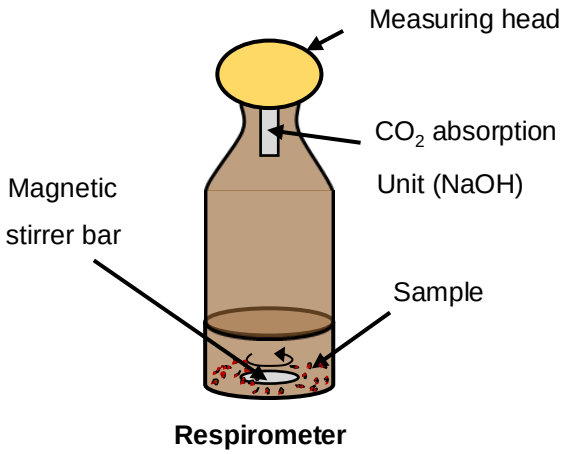

Fig. 1-6: Respirometer devise used to measure the accumulative BOD: Oxitop Control OC 110, WTW.

The rate in which bacteria utilize oxygen is identified as oxygen utilization rate (OUR) and it is used in aerobic processes to determine kinetic parameters (Gatti and Garc, 2010; Insel et al., 2002) and the biodegradability of the wastewater fractions (Fig. 1-1, Chapter 1.1) (Tran et al., 2015). However, the utilization of oxygen is associated with both microbial growth and substrate removal (Christofi, 2004). In respirometry, the use of allylthiourea (ATU) at a defined concentration is necessary to inhibit nitrification and thus to determine the oxygen used only for organic carbon removal (Tran et al., 2014).

Henze and Mladenovski (1991) studied the hydrolysis of particulate organic nitrogen through the release of ammonia nitrogen under different electron acceptor conditions. The authors found that hydrolysis of proteins is a major component for the overall hydrolysis process considering the elevated incidence of 40 - 60 % of proteins in municipal wastewater (Metcalf and Eddy, 2014). In addition, Henze and Mladenovski (1991) found that the hydrolysis rate was significantly affected by the biomass activity and that higher hydrolysis rates occur under aerobic conditions.

Drewnowski (2014) showed the impact of slowly biodegradable material on the OUR in activated sludge systems by conducting aerobic OUR experiments with low and high substrate/biomass concentration. The author compared settled wastewater (SWW) without pretreatment and SWW pretreated with a coagulation-flocculation method. The untreated

SWW consisted of easily and slowly biodegradable organic matter, while the pretreated SWW consisted of only easily biodegradable organic matter due to the removal of colloidal and particulate fractions. Drewnowski found that at low substrate/biomass ratios (i.e., MLSS between 2 and 3 g/L), the initial OUR values (after 1 h of feeding period) were 30 % higher in the experiment with untreated SWW than the experiments with pretreated SWW. At high substrate/biomass ratios (i.e., MLSS between 0.1 and 0.7 g/L), the author found in the untreated SWW experiment, an increase of the OUR values by reason of hydrolysis of slowly biodegradable organic matter. The OUR values of the pretreated SWW experiment gradually decreased to endogenous respiration levels due to the limited concentration of the easily biodegradable organic matter. The author recommended the evaluation of the OUR profile as a method to estimate hydrolysis for slowly biodegradable organic matter.

1.4.4 Measurement of specific hydrolytic intermediates or specific end-products

Measurements of substrate removal and/or the production of intermediate or end-products can be used to study hydrolysis of POM from municipal wastewater. According to Li, Brunner et al. (2018), the use of compounds with defined chemical characteristics and simple structure are often used to study hydrolysis of POM. As the intermediate or end-products of hydrolysis need to be well defined, most of the performed experiments have been conducted using artificial substrates such as glucose, starch, dextran or bovine serum albumin (Morgenroth et al., 2002). The latter is understandable when is considered the high concentration of biomass having simultaneous biomass production (release of hydrolysis products) and biomass utilization (substrate consumption) making unclear to know to what extent and how the microorganisms in a CAS system degrade the POM (Dimock and Morgenroth, 2006; Li, Brunner et al., 2018) (see also Chapter 1.4.3).

Separation techniques based on size exclusion such as membrane filtration and gel permeation chromatography can be used to measure hydrolysis products. According to Levine et al. (1991) and Sophonsiri and Morgenroth (2004), a combination of separation methods are often employed to perform the analysis. On one hand, membrane filtration processes such as microfiltration (MF) and ultrafiltration (UF) are usually applied to separate the organic matter by means of sieving. The typical pore size of a MF membrane is between 0.1 - 5 µm; MF membranes can remove suspended solids, bacteria, and blood cell. UF membranes have a pore size between 2 - 100 nm and they can remove macromolecules like albumin, viruses, or

pepsin (Li and Li, 2015; Metcalf and Eddy, 2014). Despite the broad use of the membrane technology, one major limitation is the membrane fouling caused by the DOM fraction in raw and treated wastewater (Tran et al., 2015). During filtration, fouling formation affects the separation behavior of the membrane. In addition, compounds with lower MW than the membrane cutoff may be adsorbed onto the fouling layer. Another important drawback of UF is that "UF-membrane MW distributions may not be comparable to each other because of the lack of a standardized UF method" (Esparza-Soto et al., 2006). The methods to measure the pore size and/or MW cutoff of the membranes depend on the membrane producers.

On the other hand, size exclusion chromatography (SEC) coupled with online detectors such as organic carbon and ultraviolet detector (UVD $\lambda = 254$ nm) is a method in which the DOM is separated by its molecular size. In principle, the chromatographic separation is based on the size of the compounds; lager molecules elute before (shorter retention time) from the column than smaller molecules because large molecules do not enter the pores of the column, while smaller molecules penetrate into the pores eluting later (longer retention time) (Fatoorehchi et al., 2018; Huber et al., 1994, 2011b). The retention time or elution volumes of the separated substances are reversely correlated with the molecular size and in reasonable approximation with the MW of the eluted compounds (Frimmel and Abbt-Braun, 2011). Although, "the interactions of the sample compounds with the stationary gel my lead to advanced or delayed retention behavior" (Xiao et al., 2020); compounds eluting beyond the permeation limit of the column are related to substances with hydrophobic or amphiphilic nature (Frimmel and Abbt-Braun, 2011; Huber and Frimmel, 1994, 1991; Müller et al., 2000; Müller and Frimmel, 2002; Perminova et al., 1998; Specht and Frimmel, 2000; Tran et al., 2015).

A great advantage of the SEC technique is that the whole MW range of the hydrolysis products is reflected in a chromatogram. Therefore, it is possible to measure the production and degradation of all the hydrolysis products by following the changes of the peaks´ areas through time. Although one has to keep in mind that previous analysis showed that the chromatographable dissolved organic carbon (cDOC) of wastewater is within 73 - 90 % concerning the total dissolved organic carbon (DOC) (Frimmel and Abbt-Braun, 2011). SEC provides detailed information on the molecular size of the released hydrolysis organic products. Therefore, the independent study of formation and degradation of the released products can be achieved by using the SEC technique.

Confer and Logan, (1998, 1997) studied the MW distribution of hydrolysis products during the biodegradation of bovine serum albumin and dextran and dextrin by using membrane UF techniques. The authors found that hydrolytic enzymes are cell-associated (see Chapter 1.2) and that during the hydrolysis of macromolecules, hydrolysis products are released into the bulk solution. This hydrolysis-release of products cycle is repeated until the hydrolysis products are assimilated by bacteria.

Esparza-Soto et al. (2006) investigated the changes of MW distributions of DOC and UV-absorbing compounds at seven full-scale WWTPs by using ultrafiltration techniques. The authors postulated that effluent MW distributions are greatly affected by the production of intermediate MW soluble microbial products (SMPs) and extracellular polymeric substances (EPS) during the hydrolysis process of raw wastewater by cell-associated hydrolytic enzymes.

Jin et al. (2011) studied the MW distribution of DOM in biological treated sewage effluent from eight different WWTPs by using high performance SEC as well as a total organic carbon analyzer to determine DOC and a spectrophotometer at a wavelength of 254 nm to determine SUVA values. The authors divided the DOM into polysaccharides and proteins (macromolecules), humic-like substances (refractory organic compounds) and low MW organic compounds. The same authors found that humic-like and large MW products were aggregated into the sludge during all the biodegradation processes and especially after aeration processes.

1.5 Aerobic digestion of particulate organic matter from municipal wastewater

WWTPs often use aerobic digestion for the treatment of municipal wastewater. The main objective has been the removal of contaminants from the water to protect the health of the society and the environment. The biological removal of POM in a conventional WWTP (see Fig. 1-2 in Chapter 1.1) is typically carried out in an activated sludge tank (Fig. 1-7), which treats about 75 % of the total wastewater flow in the United States of America (Boczar et al., 1992).

A CAS system is constituted by a heterogenous culture of microorganisms, which is developed and adapted to specific environmental conditions. The main function of these microorganisms is to reduce the colloidal and dissolved contaminants by adsorption and assimilation, resulting in settleable solids, which are separated from the liquid phase and as a consequence, the water quality is enhanced (Moore, 1970) (see also Chapter 1.1).

Fig. 1-7: Conventional activated sludge tanks from municipal WWTP Chapala, Mexico.

In aerobic processes, microorganisms consume oxygen to carry out metabolic reactions; the organic matter oxidation, the synthesis of new cell material (biomass) and its further degradation is carried out according to the chemical reactions (1-2) to (1-4) presented in Chapter 1.4.3. During the initial biological utilization of organic matter, more than 50 % of the organic matter is oxidized, while the remaining material is converted to new biomass, which may be further oxidized during the endogenous respiration (see Fig. 1-5 in Chapter 1.3) (Metcalf and Eddy, 2014).

In a CAS system, microorganisms agglomerate to form larger and heterogeneous structures called flocs, which are vital for the removal of organic matter (von Sperling, 2007). Typical activated sludge flocs are shown in Fig. 1-8 and a scheme is presented in Fig. 1-9. The EPS matrix of bacterial flocs (see Fig. 1-10) accounts for many compounds originated from the influent wastewater or generated during growth, utilization, and decay processes (Ramdani et al., 2012). The EPS matrix increases water retention, its mechanical stability allows the establishment of microorganisms and simultaneously provides nutrient sorption and shield against predation, viruses, antimicrobials, etc. (Seviour et al., 2019). Flocs contain adsorbed organic matter, inert material, SMPs, alive and dead cells (Ramdani et al., 2012; von Sperling, 2007). The aggregation phenomena, flocculation of dissolved and dispersed matter, is produced by exopolymers produced by bacterial cells in a CAS system (Maximova and Dahl, 2006). Flocs contain most of the hydrolytic activity in the system (Boczar et al., 1992; Kommedal, 2003). An et al. (2016) found that the bacteria *Z. ramigera* is a typical microorganism responsible for the floc´s formation. Filamentous bacteria exert a structural matrix, EPS, in the form of a gelatinous layer, where the microorganisms such as bacteria, protozoa, fungi, rotifers, nematodes adhere (Horan, 1990; von Sperling, 2007). Yu et al. (2008) found proteins and

polysaccharides within the EPS matrix, but the authors found proteins as the main component in sludge flocs. The size of a floc ranges from 50 to 200 µm (Metcalf and Eddy, 2014) with a typical size between 50 to 100 µm (Nielsen et al., 2012). Flocs present a multilayered structure (Yu et al., 2008), where a gradient in oxygen concentration is observed; from the largest oxygen concentration at the outer layer to the lowest oxygen concentration at the center of the floc (see Fig. 1-9) (von Sperling, 2007). Li, Zhao et al. (2018) stated that sludge formation is influenced by the design of the reactor, the wastewater organic load, the microbial characteristics, and environmental parameters.

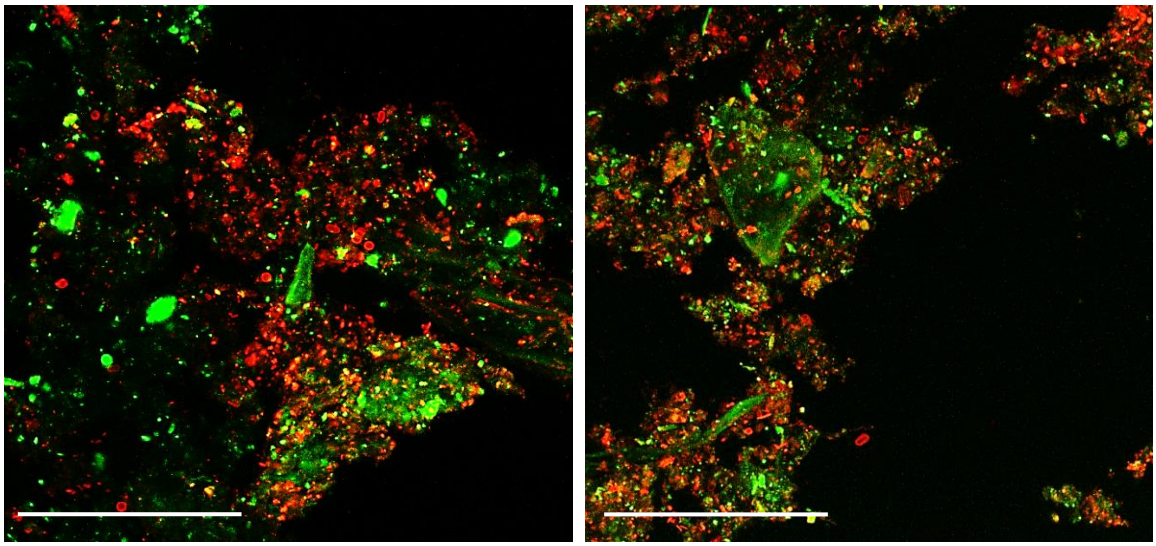

Fig. 1-8: Maximum intensity projection of CLSM-images of activated sludge flocs from the municipal WWTP of Neureut, Karlsruhe, Germany. Scale bar: 100 µm. Color: red - nucleic acids; green - EPS glycoconjugates.

The EPS formed during aerobic treatment provides adsorption sites for pollutants, thus, microorganisms can adapt and resist the toxicity of the new environment for their survival (Li, Zaho et al., 2018). Aerobic heterotrophic bacteria tolerate higher concentrations of toxic substances in comparison to autotrophic bacteria responsible for ammonia oxidation or archaea responsible for methane formation (Metcalf and Eddy, 2014). The activated sludge process is often studied by conducting aerobic batch experiments (Friedrich and Takács, 2013), where the typical dissolved oxygen (DO) concentration is 2.0 mg/L; DO concentrations higher than 0.5 mg/L have no significant effect on the degradation rate of organic matter (Metcalf and Eddy, 2014).

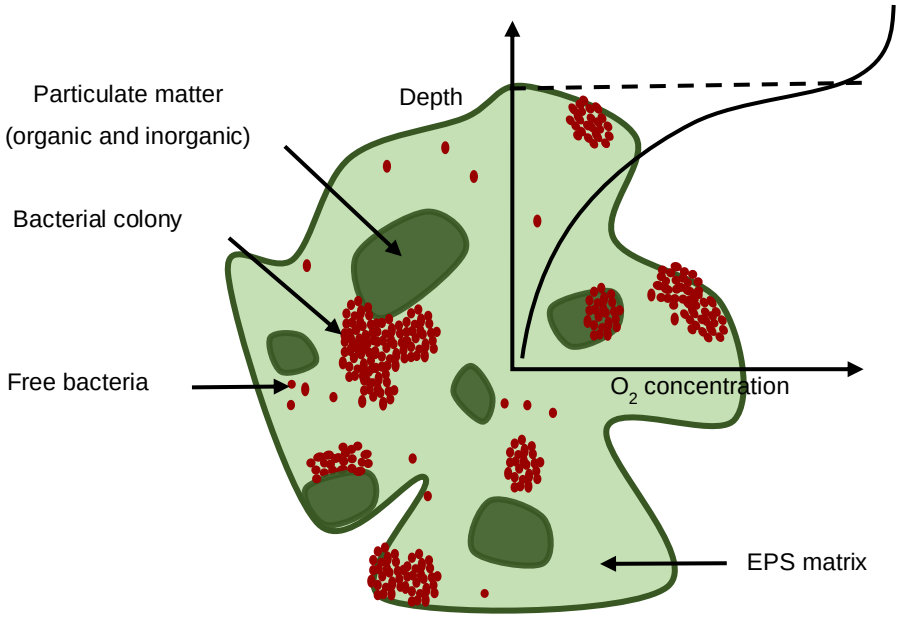

Fig. 1-9: Scheme of an activated sludge floc with oxygen concentration profile.

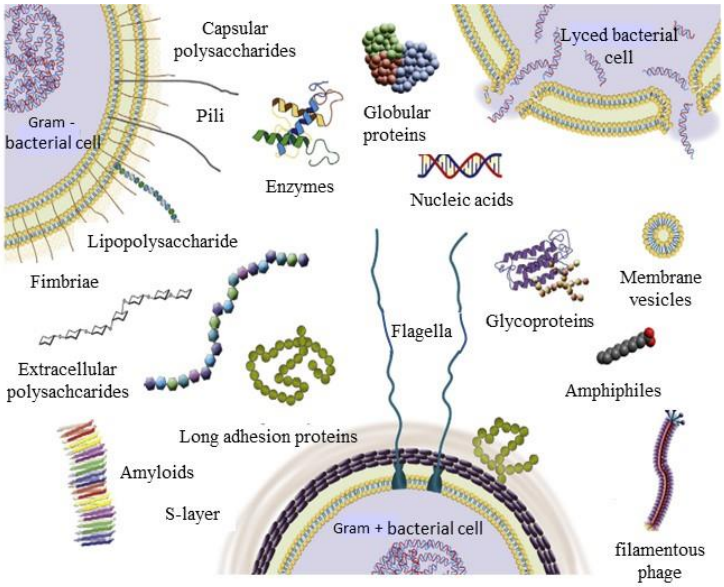

Fig. 1-10: Exopolymers typically found in EPS matrix. Taken from Seviour et al., 2019.

Moore (1970) presented an investigation about the effects of pH on aerobic sludge digestion. The author studied waste activated sludge aerobically digested over a period of 20 d and over a pH range of 3.5 - 9.5. Moore concluded that the aerobic digestion process is relatively insensitive to changes of pH and considerable solids removal can be achieved within the investigated pH range. According to Metcalf and Eddy (2014), for carbon removal, aerobic heterotrophic bacteria tolerate pH changes in the range of 6.0 - 9.0 but biological systems are commonly operated near a neutral pH, i.e., 7, since wastewater is typically alkaline, obtaining its alkalinity from the water supply, the groundwater and/or the incorporated materials

originated from domestic use. In aerobic processes where nitrification occurs, the hydrogen ion concentration may change the pH if there is not sufficient buffer capacity (alkalinity) in the system (Henze et al., 1987). Hence, to maintain the pH between 6.8 - 7.4 around 1.5 mmol/L alkalinity are required.

1.6 Anaerobic digestion of particulate organic matter from municipal wastewater

The anaerobic digestion process has been investigated over centuries (Meegoda et al., 2018). In the late 1800s and early 1900s, engineered anaerobic digestion technologies were designed to treat wastewater (Metcalf and Eddy, 2014). Throughout time, there have been continuous efforts to improve the understanding and the applicability of this technology specially because its performance is usually compared with the aerobic processes. The use of anaerobic digestion within a municipal WWTP (Fig. 1-11) can aid in the reduction of the main operational costs related to the aerobic treatment processes, i.e., oxygen consumption and sludge production together with its consequent handling, treatment and disposal (Leitão et al., 2006). In the anaerobic treatment process, there is no utilization of oxygen and the sludge production is 3 to 20 times lower than in the CAS system (Seghezzo, 2004). However, the longer time needed to start-up an anaerobic reactor, especially for high-rate anaerobic process should be considered as well as a better operational control and more qualified operators (de Lemos Chernicharo, 2005). Anaerobic conversion of carbonaceous matter produces carbon dioxide and methane as end-products as shown in reaction (1-6) producing less release of energy than in the aerobic respiration (von Sperling, 2007). In anaerobic systems, around 70 to 90 % of the biodegradable matter is converted into biogas (de Lemos Chernicharo, 2005).

$$C_6H_{12}O_6 \rightarrow 3\ CH_4 + 3\ CO_2 + \text{Energy} \qquad (1\text{-}6)$$

According to McCarty, 1964 a minimum treatment control is required to operate anaerobic processes. Anaerobic digestion is considered a two-steps process, which can be further divided into various sub-processes or stages. According to the anaerobic digestion model 1 (ADM1) (Batstone et al., 2002), a series of interconnected processes are involved in the anaerobic digestion, i.e., disintegration, hydrolysis, acidogenesis, acetogenesis and methanogenesis.

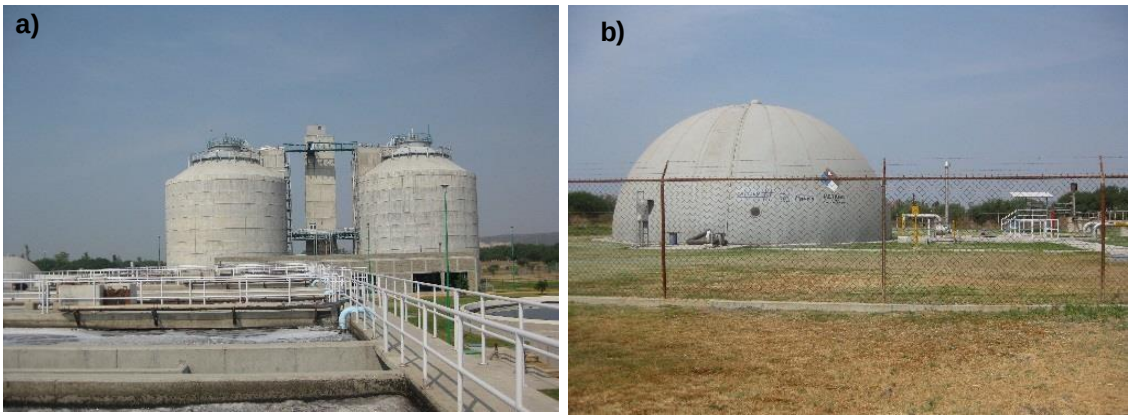

Fig. 1-11: a) Anaerobic digestion tanks for sludge treatment and b) biogas container from municipal WWTP León, Mexico.

Fig. 1-12 describes the metabolic sequences within the anaerobic digestion process in accordance with the ADM1, in which the POM is disintegrated to carbohydrates, proteins and lipids, which are further hydrolyzed into monosaccharides, amino acids and long chain fatty acids, respectively (see enzymatic hydrolysis in Chapter 1.2). According to Pavlostathis and Giraldo-Gomez (1991) and de Beer et al. (1992), the knowledge of kinetics allows an optimization of the performance, operation and control of the anaerobic digestion process. Hydrolysis is commonly represented in a first-order kinetics manner (Batstone et al., 2002; Eastman and Ferguson, 1981; Pavlostathis and Giraldo-Gomez, 1991; Vavilin et al., 2008) and if the substrate is present in particulate form, hydrolysis is considered to be the rate-limiting step from the overall process (Eastman and Ferguson, 1981; Vavilin et al., 1996). There are several degradation pathways resulting in a variety of products (Chisti, 2014); the formed products depend on the original substrate, the bacteria population and the environmental conditions (Lübken, 2009). During the acidogenesis and acetogenesis stages, the hydrolyzed products are metabolized and converted into simpler compounds such as hydrogen, carbon dioxide, and short chain organic acids called volatile fatty acids (VFA). Typical VFA produced during the anaerobic digestion are shown in Table 1-3.

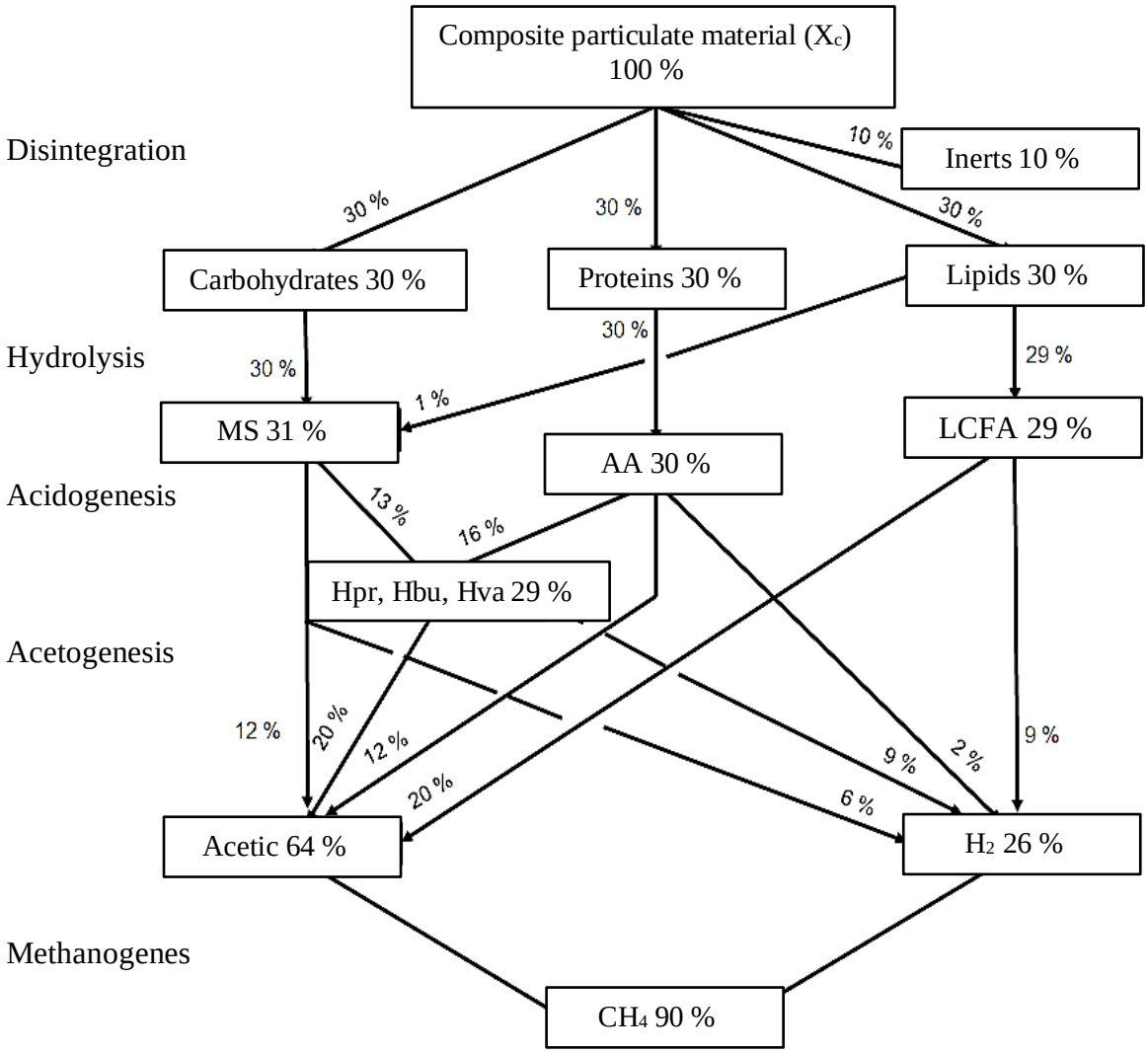

Fig. 1-12: COD flux of particulate organic matter used in the anaerobic digestion model 1 (ADM1). MS: monosaccharides; AA: amino acids; LCFA: long chain fatty acids; Hpr: propionic acid; Hbu: butyric acid; Hva: valeric acid. Taken from Batstone et al., 2002.

Table 1-3: Typical volatile fatty acids (VFA) produced during the anaerobic treatment. Taken from McCarty, 1964.

VFA	**Chemical formula**
Formic acid	HCOOH
Acetic acid	CH_3COOH
Propionic acid	CH_3CH_2COOH
Butyric acid	$CH_3CH_2CH_2COOH$
Valeric acid	$CH_3CH_2CH_2CH_2COOH$
Isovaleric acid	$(CH_3)_2CH_2CH_2COOH$
Caproic acid	$CH_3CH_2CH_2CH_2CH_2COOH$

During the last metabolic sequence, the methanogenesis stage, acetic acid and hydrogen are converted into biogas by the methanogenic archaea. For municipal wastewater, the typical composition of the biogas corresponds to 70 - 80 % of methane and 20 - 30 % of carbon dioxide (de Lemos Chernicharo, 2005). Methanogenic archaea present high specificity for the substrate; acetoclastic methanogens utilize acetic acid to produce methane, while hydrogenotrophic methanogens utilize hydrogen and carbon dioxide to form methane (Lübken, 2009; McCarty, 1964). Around 70 % of the methane is produced by the cleavage of acetic acid by acetoclastic methanogens (1-7) and the remaining 30 % is formed from the reduction of carbon dioxide (electron acceptor) by the hydrogenotrophic methanogens (1-8) (de Lemos Chernicharo, 2005; McCarty, 1964).

$CH_3COOH \rightarrow CH_4 + CO_2$ (acetoclastic methanogens) (1-7)

$CO_2 + 4\ H_2 \rightarrow CH_4 + 2\ H_2O$ (hydrogenotrophic methanogens) (1-8)

The methanogenic group is sensible to environmental changes, especially of pH (von Sperling and Lemos Chernicharo, 2005). It has been determined that the methanogenic archaea operate in a narrow pH range of around 6.5 - 7.5 having its optimal pH at 7 (Table 1-4). An anaerobic digester in a WWTP must operate within the range of tolerance of the methanogenic archaea because the presence of these methanogenic microorganisms is of vital importance for the removal of organic matter. According to Leitão et al. (2006) and Lohani and Havukainen (2017) a typical anaerobic digester is supposed to operate within the pH range of 6.8 - 7.8. Even when the pH is above 7, it has been found that the presence of VFA as acetic acid (approx. 3000 mg/L) can inhibit the methanogenic process (Stallman et al., 2012) producing a limitation for the overall anaerobic digestion process. However, the effect of pH-changes depends on the available alkalinity in the reactor (Leitão et al., 2006).

The stabilization of the organic matter requires a balance among the involved metabolic sequences or stages of the anaerobic digestion. The balance or equilibrium is indicated by the concentration of VFA, which are the intermediate products of the overall process. When the stages are in balance, methanogenic archaea utilize the VFA as fast as they are produced. However, if the production of the hydrolysis products (i.e., VFA) exceeds the consumption capacity of the methanogenic archaea, the VFA will accumulate within the system and methanogenesis will become a limiting factor of the anaerobic digestion (McCarty, 1964). This situation produces a constant drop of the pH causing an inactivation of the methanogenic

archaea resulting in a destabilization of the whole process and if no immediate remediation is performed, a sink (i.e., souring) of the reactor can be expected (von Sperling and Lemos Chernicharo, 2005).

Table 1-4: Optimal pH ranges for the different stages of the anaerobic digestion process.

Stage	Bacteria	Optimal pH	References
Hydrolysis	Fermentative bacteria	5.0 - 6.0	Lohani et al., 2018
		5.2 - 6.3	Vavilin et al., 2007
Acidogenesis	Acidogenic bacteria	5.2 - 6.5	Solera et al., 2001
		5.0 - 6.0	von Sperling and Lemos, 2005
Acetogenesis	Acetogenic bacteria	6.7 - 7.5	Solera et al., 2001
Methanogenesis	Methanogenic archaea	6.6 - 7.4	von Sperling and Lemos, 2005
		6.7 - 7 .5	Hilton et al., 1988
		6.5 - 8.0	Lohani et al., 2018
		6.6 - 7.4	Manimegalai et al., 2014
		6.8 - 7.2	Shah et al., 2014

1.7 Objectives

The main focus for the study conducted was to gain new insight into understanding hydrolysis of POM from municipal wastewater treated under aerobic and anaerobic conditions. For this purpose, three major objectives were stablished.

1) To identify the mechanism and limiting factors of hydrolysis of POM from municipal wastewater treated under aerobic and anaerobic conditions.

2) To determine the potential biodegradability of the released hydrolysis products in terms of their molecular size and UV-absorption under aerobic and anaerobic conditions.

3) To visualize the location where hydrolysis takes place, the bacteria population dynamics, and its interaction with the particulate organic matter by using confocal laser scanning microscopy under aerobic and anaerobic conditions.

To accomplish these objectives, two main experimental studies were conducted. The results of the first study are presented in Chapter 3: Hydrolysis of POM under aerobic treatment and the results of the second study are presented in Chapter 4: Anaerobic digestion of POM from municipal wastewater. Although Chapter 3 and Chapter 4 present conclusions as sub-sections within the Chapters, Chapter 5 present a comparison among the two processes and is offered as a conclusion of the work.

Preliminary experiments, i.e., POM from municipal wastewater combined with biomass (either activated sludge for aerobic experiments or anaerobic sludge for anaerobic experiments) showed that it is not possible to distinguish the release of hydrolysis products originated form the biodegradation of POM because the sludge itself is subject to hydrolysis. As the results of these preliminary experiments served as a basis for the design of the experiments shown in Chapter 3 and Chapter 4, the results of the preliminary experiments are shown in the material and methods Chapter.

The experiments shown in Chapter 3 and Chapter 4 were conducted with real municipal wastewater particles (size: 25 - 250 µm) and without addition of activated or anaerobic sludge. During the aerobic and anaerobic batch experiments, the production and utilization of the hydrolysis products were monitored by using the SEC coupled with online detectors (SEC-OCD-UV). Additionally, standard wastewater parameters such as DOC, sCOD,

dissolved total nitrogen (dTN), ammonium nitrogen (NH_4^+ - N), nitrate nitrogen (NO_3^- - N), nitrite nitrogen (NO_2^- - N) and phosphate phosphorus (PO_4^{3-} - P) were determined after defined time periods. In addition, for the aerobic experiments, aerobic respiration was measured separately from the aerobic batch reactor. For the anaerobic experiments, VFAs: acetic acid, propionic acid, butyric acid, iso-butyric acid and valeric acid were analyzed (see Chapter 2).

The findings of Chapter 3 were published as: Alondra Alvarado, Stephanie West, Gudrun Abbt-Braun, Harald Horn. Chemosphere (Alvarado et al., 2021), 263, p, 128329, https://doi.org/10.1016/j.chemosphere.2020.128329.

Chapter 2: Material and methods

2.1 Municipal wastewater sampling and preparation of the particulate organic matter fraction

Municipal wastewater was taken from the effluent of the aerated sand trap (Fig. 2-1) in the WWTP of Neureut, Karlsruhe, Germany (875.000 population equivalents). About 1200 L volume were collected in plastic tanks during each sampling for the period of 2017 to 2020. After a sedimentation time of t = 4 h, the supernatant was removed, and the settled particles were sieved with stainless steel sieves to obtain a particle fraction of 25 - 250 µm. The gathered POM fraction was rinsed with tap water (tap water of Karlsruhe, electrical conductivity: 657 µS/cm, DOC < 0.5 mg/L). The rinsed particles were re-suspended in tap water and stored at 4 °C until usage.

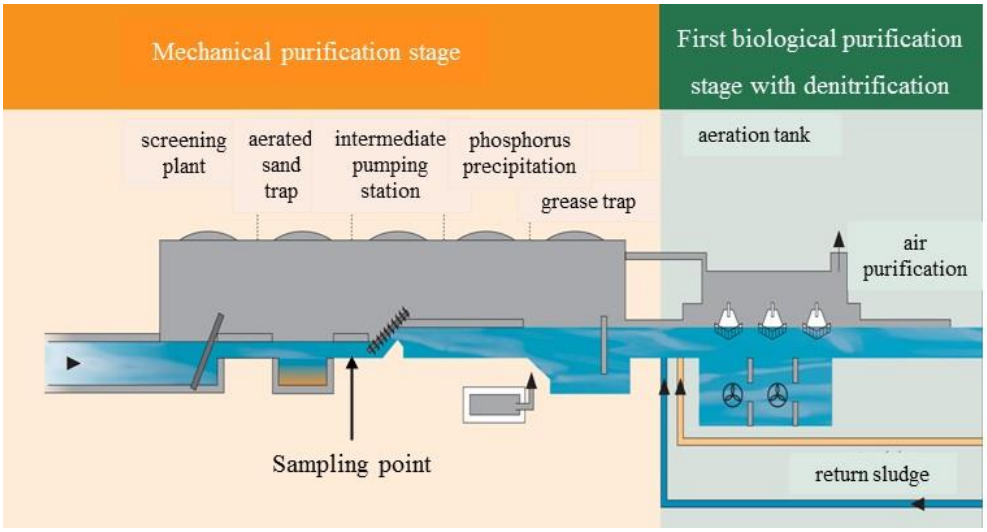

Fig. 2-1: Sampling point at the effluent of the aerated sand trap at the municipal wastewater treatment plant (WWTP) of Neureut, Karlsruhe, Germany. Taken from https://www.karlsruhe.de/b3/bauen/tiefbau/entwaesserung/klaerwerk.de.

The particle size fraction used in the current thesis work was chosen considering the results of Walters et al. (2014), Li, Brunner et al. (2018) and Behle (2011) (see Chapter 1.2). Walters et al. (2014) reported the major prevalence in wastewater corresponding to the particle size fraction between 63 - 1,000 µm (Table 2-1); while the particle size fraction between 12 - 63 µm had the major TSS contribution, i.e., 45 % from all the particle size fractions the authors studied (Table 2-1). Similarly, Li, Brunner et al., 2018 characterized particles from the effluent grit chamber of the WWTP of Neureut, Karlsruhe, Germany. The authors reported no significant

variation of the TSS concentration of all the particle fractions ranging from 28 - 500 µm resulting in an overall TSS contribution of 36.4 % (Table 2-2).

Table 2-1: Characterization, prevalence in wastewater and TSS contribution of wastewater particle fractions. Particle size: p.s. Adapted from Walters et al., 2014a.

Particle fractions	Particle size [µm]	Prevalence in wastewater [%]	TSS contribution [%]
1	1,000 < p.s.	14	26
2	63 < p.s. ≤ 1,000	33	23
3	12 < p.s. ≤ 63	27	45
4	p.s. ≤ 12	26	6

Table 2-2: Characterization of wastewater particle fractions. Particle size: p.s. Adapted from Li, Brunner et al., 2018.

Particle fractions	Particle size [µm]	Concentration of TSS [mg/L]	TSS contribution [%]
1	500 ≤ p.s.	140	42.4
2	250 ≤ p.s. < 500	30	9.1
3	100 ≤ p.s. < 250	20	6.1
4	45 ≤ p.s. < 100	30	9.1
5	28 ≤ p.s. < 45	40	12.1

2.2 Aerobic batch set-up

For each experiment, the particle concentration (fraction size: 25 - 250 µm) was set to 1 g/L TSS, 0.79 g/L VSS (washed particles diluted in tap water and without activated sludge). Fig. 2-2 describes the split of the mixture of the particle fraction and tap water into two vessels, the first one was used as an open batch reactor (aerobic batch) and the second one (respirometry) was used to measure the OUR (see Chapter 2.3).

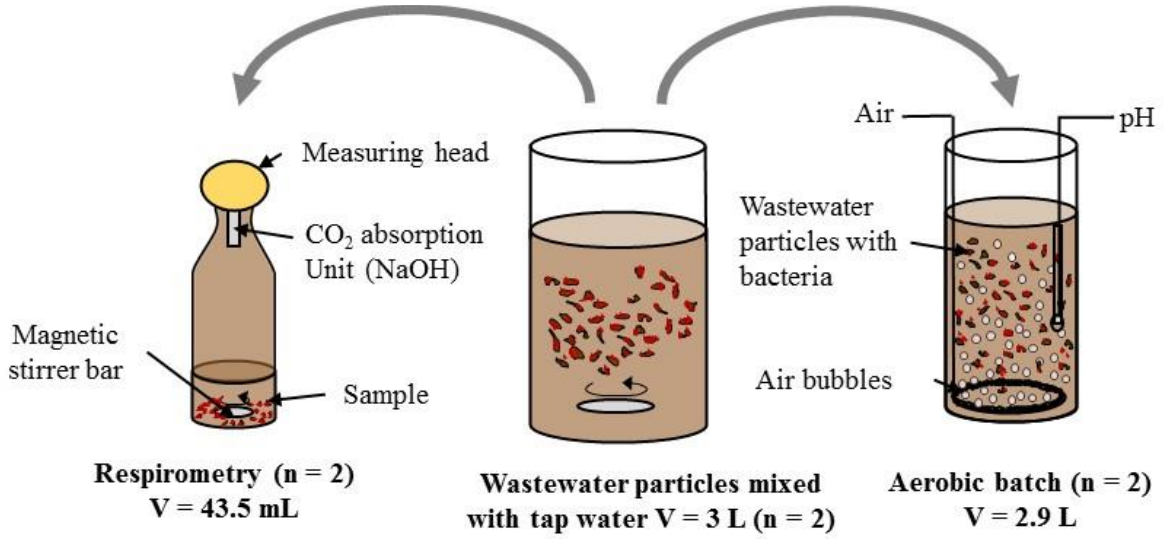

Fig. 2-2: Set-up for the aerobic batch reactor to follow the hydrolysis products, bacteria, and extracellular polymeric substances (EPS) (right) and the respirometric reactor to follow the oxygen utilization rate (OUR) (left). Allylthiourea was added to the respirometric experiments to inhibit nitrification. Taken from Alvarado et al., 2021.

The aerobic experiments were conducted in batch reactors (reaction volume V = 2.9 L) opened to air, maintained at room temperature (T = 20 °C). The reactors were aerated by air using aquarium pumps (50 L/h) and were equipped with pH probes (Endress + Hauser, Orbisint CPS11D-7AA21, Germany). The pH value was kept automatically between 6.8 - 7.2 utilizing HCl (1.4 M) and NaOH (2 M). A nutrient solution: 20 mg/L NH_4^+ - N (NH_4HCO_3), 3 mg/L PO_4^{3-} - P (KH_2PO_4) and 0.5 mg/L Fe^{3+} ($FeCl_3 \cdot 6\,H_2O$) was added to each reactor to avoid limitation. Two aerobic experiments were performed, the first one with a length of 2 d (experiment 1, Exp1-aer) and the second one of 13 d (experiment 2, Exp2-aer).

Experiments shown in Chapter 2.7, showed that degradation related only to particles started after 0.2 d. Therefore, 0.2 d was set as the starting time. As the hydrolysis products measured as soluble chemical oxygen demand (sCOD) and DOC accumulated during the first 2 days in Exp1-aer, the experiment was extended to detect when the utilization of the hydrolysis products takes place. As activated sludge systems with nitrification are generally operated with SRTs of approximately 10 d, 13 d were chosen for Exp2-aer.

2.3 Oxygen utilization rate (OUR)

The degradation of POM started after t = 4 h of aeration (see Chapter 2.7). Therefore, and in order to measure the OUR related only to the biodegradation of the POM, two aliquots of

43.5 mL were taken from the original mixture of particles and tap water after 0.2 d of aeration (see Fig. 2-2, left side). The aliquots were placed into 510 mL Oxitop bottles (Oxitop Control OC 110, WTW, Germany). To inhibit nitrification, 5 mg/L of Allylthiourea (ATU) was added to each Oxitop bottle. As the used tap water was sufficiently buffered with 6 mmol/L alkalinity, the pH was not controlled during the respiration experiment. The OUR measurement (n = 2) was ran in parallel with the aerobic batch reactor (from t = 0.2 d until t = 2 d, Exp1-aer and t = 13 d, Exp2-aer). The Oxitop Control OC 110 provides a continuous signal of BOD (accumulated BOD) throughout the experimentation (for more information see Chapter 1.4.3). The OUR in mg/(L · d) was calculated by using the slope of the daily measured values of BOD.

$$\mathrm{OUR}\ [\mathrm{mg}/(\mathrm{L}\cdot\mathrm{d})] = \Delta\mathrm{BOD}/\Delta\mathrm{t} \qquad (2\text{-}1)$$

The OUR was then further coupled to the removal of VSS. VSS concentrations were obtained from the aerated batch reactor (Fig. 2-2, right side). VSS degradation was coupled to the OUR by a 1st order reaction kinetics:

$$\mathrm{OUR}\ [\mathrm{mg}/(\mathrm{L}\cdot\mathrm{d})] = \mathrm{VSS}\cdot k_{\mathrm{hyd\_aer}}\cdot \upsilon_{\mathrm{OUR/VSS}} \qquad (2\text{-}2)$$

The coefficient $\upsilon_{OUR/VSS}$ provides the stoichiometry for oxygen used per VSS. The equivalent VSS to COD conversion coefficient of 1.56 g COD/g VSS was used (Lübken, 2009). k_{hyd_aer} is a lumped kinetic coefficient, which describes the hydrolysis and subsequent respiration.

2.4 Anaerobic batch set-up

As anaerobic digestion requires generally around 20 d of SRT, two anaerobic batch experiments were conducted for 24 d (when no more changes were observed) by using an automated methane potential test system (AMPTS II, Bioprocess Control, Sweden). The AMPTS II consists of a flow cell system to measure biogas production (measuring range 0.01 - 20 L/d) according to the principle of liquid displacement. The AMPTS II software logs data automatically and controls the rotation speed of motors that mix the contents of the reactors.

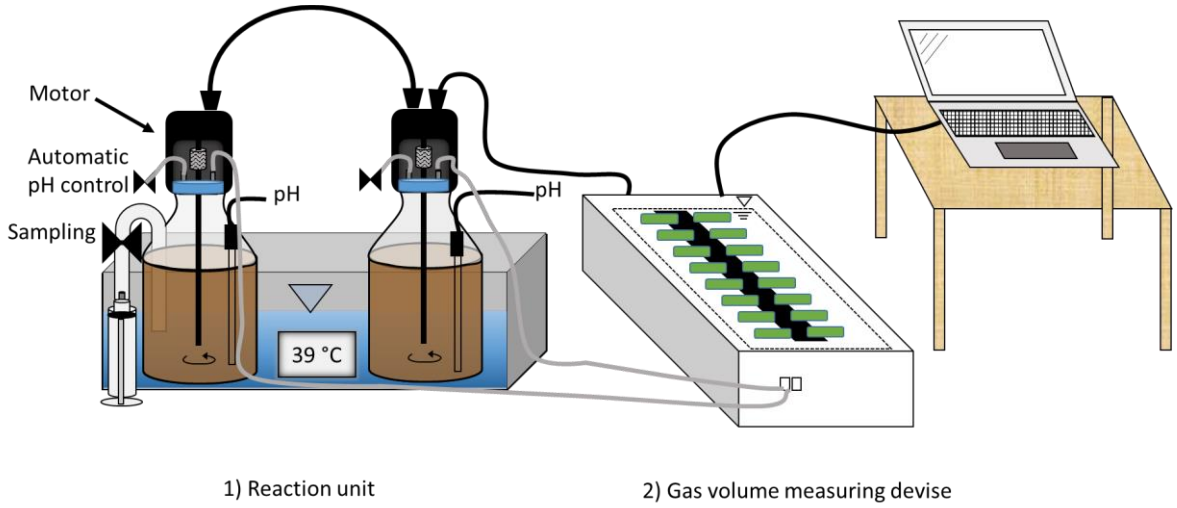

Fig. 2-3: Anaerobic batch experiment setup. 1: Reaction unit and 2: gas volume measuring devise.

The AMPTS II was divided into two units shown in Fig. 2-3; 1: reaction unit and 2: gas volume measuring device. In the reaction unit, two reactors (V = 2 L), with a working volume of 1.8 L contained washed particles diluted in tap water (see Chapter 2.1). The reactors were submerged in a water bath at T = 39 °C. To avoid limitation of nutrients, 20 mg/L NH_4^+ - N (NH_4HCO_3), 3 mg/L PO_4^{3-} - P (KH_2PO_4) and 0.5 mg/L Fe^{3+} ($FeCl_3 \cdot 6\ H_2O$) were mixed with tap water and added to each reactor. The pH was automatically controlled (pH probes: Endress + Hauser, Orbisint CPS11D-7AA21, Germany) to 6 ± 0.2 in experiment 1: Exp1-ana and to 7.0 ± 0.2 in experiment 2: Exp2-ana by using HCl (0.5 M) and NaOH (0.2 M). The stirring motors were set to 60 rpm at 60 % intensity. One of the reactors was set as a sampling reactor and the second one was used exclusively to measure biogas. The two experiments were done in duplicate. Before starting the experiments, the reactors were flushed with nitrogen gas for 2 min to ensure anaerobic conditions.

2.5 Sampling and analytical methods

Experiments were conducted under aerobic and anaerobic conditions at different pH values (Table 2-3). During the aerobic and anaerobic batch experiments, sCOD, DOC, dTN, NH_4^+ - N, NO_3^- - N, NO_2^- - N and PO_4^{3-} - P were determined after defined time periods. In addition, for the aerobic experiments, aerobic respiration was measured separately from the aerobic batch reactor (see Chapter 2.2). For the anaerobic experiments, VFAs: acetic acid, propionic acid, butyric acid, iso-butyric acid and valeric acid were analyzed.

Table 2-3: Aerobic and anaerobic experiments.

Aerobic experiments	pH	Time [d]	Anaerobic experiments	pH	Time [d]
Exp1-aer	7 ± 0.2	2	Exp2-ana	6 ± 0.2	24
Exp2-aer	7 ± 0.2	13	Exp2-ana	7 ± 0.2	24

Samples (50 mL) were taken every 4 h in Exp1-aer, daily in Exp2-aer and every two days in Exp1-ana and Exp2-ana. The samples were centrifuged at 4500 rpm for 5 min and filtered through two pre-washed Chromafil Xtra filters (first filtration: glass fiber, pore size: 1 µm; second filtration: polyether sulfones, pore size: 0.45 µm). The samples were stored at 4 °C until analysis.

The concentration of sCOD was determined following the Standard Method 5220 D (APHA et al., 2005). DOC and dTN were analyzed using oxidative combustion-infrared and oxidative combustion-chemi luminescence analysis (TOC-V CPH/CPN analyzer, Shimadzu, Japan, detection limit: 50 µg/L carbon, mean value out of three measurements, standard deviation: calculated out of the three closest values). Ammonium nitrogen was determined by using standard photometer test kits (salicylate method, Hach Lange, Germany). TSS and VSS (IDL, filter pore size: 15 µm) were measured at the beginning and at the end of the experiment following the Standard Method 2540 B (APHA et al., 2005).

The analysis of anions and organic acids was performed by using ion chromatography (IC). For anions determination, the anions method was used (IC: Metrohm 790 Personal IC, CH-9191, Switzerland; eluent: sodium bicarbonate 1 mmol/L and sodium carbonate 3.2 mmol/L; suppressor: 100 mmol/L H_2SO_4, column: Metrosep A Supp 5 100/4 polyvinyl alcohol with quaternary ammonium groups, flux: 0.75 mL/min, detection limit nitrate: 0.5 mg/L and phosphate 1 mg/L). For organic acids determination (acetic acid, propionic acid, butyric acid, iso-butyric acid), the organic acids method was employed (IC: Metrohm 881 Compact Pro, eluent: sulfuric acid 0.5 mmol, suppressor: 30 mmol LiCl, column: Metrosep organic acids 250/7.8, flux 0.70 mL/min, detection limit: 0.5 - 1 mg/L).

2.6 Size exclusion chromatography with online detection of organic carbon and UV absorption (SEC-OCD-UV)

Characterization by size exclusion chromatography with online UV (254 nm) and organic carbon detection was conducted according to Huber et al., 2011a (Fig. 2-4). The separation was performed with a TSK column (TSK HW 50S, 250 - 20 mm, Tosoh Corp., Japan). Due to the great variety of compounds present in wastewater (see Chapter 1.1), it is not possible to conduct the calibration with authentic standards (Fatoorehchi et al., 2018; Frimmel and Abbt-Braun, 2011). Therefore, the column calibration for molecular weights was conducted by using polyethylene glycols (200.000 - 200 g/mol), diethylene glycol (106 g/mol) and ethylene glycol (62 g/mol). Dextran blue ($2 \cdot 10^6$ g/mol, retention time: 28 min) and methanol (32 g/mol, retention time: 72 min) were employed to determine the exclusion and permeation volume, respectively (Frimmel and Abbt-Braun, 2011).

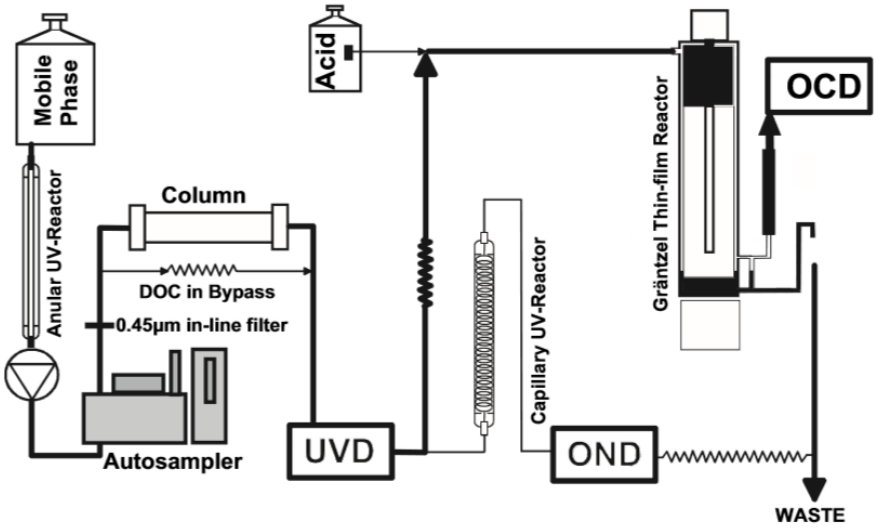

Fig. 2-4: Flow scheme of the liquid chromatographic SEC with online UV (254 nm) and organic carbon detection system. Taken from Hubber et al., 2011a.

Fig. 2-4 shows the scheme of the SEC with online detection system; the first detector after chromatographic separation was an UV detector (UVD; λ = 254 nm, Knauer S200, Berlin, Germany). After the UVD, the sample was split into a spinning thin-film reactor (Graentzel Reactor; Huber and Frimmel, 1994), which was used online for the oxidation of organic compounds, coupled with a non-dispersive infrared IR-detector (Siemens, Ultramat 6, Germany) for CO_2 detection. As eluent a phosphate buffer (1.5 g/L Na_2HPO_4 2 H_2O + 2.5 g/L KH_2PO_4) at a flow rate of 1.1 mL/min was used, the injection volume was 1000 µL.

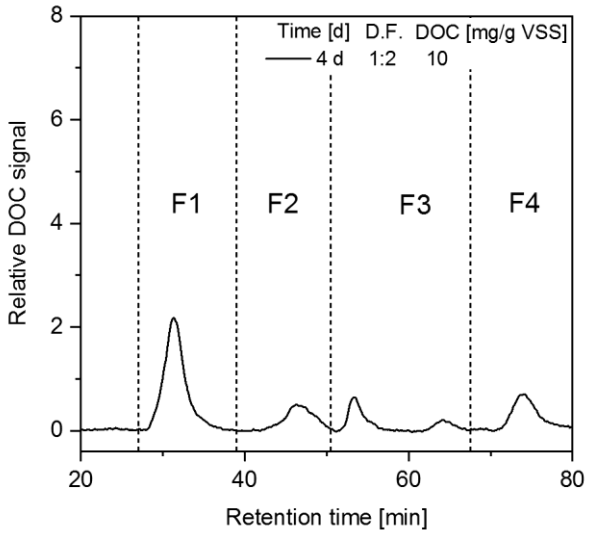

Fig. 2-5: Fractionation of the chromatographable dissolved organic carbon (cDOC) according to the retention time of the organic compounds eluted from the SEC column. Sample: municipal wastewater particle fraction (size: 25 - 250 µm) after 4 d of aeration in Exp2-aer.

The chromatograms were divided into four fractions selected in accordance with the observed changes. Fig. 2-5 shows the separation of the four fractions according to the retention time, respectively to the nominal MW. The retention time of fraction 1 (F1), fraction 2 (F2), fraction 3 (F3) and fraction 4 (F4) for the aerobic and anaerobic experiments are shown in Table 2-4 and Table 2-5, respectively. The nominal MW of the cDOC can be assigned with the molar masses of the calibration standards used. F1, F2, F3 and F4 were in the range of $2 \cdot 10^6$ - 20,000, 20,000 - 1550, 1550 - 100 and lower than 100 g/mol, respectively. The reader must keep in mind that the relative cDOC and UV signal is a response for organic carbon and UV detection, respectively. Due to system limitations, the samples were diluted down to 2 mg/L C.

ChromCALC (DOC-LABOR, Karlsruhe, Germany) software was used to integrate the peak area of the chromatograms. The results were recorded in area units. According to Frimmel and Abbt-Braun (2011), the cDOC of wastewater is within 73 - 90 % concerning the total DOC. The loss of DOC is due to the adsorption of the hydrophobic molecules onto the stationary phase. In the experiments used throughout this thesis, the DOC-peak area was set to 100 % and related to the total DOC concentration obtained with the analysis of the DOC concentration gained with the Shimadzu set-up (Chapter 2.5). Therefore, each peak area (fraction) corresponds to a determined DOC concentration. The relative amount of UV-absorbance of the peak areas of F1, F2, F3, and F4 was calculated by setting the total UV-peak area to 100 %.

Table 2-4: Retention time in min of the DOC and UV fractions at the start and end of the aerobic experiments. fraction 1 (F1), fraction 2 (F2), fraction 3 (F3), and fraction 4 (F4).

Fractions	Exp1-aer		Exp2-aer	
	Start [min]	End [min]	Start [min]	End [min]
F1	27	40	27	40
F2	40	49.5	40	49.5
F3	49.5	67.5	49.5	67.5
F4	67.5	100	67.5	80

Table 2-5: Retention time in min of the DOC and UV fractions at the start and end of the anaerobic experiments. fraction 1 (F1), fraction 2 (F2), fraction 3 (F3), and fraction 4 (F4).

Fractions	Exp1-ana		Exp2-ana	
	Start [min]	End [min]	Start [min]	End [min]
F1	26	37	26	37
F2	37	49.5	37	50
F3	49.5	67	50	67
F4	67	80	67	80

2.7 Identification of the easily biodegradable organic matter originally attached to the particulate organic matter

To study the hydrolysis of only the POM fraction, it was necessary to determine at which point the easily biodegradable organic matter originally attached to the POM was degraded. Chromatographic results indicated that after 0.2 d of aeration, the signal of all the cDOC fractions (i.e., fraction F1, fraction F2, fraction F3 and fraction F4) decreased. The decrease was specially noticed for fraction F3 (Fig. 2-6), which has been assigned as low MW organic material (Huber et al., 2011b). The nominal MW of the cDOC fraction F3 was in the range of 100 - 1550 g/mol. As molecules lower than 1000 g/mol are directly assimilated by bacteria (Chróst, 1991; Confer and Logan, 1997; Morgenroth et al., 2002) (see also Chapter 1.2), the organic matter present in fraction F3 was considered as easily biodegradable organic matter. The decrease was directly related to the degradation of the biodegradable material originally coupled to the POM.

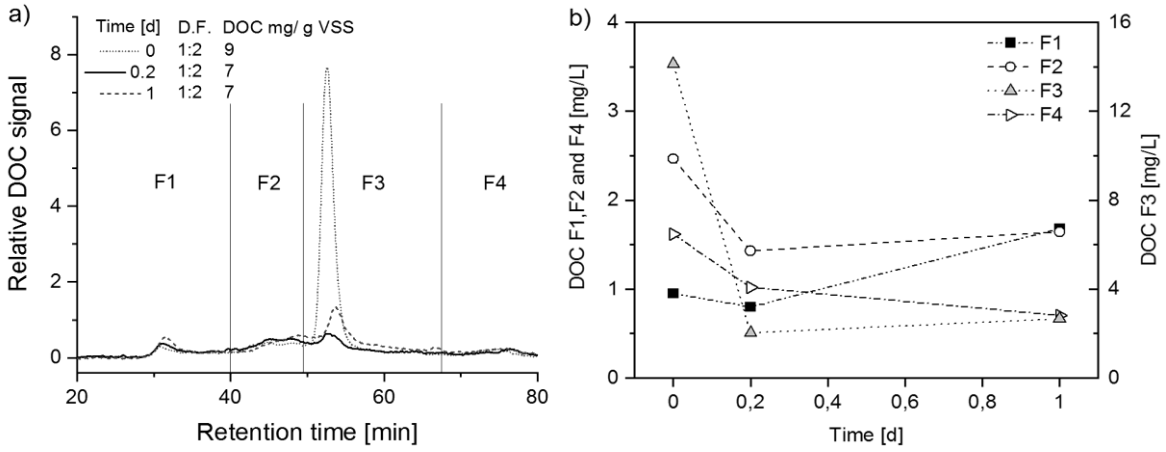

Fig. 2-6: a) Fractionation of the DOC according to its molecular size at time 0, 0.2 and 1 d. b) DOC concentration of fraction 1 (F1), fraction 2 (F2), fraction 3 (F3) and fraction 4 (F4) in Exp2-aer.

2.8 Confocal laser scanning microscopy and image analysis

In 2019, Seviour et al. highlighted the importance of targeting specific key components present in the EPS matrix. The same authors highlighted the use of imaging techniques such as CLSM for the observation of the changes of both the matrix composition and microbial cells through time. Due to the great diversity of composition (polysaccharides, proteins, nucleic acids, etc.) and structural variety of the EPS, lectins are used for the quantification of glycol-conjugates related to EPS (Staudt et al., 2003; Swerhone et al., 2015).

CLSM images stacks were obtained by using the Zeiss LSM700 confocal laser scanning microscope (Carl Zeiss Microlmaging GmbH, Jena, Germany). A water immersible lens (40x magnification; objective class Plan-Apochromat; 40x/1.0 DIC VIS-IR, Zeiss, Germany) was used to investigate the structure of the particles.

The EPS glycoconjugates were stained with Aleuria aurantia lectin (AAL) fluorescein isothiocyanate (FITC) (LINARIS Biologische Produkte GmbH, Germany) according to Staudt et al. (2003). Nucleic acids were marked with SYTO 60 (Thermo Fisher scientific, Germany). For the aerobic experiments, approximately 20 mL of the particle solution were taken from the reactor and were filtrated in order to fix the particles on the membrane filter (0.45 µm, HTTP, Millipore, Germany). Afterwards, the filter with the particles was placed in a petri dish, where it was stained with 100 µL of SYTO 60 working solution (5 µM) for 20 min, and afterward with 20 µL of AAL-FITC working solution (50 µM) for 7 - 10 min. After staining, the petri

dish was filled with tap water and the particles were visualized immediately. Samples were taken in Exp2-aer at t = 0, 2, 7 and 13 d.

For the anaerobic experiments, the methodology of Schmid et al. (2003) was followed. Approximately 20 mL of the particle solution was taken from the reactor and allowed to settle for 20 min in a conical sample tube. About 5 mL of the supernatant was filtered (0.45 µm, HTTP, Millipore, Germany) and approximately 3 mL of the settled particles were taken and placed into a well plate. There, 20 µL of AAL-FITC working solution (50 µg/mL) was added for 20 min and afterward, 20 µL of SYTO 60 working solution (20 µM) was added for another 20 min. Then, the stained sample was placed into an imaging-spacer and about 1 mL of filtered supernatant was added. The adhesive side down was applied onto the surface of a glass slide. The prepared samples were immediately visualized. Samples were taken in Exp1-ana and Exp2-ana at t = 0, 7, 14 and 24 d. To assure reliable data, for each sample day, between 15 - 30 spots were chosen randomly for the aerobic and anaerobic experiments. Image processing was performed using Carl Zeiss Zen software (black edition, 2012, version 8.1.2.484). The images had a frame size of 1020 x 1020 pixels, scaling (X·Y·Z = 0.098·0.098·1.0 µm) and were stored in 8-bit LSM format.

Three-dimensional CLSM images were processed by using Jimage Analyzer (version 1.1). Each data set was manually threshold to separate background and noise from the areas of interest (EPS and nucleic acids). Intensities below the selected threshold were not considered in the signal counting.

2.9 Simulation of the formation and utilization of the soluble hydrolysis products of particulate organic matter originated from municipal wastewater and treated under anaerobic conditions

Aquasim software version 2.1 (Reichert, 1998) was used to simulate the formation and utilization of the soluble hydrolysis products formed during the degradation of POM under anaerobic conditions. The Aquasim software was developed by the Swiss Federal Institute for Aquatic Science and Technology (EAWAG), CH-8600 Dübendorf, Switzerland and its purpose is the identification and simulation of aquatic systems. The reader is encouraged to read the Aquasim user manual (Reichert, 1998) to get familiar to the concepts and parameters used in the simulation. In addition, if the reader is interested, the nice course created by Wang and Bakke (2014) is recommended.

A set of differential equations based on first order kinetics was used (see Chapter 4.2) for the simulation in Aquasim 2.1. The simulation considers a composite particle substrate (X_c) in a batch reactor and establishes a series of processes for the hydrolysis of the POM (X_c). X_c is considered a homogeneous mixture. A constant volume reactor compartment was built in Aquasim 2.1 to simulate the metabolic sequences involved in the physical reactor during the anaerobic digestion of POM (Chapter 1.6). The metabolic sequences include hydrolysis (hydrolysis I), acetogenesis and acidogenesis (hydrolysis II) and methanogenesis (biogas formation). The rate equations used in each stage are shown in Chapter 4.2.

The stoichiometric factors used in the differential equations were determined based on the obtained results (Chapter 4.2). POM was associated to the measured VSS. Therefore, the initial input of X_c in the simulation was the initial VSS concentration measured at the beginning of the experiments (Table 4-1, Chapter 4.2). The rest of the initial input values were experimentally determined. If desired, X_c can also be presented in terms of COD by using the equivalent coefficient of 1.56 g COD/g VSS (Lübken, 2009).

2.10 Preliminary studies: Hydrolysis experiments with biomass and particulate organic matter

The hydrolysis process was initially investigated by conducting aerobic and anaerobic experiments with activated sludge (AS) and anaerobic sludge (ANS) as biomass and POM as substrate. The objectives were to investigate the hydrolysis of POM in combination with biomass and to identify the hydrolysis products of the POM from municipal wastewater. These experiments served as a basis for the design of the experiments shown in Chapter 3 and Chapter 4 of this thesis.

2.10.1 Preliminary experiments: activated sludge and particulate organic matter

The POM fraction was prepared in accordance to Chapter 2.1. The activated sludge was taken from the return sludge at the WWTP of Neureut, Karlsruhe, Germany (875.000 population equivalents). The activated sludge was filtrated (VWR, Filter: 516 - 0307, particle size retention: 10 - 20 µm) and aerated for 24 h to deplete the major quantity of organic matter. After aeration, TSS and VSS from the activated sludge were measured following the standard methods (APHA et al., 2005). Three experiments were conducted in open air batch reactors

with a working volume of V = 2 L (Table 2-6). The batch reactors were aerated using aquarium pumps (50 L/h). The reactors were kept at room temperature (T = 20 °C). The sampling was done every 4 h during the first 24 h and afterwards every 12 h. The samples were treated according to Chapter 2.5.

Table 2-6: Preliminary aerobic experiments with activated sludge (AS) and particulate organic matter (POM). AS concentration: 3 g/L TSS.

Experiment [n = 3]	**Inoculum**	**Substrate**	**TSS [g/L]**
Exp-a	-	POM	0.25
Exp-b	AS	POM	0.25
Exp-c	AS	-	-

2.10.1.1 Results of preliminary experiments: activated sludge and particulate organic matter

Fig. 2-7 shows the released sCOD and DOC throughout the experimentation. The highest release of organic matter occurred in the experiments with activated sludge alone (Exp-c) and in the experiments with a combination of biomass and POM (Exp-b). The similar results suggest that the respiration of the activated sludge was too high to be separated from the respiration of the wastewater particles. Experiments with only POM (Exp-a) showed a slight release of sCOD and DOC after 36 to 48 h indicating activity of the microorganisms originally attached to the particles.

By reason of the high release of organic matter due to the self-hydrolysis of the activated sludge (Exp-c) and the release of organic matter found in Exp-a, the experiments presented in Chapter 3 were conducted only with POM at a higher concentration to discern changes and with nutrients addition to ensure microbial growth (Chapter 2.2).

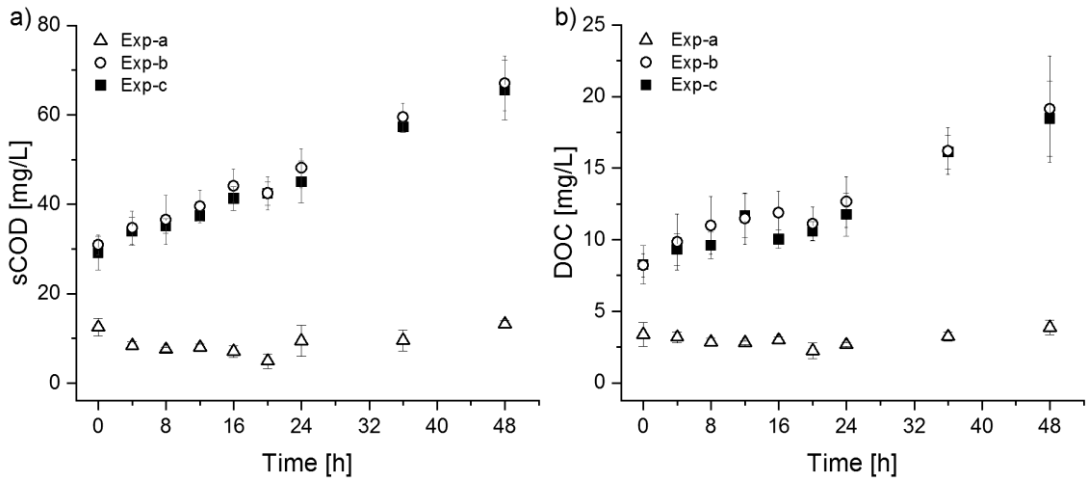

Fig. 2-7: Preliminary experiments: a) sCOD and b) DOC in Exp-a Exp-b and Exp-c. No nutrients addition.

2.10.2 Preliminary experiments: anaerobic sludge and particulate organic matter

Anaerobic sludge (ANS) was taken from the anaerobic digestion tank in the WWTP of Bruchsal, Germany (80,000 population equivalents) and was pre-incubated for four days at T = 30 °C to deplete the major quantity of biodegradable matter that could be attached to the sludge and therefore, to minimize the amount of produced biogas related to self-degradation. The POM was prepared in accordance to Chapter 2.1. TSS and VSS were determined according to the standard methods (APHA et al., 2005). Three experiments were conducted over a period of 10 d. Table 2-7 shows the volume of biomass (ANS) and substrate (POM) used for each experiment with their corresponding initial and final concentration of TSS and VSS. A nutrient solution was added to each reactor to ensure microbial growth: 20 mg/L NH_4^+ - N (NH_4HCO_3), 3 mg/L PO_4^{3-} - P (KH_2PO_4) and 0.5 mg/L Fe^{3+} ($FeCl_3 \cdot 6\,H_2O$). The AMPTS II set-up was used (see Chapter 2.4). The experiments were conducted in duplicate. The stirring units were set to 60 s of stirring time and 60 s of down time at 60 % intensity. The pH was manually maintained between 6.7 and 7.5 for all the experiments. The samples were treated accordingly to Chapter 2.5 and Chapter 2.6. The fractionation of cDOC was done based on the observed changes.

Table 2-7: Volume of biomass (ANS) and substrate (POM) used in Exp-d, Exp-e and Exp-f with their corresponding initial and final concentration of TSS and VSS. Reactor volume = 2 L. Duration of the experiments: 10 d. pH: 6.7 - 7.5.

Experiment [n = 2]	**POM [mL]**	**ANS [mL]**	**$TSS_{initial}$ [g/L]**	**TSS_{final} [g/L]**	**$VSS_{initial}$ [g/L]**	**VSS_{final} [g/L]**	**$VSS_{removal}$ [%]**
Exp-d	1800	0	2.9	1	2.7	0.4	85.2
Exp-e	1400	400	7.9	5.5	6.6	2.6	60.6
Exp-f	0	400	5.7	4.2	4.5	2.0	55.6

2.10.2.1 Results of preliminary experiments: anaerobic sludge and particulate organic matter

The anaerobic hydrolysis process was investigated by observing the release of organic matter, i.e., sCOD, DOC and VFA. The production and utilization of the hydrolysis products (DOC-fractions) was followed by using the SEC with online detectors (Chapter 2.6). The conversion of the intermediate products (VFA) into biogas was recorded with the AMPTS II system (Chapter 2.4).

Fig. 2-8 shows the release of organic matter and biogas during the anaerobic digestion of ANS and POM. Experiments with POM alone (Exp-d) released the largest amount of hydrolysis products (Fig. 2-8a). The release of sCOD, DOC and VFA in Exp-d started within the first day indicating hydrolysis of POM into DOM. The equilibrium between the hydrolysis rate and the utilization rate was reached a t = 4 d (Fig. 2-8a). The biogas production slowly increased from t = 0 to t = 4 d and remained with an approximate value of 20 mL/g VSS_{added} during the rest of the experiment. Although the presence of biogas in Exp-d indicates the existence of methanogenic microorganisms originally attached to the POM, the accumulation of the hydrolysis products is attributed to a small population of the methanogenic microorganisms and its slow growth rate.

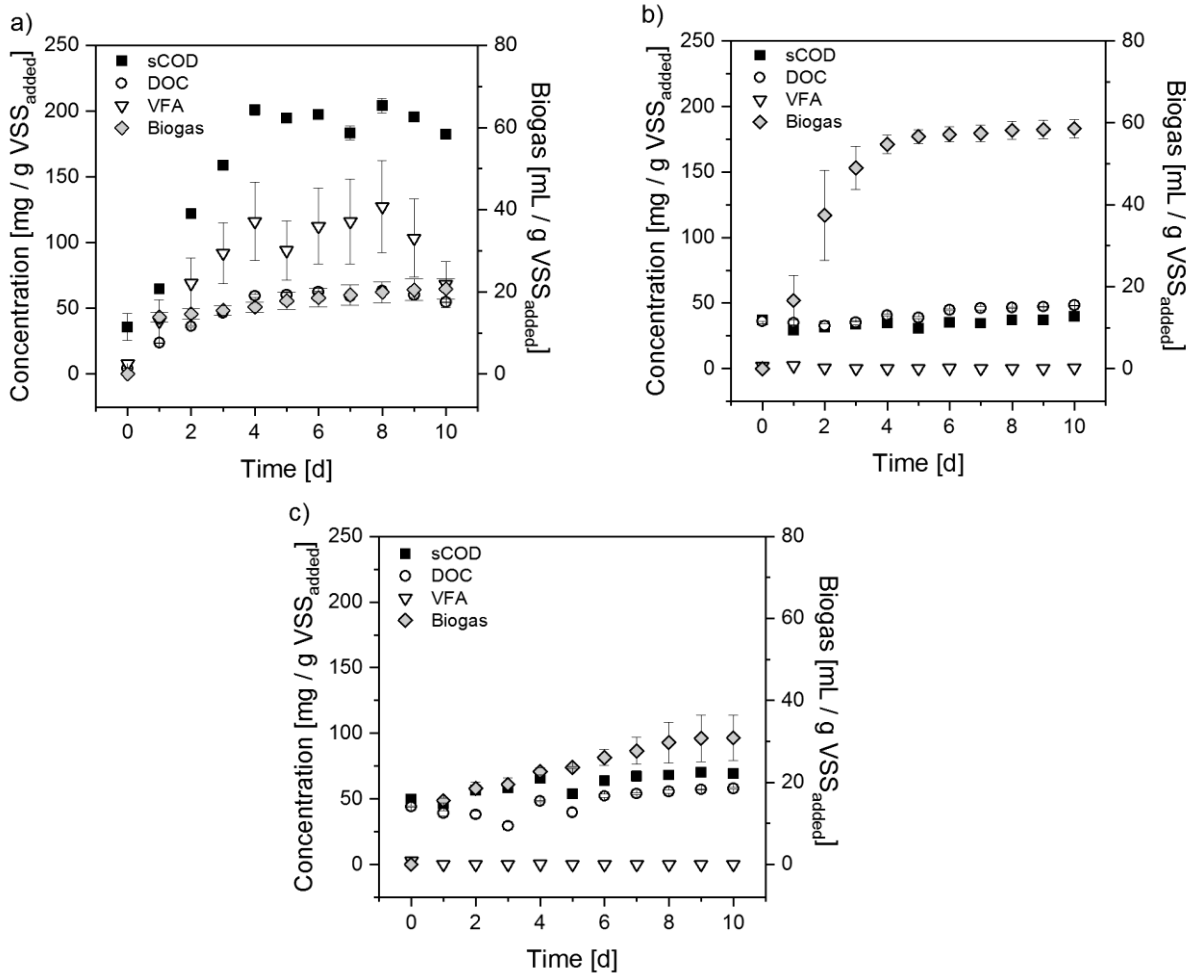

Fig. 2-8: Concentration of organic matter and accumulated biogas. a) Exp-d, b) Exp-e, c) Exp-f.

Exp-e (combination of ANS and POM) and Exp-f (only ANS) produced similar results for the hydrolysis products measured as sCOD, DOC and VFA (Fig. 2-8b-c). It appears that the microorganisms present in the ANS dominated the hydrolysis process. Hydrolysis products were neither accumulated in Exp-e nor Exp-f during the whole experimentation. However, the biogas increased from t = 0 to t = 4 d in both experiments. The combination of POM and ANS in Exp-e produced the highest values of biogas from all the experiments reaching 60 mL/ g VSS. After t = 4 d, no significant changes in the accumulated biogas were observed in Exp-e. Exp-f continuously produced small amounts of biogas during the whole experiment reaching about 30 mL/ g VSS $_{added}$ (Fig. 2-8c). Although methanogenic microorganisms were present in the anaerobic sludge, the lower biogas production in Exp-f compared to Exp-e was attributed to the lack of easily biodegradable organic matter, which was mostly depleted during the pre-incubation period of the anaerobic sludge.

It seems that the initial increase of biogas from t = 0 to t = 4 d, in the three experiments, was the result of the degradation of the easily biodegradable and easily hydrolysable organic matter originally attached to the POM or/and the ANS at the beginning of the experimentation.

SEC with online detection (Chapter 2.6) was used to obtain detailed information of the production and utilization of the hydrolysis products. Fig. 2-9 shows the DOC and UV (254 nm) chromatograms of Exp-d (a-b), Exp-e (c-d) and Exp-f (e-f). Experiments where anaerobic sludge was used (Exp-e and Exp-f) showed formation of products with different nominal MW; four DOC-peaks/fractions were distinguished (Fig. 2-9c-f). In Exp-d, where only POM was used, only one DOC-peak was observed. The single peak observed in Exp-d (Fig. 2-9a), corresponded to low MW compounds, which are related to VFA. The maximum accumulation occurred at t = 8 d (see peak in Fig. 2-9a). The decrease of this peak is related to the utilization of the VFA by the methanogens.

Different from the single peak observed in the experiment with POM (Fig. 2-9a), in all the experiments where ANS was used, broader MW distribution of the products were observed (Fig. 2-9c, e). The combination of ANS and POM in Exp-e produced the same results as the experiments with only ANS in Exp-f (Fig. 2-9c-f). Therefore, it can be assumed that the anaerobic microorganisms originally coupled to the ANS dominated the process and it was not possible to distinguish the effect of the POM on the overall process when the POM was combined with ANS. In addition to the broader MW compounds originated from the ANS (Fig. 2-9c-f), it was also noticed during Exp-e and Exp-f that the formed HMW organic compounds (see first peak in Fig. 2-9c-f) were not totally degraded and intermediate products with a strong UV-response were formed and accumulated during the anaerobic digestion process (see second peak in Fig. 2-9c-f). The recalcitrant organic matter originated from the hydrolysis of ANS, probably contributed to the lower 58 % of VSS removal achieved in the experiments with biomass in comparison to 85 % of VSS removal achieved in the experiments with only POM (see Table 2-7).

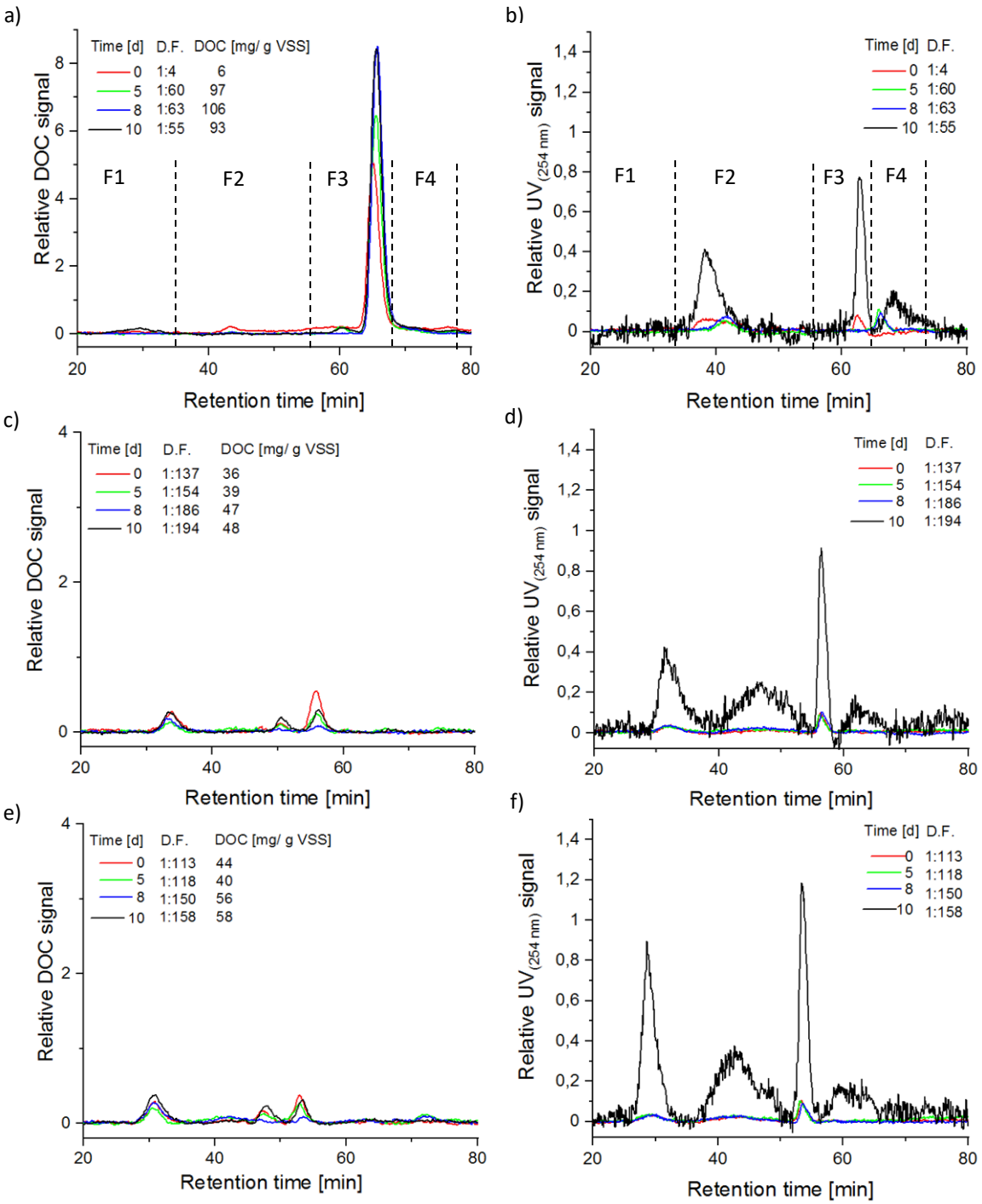

Fig. 2-9: DOC and UV (254 nm) chromatograms of samples from anaerobic experiments with anaerobic sludge (ANS) and particulate organic matter (POM). (a-b): Exp-d; (c-d): Exp-e; (e-f): Exp-f. The baseline and time shift of the detectors were corrected.

Chapter 3: Results of hydrolysis experiments of particulate organic matter from municipal wastewater under aerobic treatment

This Chapter presents the findings published as Alondra Alvarado, Stephanie West, Gudrun Abbt-Braun, Harald Horn. Chemosphere (Alvarado et al., 2021), 263, p, 128329, https://doi.org/10.1016/j.chemosphere.2020.128329. The introduction and material and methods Chapters were incorporated to Chapter 1 and Chapter 2.1 - 2.3, respectively.

3.1 Size exclusion chromatography coupled with online carbon and UV (254 nm) detectors

The formation and biodegradability of the hydrolysis products released by the aerobic treatment of the POM fraction (25 - 250 µm) (see Chapter 2.1) were investigated by means of the SEC-OCD-UVD technique during t = 2 d (Exp1-aer) and t = 13 d (Exp2-aer) by using samples from the aerobic batch reactors (see Chapter 2.1 - 2.3). The data of Exp1-aer showed information during the first 2 d, while Exp2-aer provided a long-term overview (until t = 13 d) of the hydrolysis process mimicking a realistic SRT in an activated sludge process. Fig. 3-1 shows the changes of the cDOC and UV (254 nm) signals in Exp2-aer for t = 0.2, 4 and 13 d.

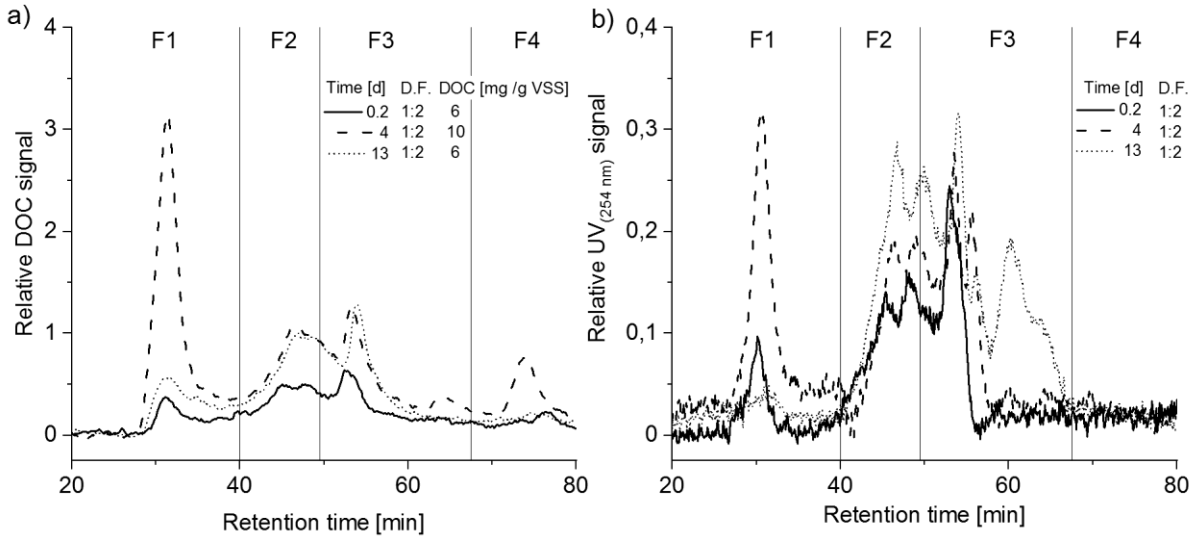

Fig. 3-1: a) Fractionation of DOC and b) fractionation of UV (254 nm) according to its molecular size in Exp2-aer at t = 0.2, 4 (maximum accumulation of fraction F1) and 13 d.

One of the main advantages of the SEC technique is that the whole MW range of the hydrolysis products is reflected in the chromatograms. Therefore, it is possible to follow the production and degradation of the hydrolysis products by observing the changes of the peaks-areas (relative

amount) of the four size fractions through time in Exp2-aer. During the entire process studied, the hydrolysis products (represented as DOC) showed the full range of MW distribution (hydrolysis products with different MW). The relative amount (peaks area) of the four size fractions is changing over the entire time of Exp2-aer as can be seen in. Fig. 3-1.

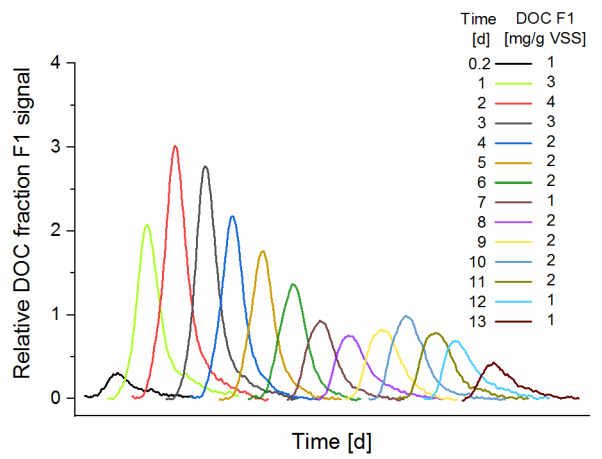

Fig. 3-2: Development of relative DOC fraction F1 during Exp2-aer. Dilution factor of two in all the samples.

The main changes correspond to fraction F1 (Fig. 3-1). The development of the DOC-peak fraction F1 during the whole experiment is shown in Fig. 3-2. Fraction F1 increased significantly from t = 0.2 d to t = 2 d and then gradually decreased until t = 13 d. The accumulation of fraction F1 is a clear indication of the continuous hydrolysis of POM into dissolved high molecular weight (HMW) organic products. The DOC-peaks in F1, F2, and F3 appear in the UV-chromatograms (Fig. 3-1). The UV-signal shows that the organic matter of the different DOC-fractions contain chromophores with conjugated C=C (e.g., aromatic compounds) and C=O double bonds structures (Frimmel and Abbt-Braun, 2011). The UV-absorbing fraction in F3 at t = 60 min was attributed to nitrate, as there is no distinct signal in the cDOC chromatogram. Fig. 3-3 shows the development of the nitrogen-species during the aerobic experiments Exp1-aer and Exp2-aer. It is clearly seen the ammonia oxidation as nitrite and nitrate confirm the increase of nitrate after t = 6 d. NH_4^+ - N was depleted on t = 9 d. However, nitrate was present until the end of the experiment.

Due to interactions of the sample with the material of the chromatographic column, DOC fraction can appear after the permeation limit of the column (permeation limit: t = 72 min). The organic fraction, F4, can be characterized by a hydrophobic or amphiphilic character (Huber and Frimmel, 1994; Müller et al., 2000; Müller and Frimmel, 2002; Perminova et al., 1998;

Specht and Frimmel, 2000). The peak in fraction F4 at = 4 d showed no UV-response and disappears at the end of the experiment (Fig. 3-1).

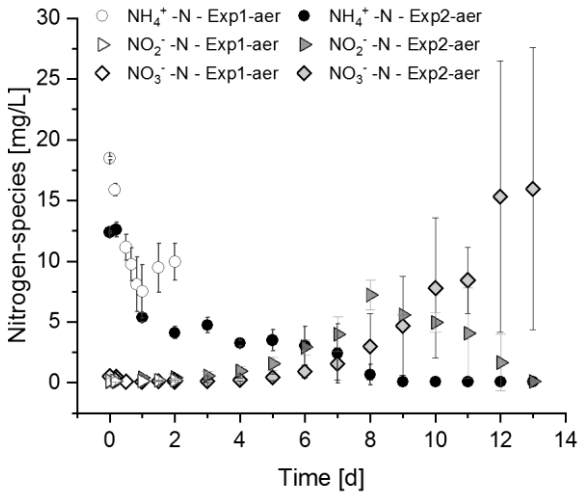

Fig. 3-3: Nitrogen-species behavior though the Exp1-aer and Exp2-aer.

Fig. 3-4 shows the time series of the DOC concentration and the relative amount of UV of each fraction in Exp1-aer and Exp2-aer. The DOC concentration of the HMW fraction (F1: 20,000 - $2 \cdot 10^6$ g/mol) increased during the first three days. However, the concentration of maximum 2.5 mg/L on t = 3 d is still low compared to the huge amount of initial TSS, i.e., 1 g/L. After 3 d, F1 continuously decreased until t = 13 d (Fig. 3-4a). The relative amount of UV of fraction F1 ($F1_{UV}$) (Fig. 3-4a) showed a similar trend to F1 (Fig. 3-4a), although the differences are not very pronounced. The main drop of $F1_{UV}$ started after t = 4 d, and reached negligible values on t = 6 d. This indicates that 2 d were needed by the bacteria to develop the necessary enzymes to hydrolyze UV-absorbing substances into smaller molecules in parallel to the biodegradation of fraction F1. This suggests a similarity in the composition of the organic matter in fraction F1 (Fig. 3-5). After 13 d of aeration, the dissolved organic carbon represented by F1 was degraded.

The results do match the findings of Benneouala et al. (2017), who studied the role of activated sludge on the hydrolysis of the particulate settleable solids by using batch reactors and calculated oxygen utilization rates (OUR). They found that the degradation time of large particles was at least 10 d. Unfortunately, the size of those particles was not shown.

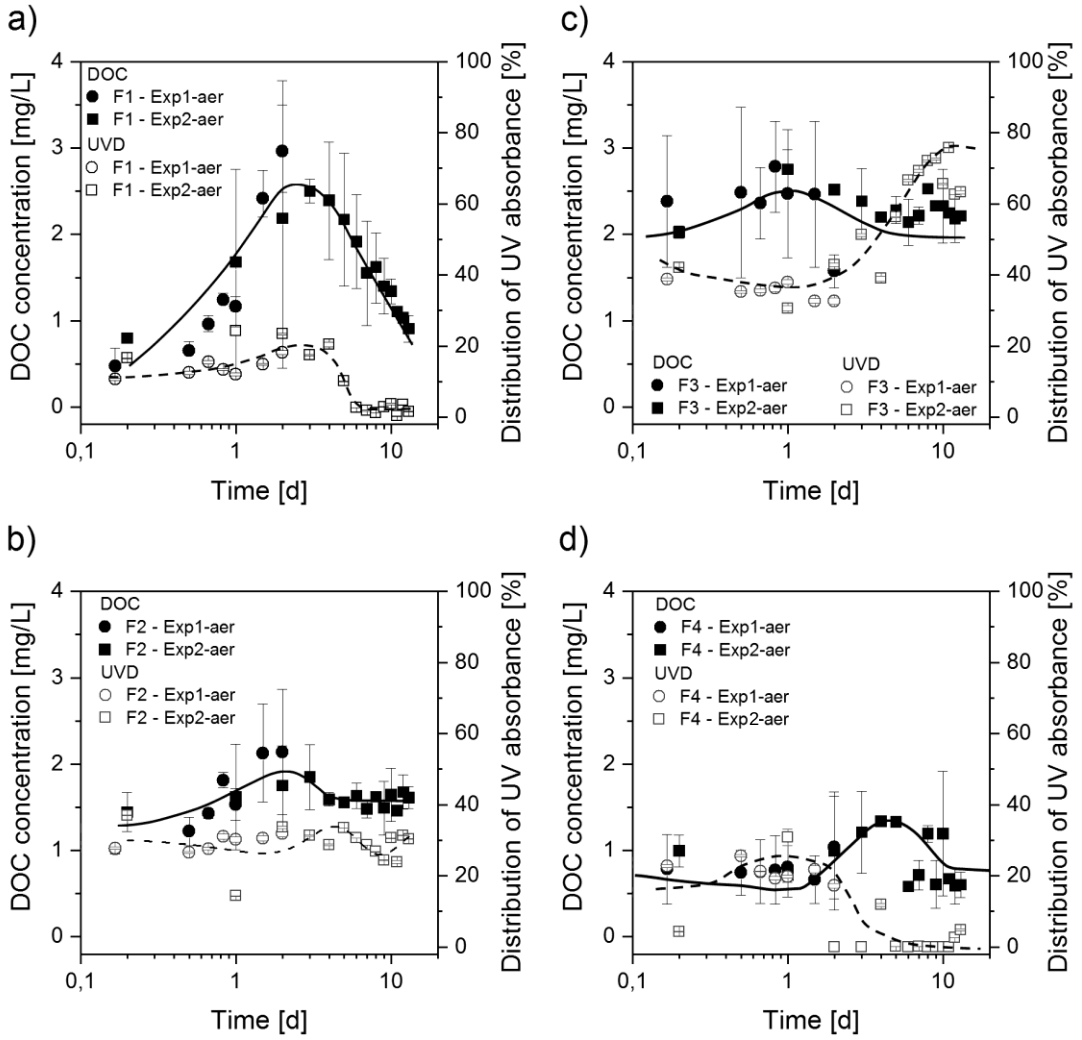

Fig. 3-4: Calculated DOC concentration [mg/L] and relative amount distribution of UV (254 nm) absorbance [%] for Exp1-aer (n = 3) and Exp2-aer (n = 2). a) fraction 1 (F1); b) fraction 2 (F2), c) fraction 3 (F3) and d) fraction 4 (F4).

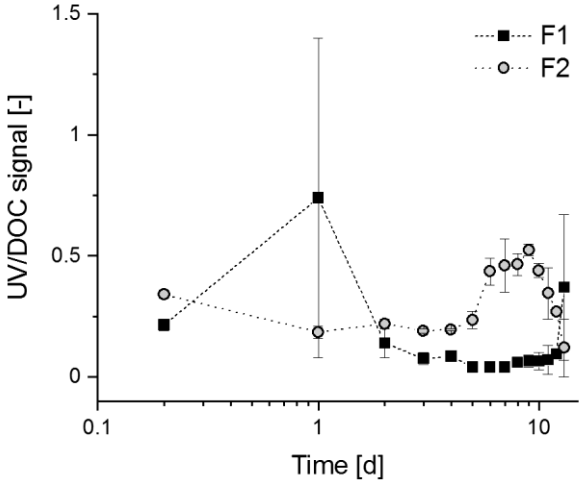

Fig. 3-5: UV/DOC signal of fraction 1 (F1) and fraction 2 (F2) during Exp2-aer. The signals were stablished at the highest point of the peaks.

Intermediate MW organic material, fraction F2, (nominal MW: 1550 - 20,000 g/mol) accumulated within the first 3 d, and then slightly decreased at t = 4 d, remaining stable until the end of the experiment (Fig. 3-4b). No major changes in the relative amount of UV of fraction F2 ($F2_{UV}$) were observed. F2 was mainly in the range of 25 - 35 % during the experimentation. The compounds in F2 show a higher amount of UV-absorbing compounds compared to F1 (Fig. 3-5). This could be attributed to an incomplete biodegradation of refractory compounds during the aerobic treatment (Luo et al., 2014; Metcalf and Eddy, 2014; Tran et al., 2015). Toilet paper (cellulose) is the main component of POM in raw wastewater (Ruiken et al., 2013). Cellulose consists of chains of glucose linked by strong hydrogen bonds forming microfibrils, which are very recalcitrant to degradation (Dyk and Pletschke, 2012; Himmel et al., 2007). According to Dyk and Pletschke (2012), the cellulose is embedded in a matrix of hemicellulose, pectin and lignin. The same authors stated that lignin is the most important factor limiting enzymatic hydrolysis by cellulolytic and hemicellulolytic enzymes. Cellulase enzymes function one to two order of magnitude slower than other polysaccharidases (Himmel et al., 2007). Furthermore, Confer and Logan (1997) worked with products of bovine serum albumin and found that the major part of the recalcitrant protein was intermediate molecular weight material (2000 - 10,000 g/mol). This is especially interesting due to about 50 % of biomass dry weight is protein (Metcalf and Eddy, 2014). In addition, amyloids originated from proteins, are abundant in bacterial biofilms, and are resistant to degradation by proteases (Schlafer and Meyer, 2017). Jin et al. (2011) studied the biological treated sewage effluent from eight different WWTPs by using high performance liquid chromatography-SEC. The authors found an increase of compounds with a nominal MW > 10,000 g/mol. They attributed these compounds as SMP or EPS such as polysaccharides and proteins.

Previous investigations concluded that easily biodegradable organic matter, i.e., organic matter with a MW < 1000 g/mol, can be assimilated directly by bacteria (Confer and Logan, 1998; Kommedal, 2003; Morgenroth et al., 2002; Sophonsiri and Morgenroth, 2004). Fraction F3 had a nominal MW of 100 - 1550 g/mol. The low MW fraction F3 had its maximum accumulation on the first day (Fig. 3-4c). Afterwards, F3 decreased until t = 4 d and then remained stable. Probably up to this fraction on the DOC was directly used for biomass growth. The relative amount of the UV-absorbing organic matter in F3 ($F3_{UV}$) is quite stable during the first three days. The sharp increase of $F3_{UV}$ observed after this time (Fig. 3-4c) was related to a formation of nitrite and nitrate due to nitrification (Fig. 3-3). The increase of the first UV-peak in F3 showed in Fig. 3-1, together with the decrease of the UV-signal of F1 during this time, suggest

that the recalcitrant material could be originated from the hydrolysis of F1 due to incomplete biodegradation of refractory compounds in the aerobic treatment (Luo et al., 2014; Metcalf and Eddy, 2014; Tran et al., 2015).

The nominal MW of fraction F4 was < 100 g/mol, F4 remained stable during the first 1.5 d. Afterwards an increase was observed until t = 4 d (Fig. 3-4d) probably due to the degradation of the higher MW fractions. It seems that during this time the hydrolysis rate was faster than the utilization rate. The relative UV-absorbance in F4 ($F4_{UV}$) remained stable during the first 2 days in Exp1-aer, while in Exp2-aer $F4_{UV}$ increased on the first day and reached negligible values from the second day until the end of the experiment (Fig. 3-4d). The latter is in accordance with Huber et al. (2011b) who found no or little UV-response corresponding to the MW of this fraction (F4) that they called low molecular weight neutrals. The reader must be aware that F4 was affected by interactions of the organic matter with the material of the column (see Chapter 1.4.4).

3.2 Sum parameters from batch reactor and respirometer

The release of hydrolysis products during the aerobic treatment of POM was additionally investigated on the batch-scale by measuring the sCOD and DOC. Fig. 3-6 illustrates the development of the released hydrolysis products (sCOD and DOC) in the batch reactors for the short (Exp1-aer and Exp2aer: t = 0.2 d until t = 2 d) and the long-term experiment (Exp2-aer: t = 0.2 d until t = 13 d). Short-term experiments can be used to show the accumulation of organic compounds, whereas the long-term experiments can follow the degradation of the hydrolysis products. Previous studies have shown that around 10 d are needed to degrade POM (Benneouala et al., 2017). In Fig. 3-6 the accumulated BOD obtained from the respirometric experiments is shown. An increase of sCOD and DOC during the first 3 d is observed, suggesting that during this time the hydrolysis rate (production) was faster than the utilization rate. Starting at t = 4 d, the sCOD and DOC gradually decreased until the end of the experimentation. The behavior is more evident for the sCOD. This probably occurred due to the constant biodegradation of the hydrolysis products by the microorganisms. The BOD concentration increased continuously, reaching a maximum value of 800 mg/L O_2, suggesting a nearly complete degradation of the particulate material (Table 3-1). Due to the addition of ATU, the oxygen consumption was related only to the utilization of the organic carbon (originating from POM).

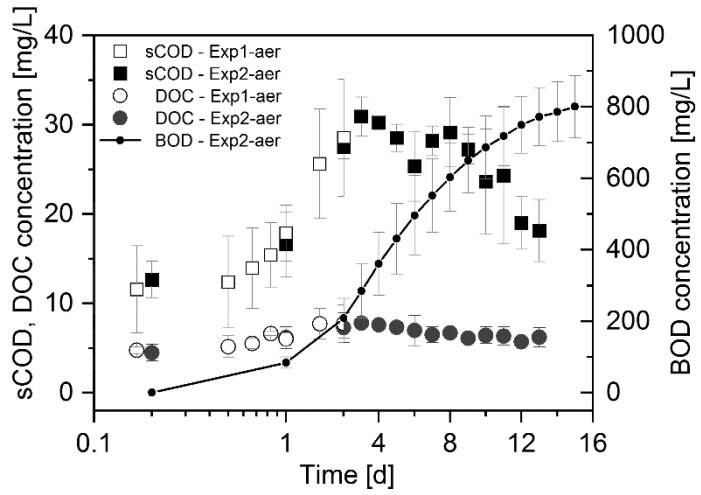

Fig. 3-6: sCOD and DOC concentration (Exp1-aer and Exp2-aer). BOD concentration (Exp2-aer). It has to mentioned that the sCOD and DOC are measured in the aerobic batch reactor and BOD is measured with the respirometer (nitrification was inhibited). Time in logarithmic scale until day 2 (Exp1-aer), afterwards in linear scale (Exp2-aer).

Fig. 3-7a shows values of VSS measured at t = 0, t = 2 d and t = 13 d. The VSS removal curve was fitted by a first order reaction kinetics. Fig. 3-7b shows the OUR calculated with equation (2-1) (see Chapter 2.3) together with the concentration of F1 in Exp2-aer. As shown previously in Fig. 3-2 and Fig. 3-4a fraction F1 is the one which seems to be the best indicator for the hydrolysis process. The maximum OUR value was 124 mg O_2/L · d on t = 2 d. During this period, the maximum microbial activity was observed. According to Insel et al. (2002), the shape of the OUR curve after the first plateau is mainly governed by the hydrolysis rate.

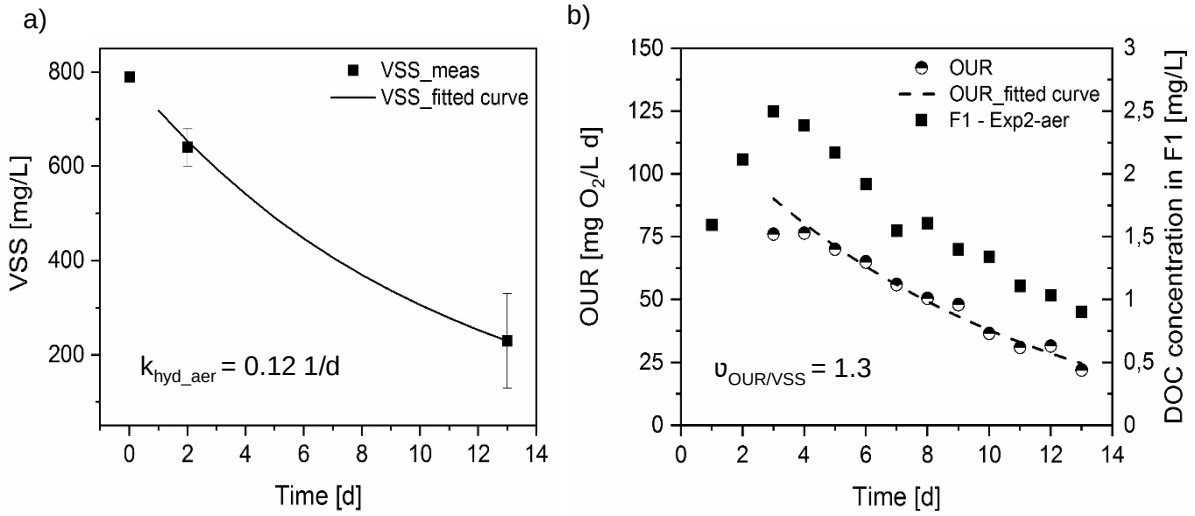

Fig. 3-7: a) VSS-fitted curve and measured VSS at t = 0, t = 2 d and t = 13 d. b) OUR, OUR-fitted curve and concentration of DOC fraction F1. DOC and VSS were measured in the aerobic batch reactor, and BOD was measured with the respirometer (nitrification was inhibited).

The fitted curve of OUR (Fig. 3-7b) was coupled to the VSS (Fig. 3-7a) according to equation (2-2) (see Chapter 2.3). The hydrolysis reaction constant k_{hyd_aer} was found to be 0.12 1/d and the stoichiometric coefficient $\upsilon_{OUR/VSS}$ for oxygen used per VSS degraded was fitted to 1.3. The fitted curve of OUR was set up from the third day when the hydrolysis and consumption rate reached the equilibrium (Fig. 3-7a). Li, Wu et al. (2019) investigated the effects of SRT and microbial community in the degradation kinetics of toilet paper fiber by using sequencing-batch activated sludge systems. The authors published hydrolysis rate constants for toilet paper in the range 0.025 to 0.034 1/d for SRT of 20 d and 0.116 to 0.137 1/d for a SRT of 40 d. The authors explained the higher rate constants with a better adaptation of older sludge to hydrolyze cellulose and hemicellulose fibers. The development of fraction F1 shows that the adaptation process in the system was more or less finished after 2 to 3 d.

Fig. 3-7 clearly shows that most of the hydrolysis products cannot be found in the liquid phase (see also Chapter 1.2 and Chapter 1.4.1). Although it is not possible to know an exact stoichiometry involved in the biological oxidation of wastewater (Metcalf and Eddy, 2014), the COD of the DOC can be determined by writing a balanced stoichiometric reaction for the oxidation of DOC to carbon dioxide as follows:

$$(CH_2O)_n + n\ O_2 \rightarrow n\ CO_2 + n\ H_2O \qquad (3\text{-}1)$$

Therefore,

$$\frac{\Delta\ O_2}{\Delta\ \mathrm{DOC}} = \frac{32\ \frac{\mathrm{g}}{\mathrm{mole}}}{12\ \frac{\mathrm{g}}{\mathrm{mole}}} \approx 2.5 \frac{\mathrm{g}\ O_2}{\mathrm{g\ DOC\ oxidized}} \qquad (3\text{-}2)$$

Fraction F1 represents a newly formed hydrolysis product, the maximum concentration of 2.5 mg/L F1 at t = 3 d is small compared to the 100 mg/(L · d) OUR at this time. The latter value can be used to calculate the stoichiometric comparable amount of organic carbon (3-2), which was approximately 40 mg/(L · d).

It is assumed that most of the hydrolyzed organic matter will not leave the aggregated bacteria fixed to the particulate material. The latter is supported by the CLSM images (see Chapter 3.3), where it is observed that most of the microorganisms are attached to the particles. Therefore, the degradation occurs at the particles surface and/or at the vicinity of the particles. Different investigations support the findings (see Chapter 1.2 and Chapter 1.4.1). Goel et al. (1998) identified that only 4 % of the hydrolytic enzyme activity in activated sludge is located at the

bulk phase, indicating an entrapment of microorganisms in the extra-cellular polymers. Likewise, Guellil et al. (2001) studied extracellular enzymes extracted from activated sludge flocs and found that glycolytic activity was mainly related to wastewater organic colloids. Li and Chrost (2006) also revealed that the enzyme activity is cell-associated and that the EPS matrix of the flocs immobilize the microorganisms within the matrix.

The characteristics of the mixed liquor (wastewater particles plus tap water) at the beginning and end of Exp1-aer and Exp2-aer are presented in Table 3-1. The VSS removal for Exp1-aer was 19 % and 69 % for Exp2-aer (Table 3-1).

Table 3-1: Wastewater standard parameters in Exp1-aer at day 0.2 and 2 and in Exp2-aer at t = 0.2 and 13 d. All parameters beside BOD have been measured in the aerobic batch reactor, BOD has been measured in the respirometer.

Parameters	**Exp1-aer [n = 3]**		**Exp2-aer [n = 2]**	
[mg/L]	**Start**	**End**	**Start**	**End**
TSS	1000	790 ± 40	1000	350 ± 130
VSS	790	640 ± 40	790	230 ± 100
sCOD	12 ± 5	29 ± 7	14 ± 2	16 ± 2
DOC	5 ± 1	8 ± 2	5 ± 1	5 ± 1
Aerobic respiration BOD	0	209 ± 56	0	772 ± 80
dTN	19 ± 1	14 ± 3	14 ± 1	19 ± 3
NH_4^+- N	16 ± 1	10 ± 2	13 ± 1	0 ± 0
NO_3^- - N	0.3 ± 0.2	0.2 ± 0.1	0.5 ± 0.1	16 ± 12
PO_4^{3-} - P	2 ± 1	0.7 ± 0.7	0.4 ± 0.2	0.3 ± 0.1

3.3 Confocal laser scanning microscopy (CLSM)

In addition to the chemical analysis of the hydrolysis products in the aerobic batch reactor (here measured as sCOD and the DOC-fractions: F1, F2, F3, and F4), the CLSM can be used to partly quantify the amount of bacteria, which develop during the experiment. Important is, to keep in mind, that Benneouala et al. (2017) could show that activated sludge added as inoculum does not significantly influence the hydrolysis rate. In this work, the development of the initial amount of bacteria attached to the particles and its growth dynamics together with the EPS production during hydrolysis was visualized using CLSM.

Fig. 3-8 shows the maximum intensity projections of the CLSM stacks in Exp2-aer. A decrement in the particle size over time, corresponding to the hydrolysis process can be observed. Small agglomerations of bacteria were noticed at t = 0 (Fig. 3-8a). This was directly related to the bacteria originally attached to the particles at the beginning of the experiment. After two days of aeration (Fig. 3-8b), an increase of the bacteria and EPS-glycoconjugates signal was observed, which is supported by the increase of fraction F1 during this time period together with the high OUR. Cadoret et al. (2002) found that the higher MW of the substrate the more hydrolytic activity is associated to the EPS.

Beside the detection of bacteria (nucleic acid signal, NA) the glycoconjugate signal can be used to count the amount of EPS (Staudt et al., 2003). The result corresponds to the conceptual model offered by Vavilin et al. (2008), which formulates that the hydrolytic bacteria in the liquid medium colonize the surface of the particles, producing enzymes to hydrolyze the organic matter and in such a manner being able to assimilate the hydrolysis products released by the enzymatic reaction. Likewise, Confer and Logan (1998, 1997) explained that hydrolysis is a stepwise process in which the macromolecules diffuse to the surface of the cells where they are hydrolyzed and the hydrolytic fragments are released to the bulk solution or to other cells, repeating the process until the hydrolytic fragments are small enough to be directly assimilated into the cells (see also Chapter 1.2).

A slight reduction of the bacteria population together with a parallel increase of EPS can be observed at t = 7 d (Fig. 3-8c) and t = 13 d (Fig. 3-8d) compared to t = 2 d (Fig. 3-8b). Consequently, a decrease in the NA/EPS ratio can be calculated (Fig. 3-9a-b). However, there is a certain risk that more and more smaller aggregates over time lead to a loss in signal intensity for the detached bacteria.

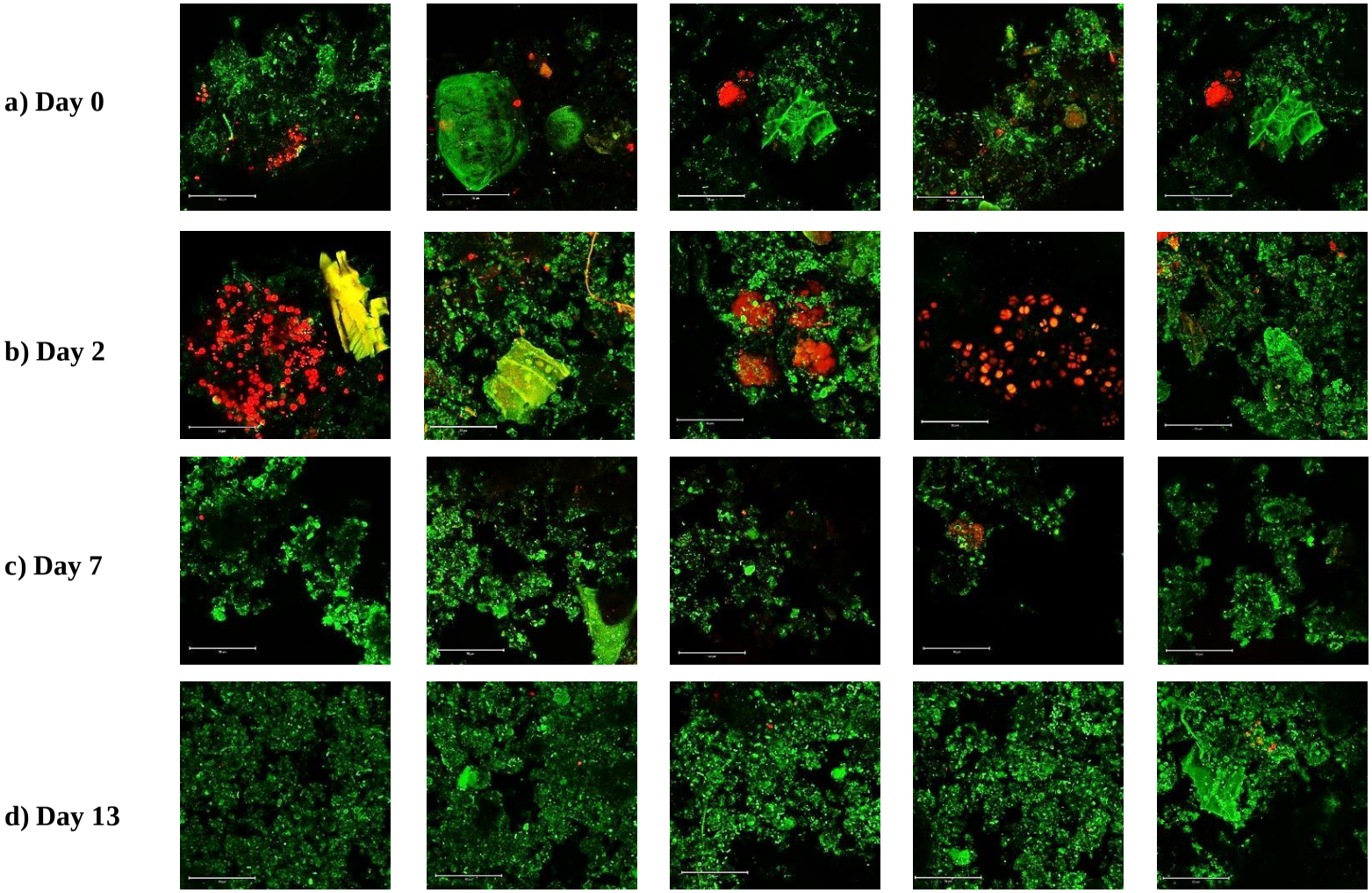

Fig. 3-8: Maximum intensity projections of CLSM images acquired to visualize the hydrolysis process and the bacteria population during Exp2-aer. Stacks at t = 0, 2, 7 and 13 d. Total stacks per day = 16. Color: red-nucleic acids; green-EPS glycoconjugates. Scale bar = 40 µm.

Rusanowska et al. (2019) studied the effect of the organic load on aerobic granule diameters and EPS composition in granules with different sizes. They found that the amount of loosely bound EPS increased as the granule diameters decreased. It is known that EPS can be produced during the growth, substrate utilization and decay processes involved in the aerobic treatment (Henze et al., 1987; Ramdani et al., 2012).

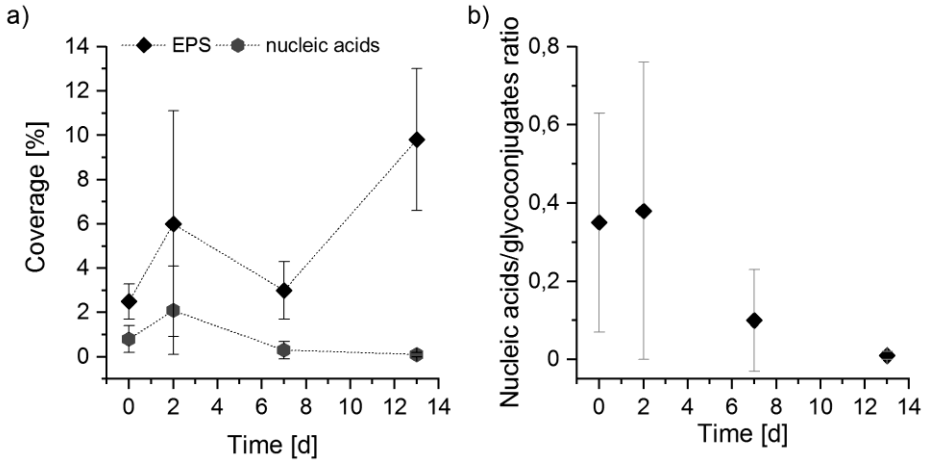

Fig. 3-9: Coverage for nucleic acid (NA) and EPS glycoconjugates signals (a) and ratio of both (b) at t = 0, 2, 7 and 13 d in Exp2-aer.

3.4 Conclusions of hydrolysis experiments of particulate organic matter from municipal wastewater under aerobic treatment

Based on the obtained results, more detailed insight into the aerobic hydrolysis process of particulate organic matter (POM) originated from municipal wastewater was gained by combining two reactor systems with comparable conditions, i.e., an aerobic batch reactor and a respirometer. The conversion of POM into DOM was detected through measurements of sCOD and DOC during the entire experiment. By means of size exclusion chromatography coupled with online carbon and UV detectors (SEC-OCD-UV), it was possible to separate the released hydrolysis products into four molecular weight organic fractions of DOC (F1 through F4) in the aerobic batch reactor. These DOC-fractions were evaluated according to their biodegradability during the aerobic treatment of POM. The lower molecular weight fractions, i.e., F4 and F3, were recognized as easily biodegradable organic matter and it was determined that these two organic fractions were used for microbial growth. F2 was identified as the intermediate MW fraction, which mainly consisted of a more refractory type of organic matter by reason of an incomplete biodegradation of the organic matter during the aerobic treatment. F1, i.e., high molecular weight (HMW) organic matter, was found to be the most representative

fraction for the aerobic hydrolysis process. The occurrence of HMW organic matter produced during the hydrolysis of POM within the first three days of aerobic treatment indicated that during this time, the hydrolysis rate was faster than the utilization rate. The respirometer, operated in parallel, provided the oxygen consumption of the active bacteria. According to the oxygen utilization rate (OUR) evidence, the maximum microbial activity occurred on the second day. Supporting the data, the growth dynamics of bacteria originally associated to wastewater particles was visualized during the hydrolysis of POM by using the CLSM technique. Maximum intensity projection images showed that hydrolysis takes place on the surface of the wastewater particles and that the maximum bacteria activity occurred on the second day. Afterwards, the bacteria population decreased by reason of substrate depletion.

Comparing the OUR together with the released DOC it was concluded that most of the hydrolysis products were directly consumed by bacteria. Only within the first three days, the largest size fraction, i.e., HMW organic compounds, accumulated in the liquid phase indicating that bacteria need a certain time to provide the enzymatic pathways for degradation of this DOC-fraction. The hydrolysis of these HMW organic compounds was identified as the limiting factor of hydrolysis. Most of the HMW organic fraction was degraded after 13 d; the non-biodegradable organic matter was associated to refractory compounds resulted from the incomplete biodegradation during the aerobic treatment.

Chapter 4: Results of anaerobic digestion of particulate organic matter originated from municipal wastewater

4.1 Molecular weight distribution of the hydrolysis products released during the anaerobic digestion of particulate organic matter from municipal wastewater

This Chapter highlights the nominal MW distribution of the hydrolysis products released during the anaerobic digestion of POM originated from municipal wastewater. Anaerobic digestion experiments were conducted in batch reactors at a constant temperature of 39 °C and at optimal pH conditions for hydrolytic and acidogenic bacteria, i.e., pH 6 ± 0.2 in experiment 1: Exp1-ana and at optimal pH conditions for acetogenic and methanogenic microorganisms, i.e., pH 7.0 ± 0.2 in experiment 2: Exp2-ana (Chapter 2.4). The SEC-OCD-UV technique (Chapter 2.6) was used to study the biodegradability of the released DOC-fractions (F1 through F4) produced in both experiments.

The chromatographic results presented in Fig. 4-1 indicated that during the entire studied time, most of the hydrolysis products had a nominal MW distribution between 150 - 1550 g/mol corresponding to the DOC fraction F3 in Exp1-ana and Exp2-ana (see fractionation of DOC in Table 2-5, Chapter 2.6). The time resolved development of the main fraction F3 is shown in Fig. 4-2. Clearly the quick increase within the first days can be seen. F3 mainly refers to VFA, which seems to be degraded after 2 - 3 d. Fig. 4-1 shows on the other hand that a minor formation of other hydrolysis products with a different MW range than F3 were produced. Even though, strong UV-absorbance was observed for fraction F1 in Exp1-ana and fractions F1 and F2 in Exp2-ana indicating the presence of C=O double bonds or chromophores with conjugated C=C (e.g., aromatic compounds) (Frimmel and Abbt-Braun, 2011). Kuo and Parkin (1996) studied the production of SMP during the anaerobic treatment at pH of 7.0 ± 0.5 by using ultrafiltration. The authors found that the MW distribution of the SMP was bimodal, the first MW range was < 1000 g/mol and the second MW range was > 10,000 g/mol.

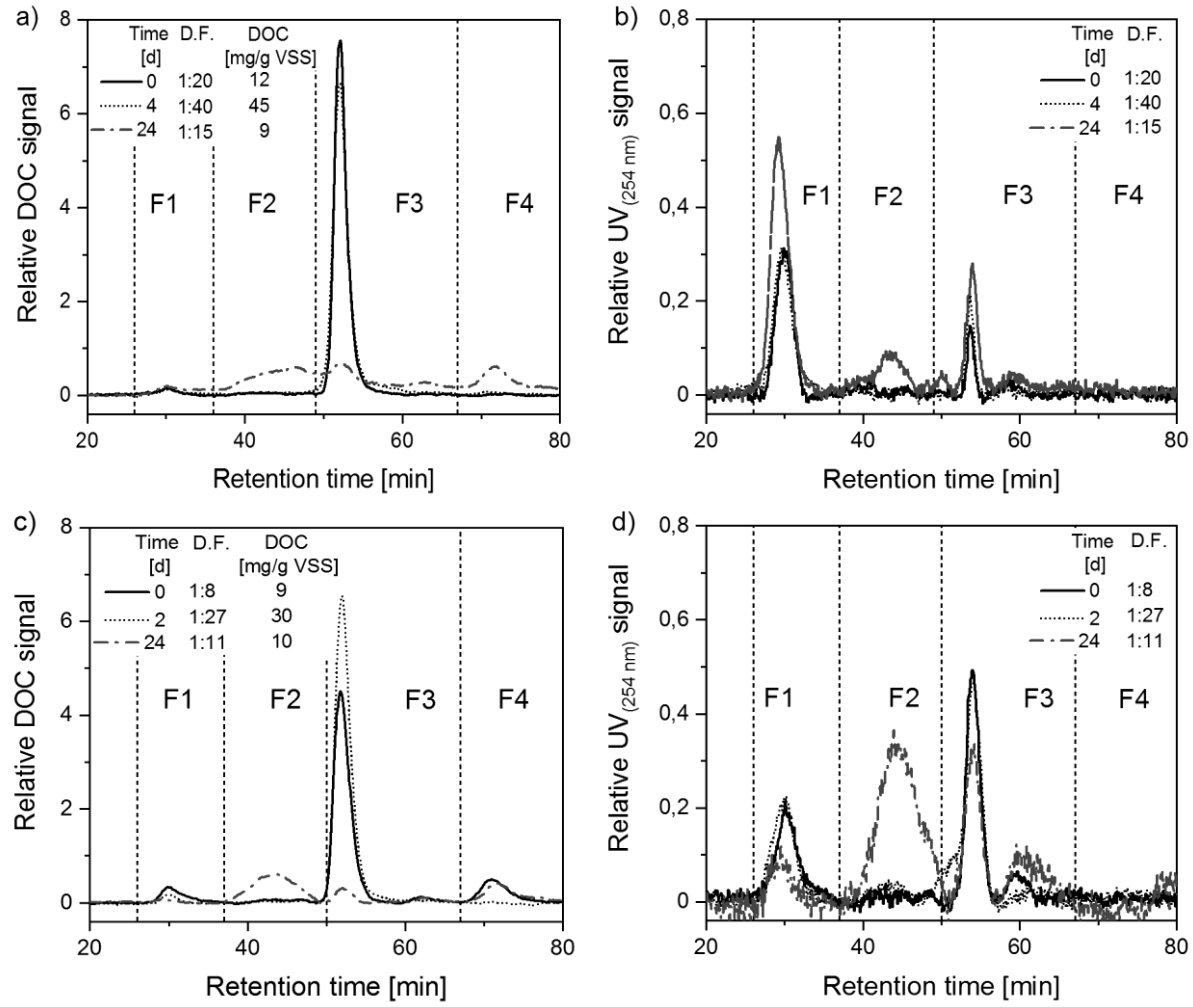

Fig. 4-1: Fractionation of DOC and UV (254 nm) according to its molecular size in Exp1-ana (pH = 6.0 ± 0.2) (a-b) at t = 0, t = 4 d (maximum accumulation of fraction F3) and t = 24 d; and in Exp2-ana (pH = 7.0 ± 0.2) (c-d) at t = 0, t = 2 d (maximum accumulation of fraction F3) and t = 24 d. The baseline and time shift of the detectors were corrected.

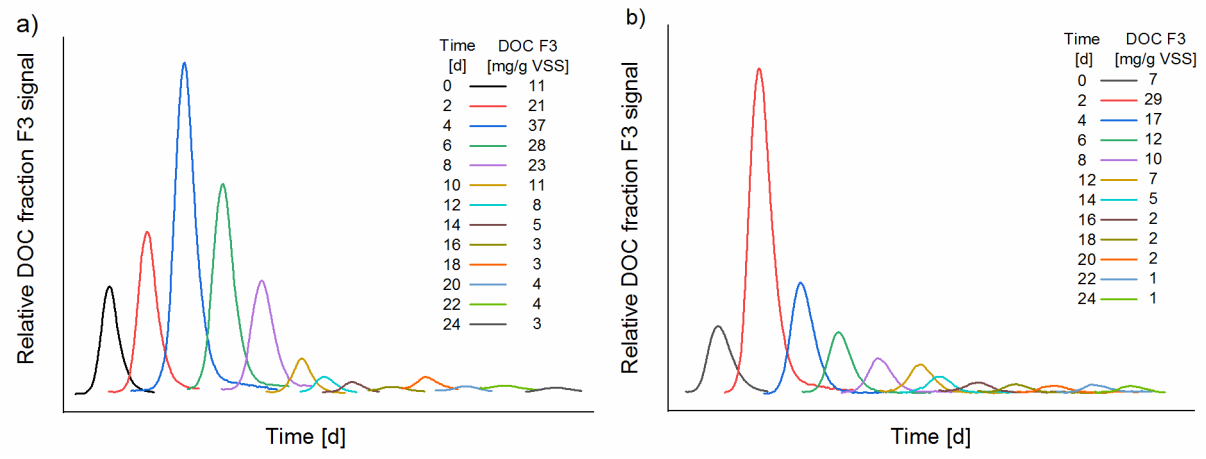

Fig. 4-2: Development of the relative DOC fraction F3 in Exp1-ana (pH 6 ± 0.2) and Exp2-ana (pH 7 ± 0.2). The dilution factor of all the samples had to be adopted.

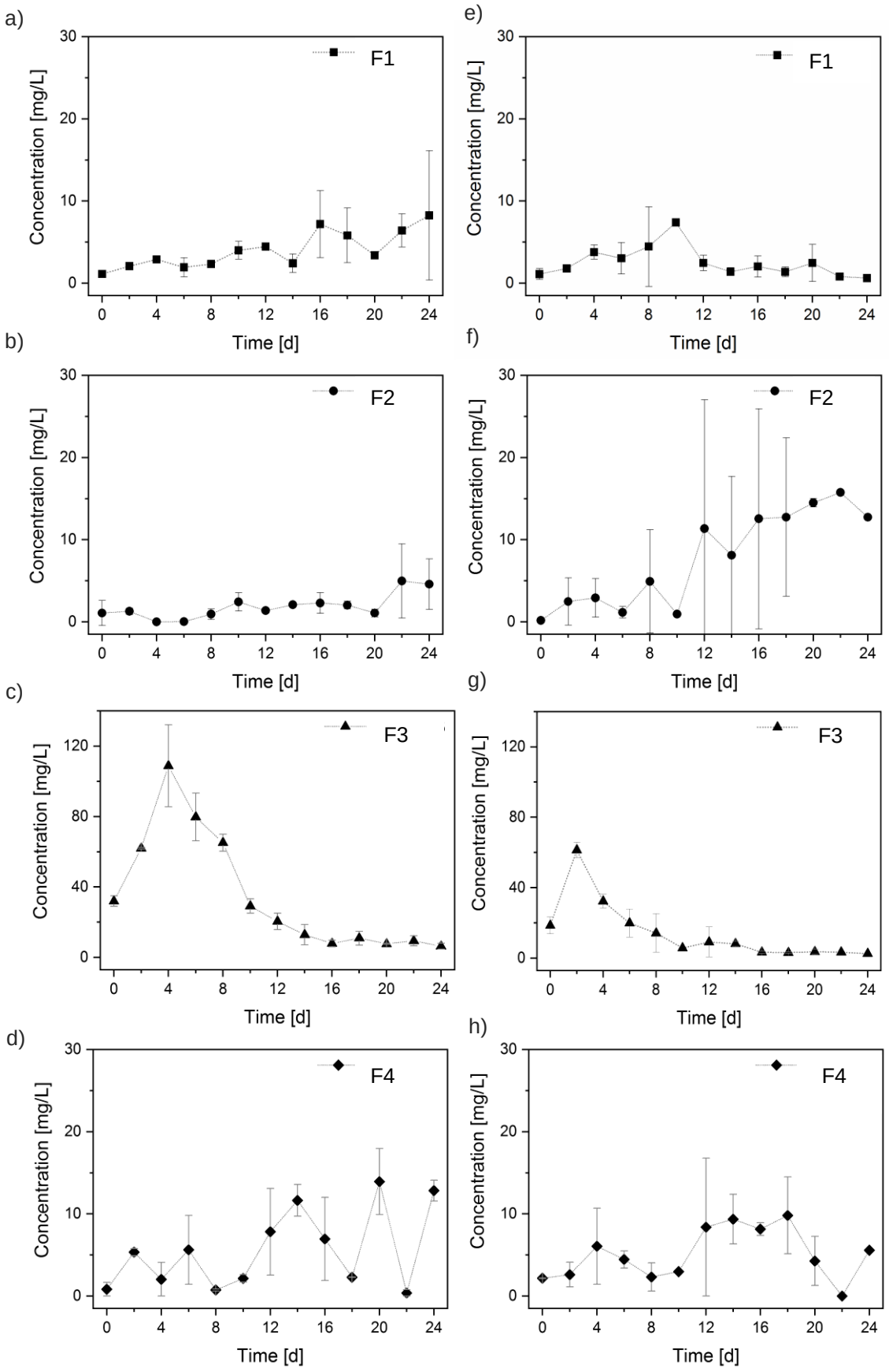

Fig. 4-3: Calculated DOC concentration [mg/L] in Exp1-ana (a-d) (n = 2) and Exp2-ana (e-h) (n = 2); fraction 1 (F1); fraction 2 (F2), fraction 3 (F3) and fraction 4 (F4).

Fig. 4-3 illustrates the time series of the DOC concentrations of the four MW fractions. The HMW organic fraction (F1) had a nominal MW distribution of 20,000 - $2 \cdot 10^6$ g/mol. Because of the persistence of fraction F1 throughout the experimentation, fraction F1 was related to non-biodegradable organic matter. The concentration of fraction F1 remained with values lower than 10 mg/L in both experiments (Fig. 4-3 a, e), while the strong amount of UV of fraction F1 ($F1_{UV}$) indicated the presence of double bond or aromatic structures, which were only to some extent degraded during 24 d of anaerobic treatment (Fig. 4-1b, d).

Intermediate MW organic matter, fraction F2, had a nominal MW between 1550 - 20,000 g/mol. Exp1-ana (pH 6 ± 0.2) showed no significant production of F2 and no UV-response of fraction F2 ($F2_{UV}$). However, in Exp2-ana (pH 7 ± 0.2) a strong increase of F2 was observed at t > 12 d (Fig. 4-3f) as well as an increase of $F2_{UV}$ (Fig. 4-1d) at the same time. The results match the findings of Kuo and Parkin (1996), who worked with a pH of 7.0 ± 0.5 and found that the concentration of SMPs with a nominal MW > 10,000 g/mol increased together with the SRT. Likewise, Jin et al. (2011) used high performance liquid chromatography SEC with a series-connected ultraviolet (UV) and Fluorescence (FL) detectors to characterize the effluent of eight different pilot WWTPs. The authors used sodium Polystyrene Sulfonates (PSS, Fluka) with a molecular weight of 210, 1400, 3400, 13,000, 32,000 g/mol as standards. The authors found an increase in compounds with a MW of 1700 g/mol; the fraction was related to humic-like substances. The same authors also found an increase of the MW fraction > 10,000 g/mol, which was related to SMPs or EPS formation. It seems that at optimal pH conditions for the hydrolytic bacteria (i.e., Exp1-ana: pH of 6 ± 0.2) there was no significant formation of fraction F2 (refractory organic matter) (Fig. 4-1b and Fig. 4-3b), while at optimal pH conditions for the methanogenic group (i.e., Exp2-ana: pH of 7 ± 0.2), refractory organic matter was produced. According to Xiao et al., 2020, the inert fraction of humic substances interacts with biopolymers forming granular aggregates, which decrease the active sites for enzymatic activity leading to inhibition of hydrolysis.

Fraction F3 had a nominal MW of 150 - 1550 g/mol. This is the most representative fraction of hydrolysis products formed during the hydrolysis of POM from municipal wastewater and treated under anaerobic conditions (Fig. 4-2). The DOC concentration of the low MW fraction F3 reached a maximum concentration of 108 mg/L at t = 4 d in Exp1-ana and 62 mg/L at t = 2 d in Exp2-ana (Fig. 4e, f). Afterwards, a continuous decrease of F3 was observed in both experiments (Fig. 4-2). The decrease of DOC probably occurred due to a further conversion of the organic matter into smaller MW compounds, which were probably used as fast as they were

produced. The UV-absorption of F3 ($F3_{UV}$) goes along with fraction F3 indicating a similar molecular composition (Fig. 4-1). It is recognized that low MW acids are easily removed by biological processes (González et al., 2013). Jin et al., (2011) found for several pilot WWTPs a decrease in the MW fraction of 1000 g/mol. They related the decrease with the sludge age, the longer the SRT the higher degradation obtained. They based their assumptions on specific UV-absorbance (SUVA) comparisons. However, the differences in their comparisons were overemphasized (i.e., SBR 1, SRT: 10 d, SUVA: 1.81 ± 0.10 vs SBR 2, SRT: 15 d, SUVA: 1.72 ± 0.10).

The nominal weight of fraction F4 was < 100 g/mol. Fraction F4 showed no UV-response ($F4_{UV}$) (Fig. 4-1), this was consistent with the results of aerobic hydrolysis of POM (see Chapter 3.1) and the findings of Huber et al., (2011a), who found no or little UV-response in this MW range. The reader must be aware that F4 may have been affected by interactions of the organic matter with the material of the column by reason of the hydrophilic or amphiphilic nature of the organic compounds eluting close to or slightly after the permeation volume of the SEC column (see Chapter 1.4.4).

4.2 Flux of organic matter during the anaerobic digestion of particulate organic matter from municipal wastewater

During the current investigation, the biodegradation of the POM fraction (size: 25 - 250 µm) (Chapter 2.1) was studied under anaerobic conditions by using anaerobic batch experiments and the analytical methods described within Chapter 2, from Chapters 2.4 - 2.6 and Chapter 2.8. Table 4-1 shows the characteristics of the MLSS (wastewater particles plus tap water) at the beginning and at the end of Exp1-ana and Exp2-ana, while Table 4-3 present the determined and estimated kinetic parameters used within this Chapter. In Fig. 4-4 the organic matter flux during the anaerobic digestion of the POM fraction is depicted. The metabolic sequences or sub-processes (i.e., hydrolysis, acidogenesis and acetogenesis, and methanogenesis) shown in Fig. 4-4 are interconnected and occur simultaneously in an anaerobic digester (see Chapter 1.6).

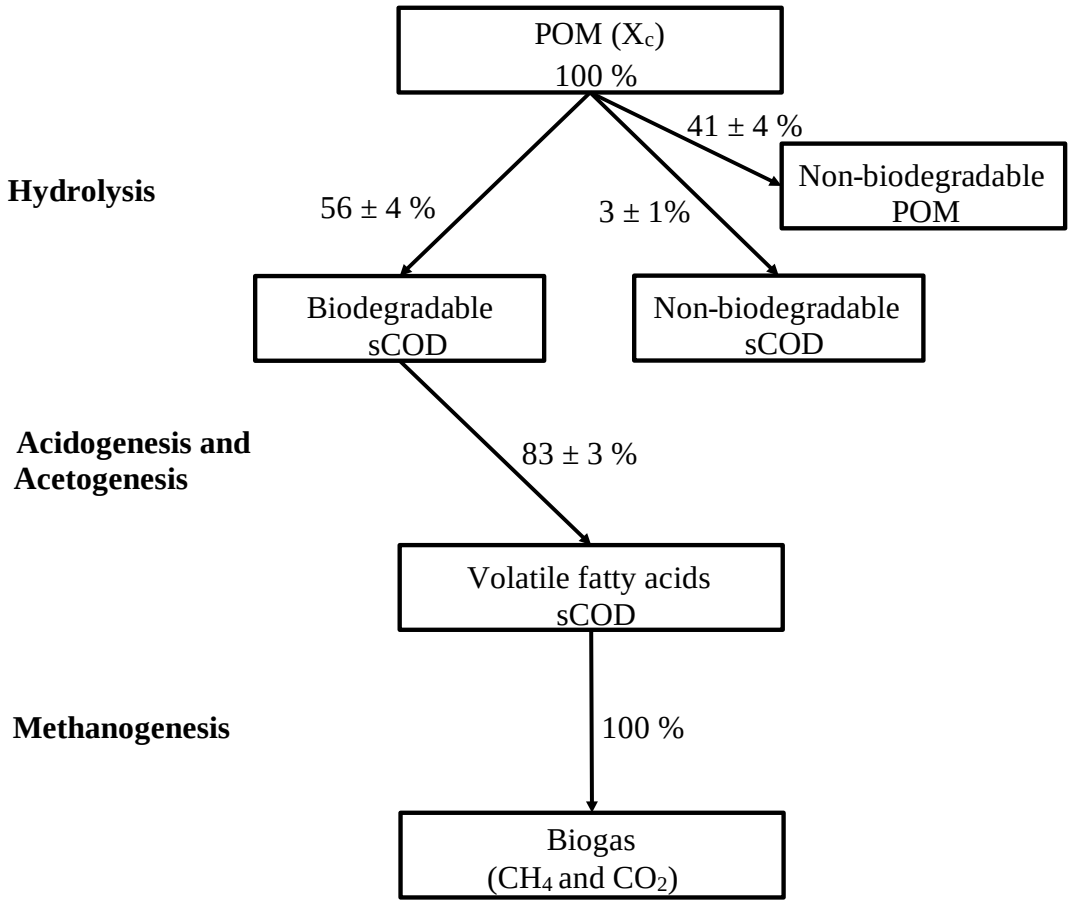

Fig. 4-4: Organic matter flux during the anaerobic digestion of POM and metabolic sequences of anaerobic digestion: hydrolysis, acidogenesis and acetogenesis, and methanogenesis. The percentages are averages from Exp1-ana and Exp2-ana measurements. The content of the initial POM was established to 100 %. Percentages obtained from results.

Table 4-1: Wastewater standard parameters in Exp1-ana and Exp2-ana at the beginning and end of the experiments.

Parameters	Unit	Exp1-ana [n = 2]		Exp2-ana [n = 2]	
		Start	End	Start	End
Time	d	24		24	
pH	-	6 ± 0.2		7.0 ± 0.2	
TSS	g/L	4.3 ± 0.3	2.1 ± 0.1	3.2 ± 0.1	1.9 ± 0.2
VSS	g/L	3.0 ± 0.2	1.3 ± 0.4	2.3 ± 0.1	1.1 ± 0.1
sCOD	mg/L	103 ± 11	86 ± 40	59 ± 5	64
DOC	mg/L	35 ± 1	34 ± 8	23 ± 3	22
VFA	mg/L	56 ± 4	4 ± 1	21 ± 5	1 ± 1
Accumulated biogas*	mL	800		600	
dTN	mg/L	15 ± 1	59 ± 17	20 ± 1	52
NH_4^+- N	mg/L	11 ± 5	41 ± 10	12 ± 2	20 ± 10

* The accumulated biogas was obtained from simulation.

The ADM1 (Batstone et al., 2002) considers disintegration and hydrolysis separately. Disintegration is the step in which the composite material (e.g., sludge waste, primary sludge) is converted into carbohydrates, proteins, and lipids, which are then further hydrolyzed into monosaccharides, amino acids, and long-chain fatty acids, respectively. Disintegration and hydrolysis are extracellular biological and non-biological processes that carry out the breakdown of POM (Batstone et al., 2002). Wastewater engineering literature does not have a clear distinction to whether the mechanisms of POM solubilization are hydrolytic or not (Kommedal, 2003). Therefore, in this work, the disintegration step was included in the term hydrolysis.

It is accepted that hydrolysis of POM is the rate-limiting step of the overall anaerobic digestion process (Eastman and Ferguson, 1981; Vavilin et al., 2008, 1996) (see also Chapter 1.6). Therefore, hydrolysis of POM is the most important kinetic parameter because the subsequent hydrolysis of soluble organic matter occurs faster than the solubilization of POM into DOM (Batstone et al., 2002). Hydrolysis of POM can be estimated by following the VSS degradation

together with the production and utilization of the hydrolysis products, that is, DOM, which was measured within this work as sCOD and DOC. Hydrolysis of POM is commonly expressed in a first order manner (Batstone et al., 2002; Eastman and Ferguson, 1981; Pavlostathis and Giraldo-Gomez, 1991). Hence, equation (4-1) depicts the solubilization of POM (VSS) into sCOD based on a first-order reaction kinetics. The integrated equation is shown in equation (4-2).

$$\frac{dVSS}{dt} = -k_{hyd_{anaer}} * VSS \quad (4\text{-}1)$$

$$VSS = VSS_0 * e^{-khyd\_anaer*t} \quad (4\text{-}2)$$

Where the VSS concentration at a time *t* depends on the initial VSS concentration and a kinetic constant (k_{hyd_anaer}). The k_{hyd_anaer} was found to be 0.034 1/d for Exp1-ana and Exp2-ana. Fig. 4-5 shows the simulation of the POM biodegradation for both experiments (see Chapter 2.9). After t = 24 d of experimentation, the VSS removal in Exp1-ana and Exp2-ana was 58 % and 53 %, respectively (Table 4-1).

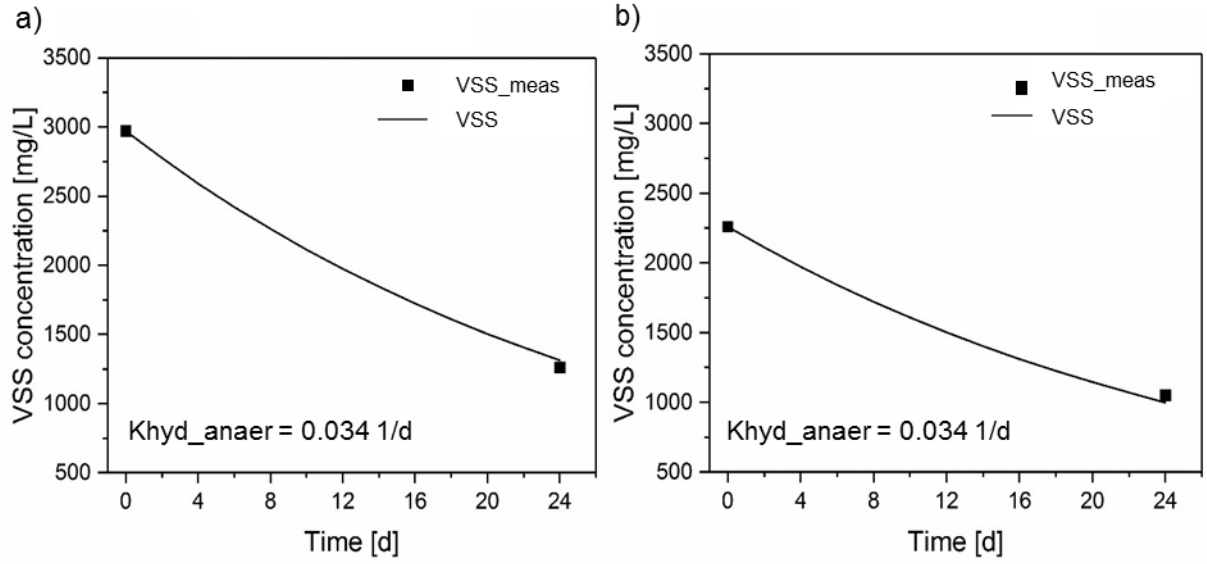

Fig. 4-5: VSS concentration in a) Exp1-ana and b) Exp2-ana. Symbols: Measured VSS at the beginning and end of the experiments. Lines: Simulation of VSS degradation.

The main component in municipal solid waste is cellulose from toilet paper (Chen et al., 2017; Song and Clarke, 2009). After sieving of raw wastewater, Ruiken et al. (2013) found that the cellulose fraction in raw wastewater corresponds to 84 % of the organic mass. According to Grabber et al. (2009) and Lübken (2009) the particulate inert (non-biodegradable) matter is mainly determined by the lignin content. In the ADM1, Batstone et al. (2002) used a hypothetical composite material with only 10 % of non-biodegradable particulate matter.

Nonetheless, the VSS measurements shown in Table 4-1 indicate that the non-biodegradable particulate VSS fraction corresponds to 41 %. The results are in accordance with Ramdani et al. (2012), who stated that the influent non-biodegradable particulate organic matter may contribute to 25 % or more of the VSS in the MLSS, depending on the characteristics of the wastewater.

Non-biodegradable soluble organic matter was estimated to 3 % (Fig. 4-4). The estimation was based on the chromatographic results presented in Chapter 4.1, where it is shown the persistence of the HMW (F1) and intermediate MW (F2) organic matter originated from the influent wastewater particles or formed during the anaerobic digestion of POM (Fig. 4-3, Chapter 4.1). The non-biodegradable soluble organic matter fraction was estimated when the maximum hydrolytic activity was registered, at t = 4 d in Exp1-ana and at t = 2 d in Exp2-ana (see Chapter 4.1).

As DOC is formed at the same rate as the degradation of POM, the production of DOC in terms of sCOD (4-3) is determined by the VSS fraction being hydrolyzed to sCOD and the degradation kinetic constant of VSS (k_{hyd_anaer}). The integrated form is presented in equation (4-4).

$$\frac{dsCOD}{dt} = k_{hyd\_anaer} * \upsilon_1 * VSS \qquad (4\text{-}3)$$

$$sCOD = sCOD_0 + \upsilon_1 * VSS_0 \left(1 - e^{-khyd\_anaer*t}\right) \qquad (4\text{-}4)$$

Where k_{hyd_anaer} is the degradation kinetic constant of VSS in 1/d and υ_1 represents the fraction of VSS converted to sCOD (biodegradable and non-biodegradable). υ_1 was estimated to 0.63 for both experiments (Fig. 4-4).

The chromatographic results demonstrated that during the anaerobic digestion of POM, the biodegradable fraction of the DOC is mainly represented by F3 (see Fig. 4-1 and Fig. 4-2 in Chapter 4.1). The measured DOC in F3 can be converted to sCOD by using the equations (3-1) and (3-2) presented in Chapter 3.2. $sCOD_{F3}$ can be determined through simulation by using equation (4-5).

$$\frac{dsCOD_{F3}}{dt} = k_{hyd\_anaer} * \upsilon_2 * VSS \qquad (4\text{-}5)$$

Where υ_2 accounts only the conversion of VSS (POM) into biodegradable soluble organic matter ($sCOD_{F3}$). υ_2 was estimated to 0.6 for both experiments (see VSS in Table 4-1). The reader must be aware that the simulation reflects the behavior of the sCOD considering the interaction of the metabolic sequences during the anaerobic digestion. Therefore, the simulation contemplates the formation and the utilization of the sCOD.

The amount of VFA formed by the degraded fraction of the $sCOD_{F3}$ can be calculated by using equation (4-6).

$$\frac{dVFA}{dt} = k_{hyd\_anaer\,II} * \upsilon_3 * sCOD_{F3} \qquad (4\text{-}6)$$

Where $k_{hyd\_anaer\,II}$ is the degradation kinetic constant of $sCOD_{F3}$ in 1/d. As the $sCOD_{F3}$ represents only the biodegradable fraction of the sCOD, a higher kinetic constant for the transformation of sCOD into VFA is expected (Batstone et al., 2002). Through data simulation, $k_{hyd\_anaer\,II}$ was set to 0.55 1/d for both experiments. The hydrolysis constant was comparable to the values found by Song and Clarke (2009), who worked with a mixed culture from landfill waste in a continuous reactor and found the hydrolysis rate value of 0.45 ± 0.07 1/d. Likewise, for primary sludge substrate, the ADM1 - appendix A shows hydrolysis constants of carbohydrates and proteins of 0.41 and 0.39 1/d, and 0.58 and 0.58 1/d at pH of 5.85 and 6.67, respectively. υ_3 is the fraction of $sCOD_{F3}$ being transformed into VFA and it was estimated to 0.8 for both experiments. The estimation was based on the found values of $sCOD_{F3}$ at the end of the experiments. The latter was in accordance with de Lemos Chernicharo (2005), who stated that 70 to 90 % of the biodegradable matter in an anaerobic digester is converted into biogas.

It is important to clarify that acidogenesis and acetogenesis were contemplated as a lump stage (Fig. 4-4) because the reaction products of the acidogenesis and acetogenesis stages are H_2 gas and $COOH^-$, which are both substrates of the methanogenic bacteria (Anukam et al., 2019). Table 4-2 shows the maximum measured VFA concentrations found in Exp1-ana (pH 6 ± 0.2) and Exp2-ana (pH 7 ± 0.2). The percentage of acetic acid: propionic acid: butyric and iso-butyric acid at t = 4 d in Exp1-ana and at t = 2 d in Exp2-ana were 60:34:6 and 76:17:7, respectively. A larger amount of propionic acid was formed in Exp1-ana, while mostly acetic acid was formed in Exp2-ana. This is related to the optimal pH conditions for acidogenic and acetogenic bacteria (see Table 1-4 in Chapter 1.6).

Table 4-2: Maximum concentration of the organic acids in Exp1-ana (pH 6 ± 0.2) at t = 4 d and in Exp2-ana (pH 7 ± 0.2) at t = 2 d.

VFA	**Exp1-ana**	**Exp2-ana**
	[mg/L]	**[mg/L]**
Acetic acid	97 ± 23	41 ± 8
Propionic acid	55 ± 3	9 ± 8
Butyric acid	3 ± 2	1 ± 0
Iso-butyric acid	6 ± 2	3 ± 0

The found VFA corresponded to the most important products of glucose degradation depicted in the ADM1:

Acetate $C_6H_{12}O_6 + 2\ H_2O \rightarrow 2\ CH_3COOH + CO_2 + 4\ H_2$ (4-7)

Acetate, propionate $3\ C_6H_{12}O_6 \rightarrow 4\ CH_3CH_2COOH + 2\ CH_3COOH + 2\ CO_2 + 2\ H_2O$ (4-8)

Butyrate $C_6H_{12}O_6 \rightarrow CH_3CH_2CH_2COOH + 2\ CO_2 + 2\ H_2$ (4-9)

Lübken (2009) reported that glucose degradation occurred via reaction (4-7): 50 %, (4-8): 35 %, and (4-9): 15 %.

Fig. 4-6 shows the measured and simulated soluble organic matter. The maximum measured accumulation of sCOD and VFA was perceived at t = 4 d in Exp1-ana (Fig. 4-6a) and at t = 2 d in Exp2-ana (Fig. 4-6b). The higher accumulation of sCOD in Exp1-ana (Fig. 4-6a) can be attributed to a major quantity of VSS and/or to a major activity of the acidogenic bacteria, being the pH of 6 within the optimal range for those microorganisms (Vavilin et al., 2008). The faster decrease of VFA in Exp2-ana was in agreement to von Sperling and Lemos Chernicharo (2005); who stated the optimal pH range for the degradation of acetate between 6.5 - 7.1 and for propionate between 7.2 - 7.5. After t = 14 d no major changes were observed in none of the experiments. The decrease of VFA was directly related to the formation of methane (de Beer et al., 1992). Even when the decrease of VFA started two days before in Exp2-ana at pH 7 than in Exp1-ana at pH 6, the VSS removal after 24 d was similar (i.e., Exp1-ana = 58 % and Exp2-ana = 53 %).

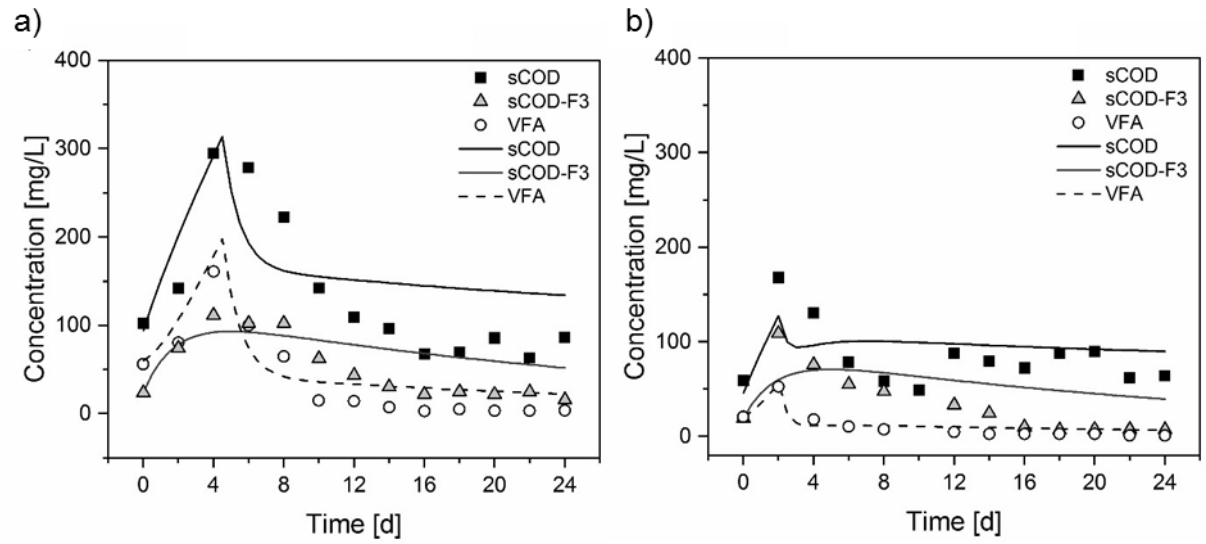

Fig. 4-6: Formation and utilization of soluble organic matter originated from the hydrolysis of municipal wastewater particles in Exp1-ana (a) and Exp2-ana (b). Symbols represent measured values and lines data simulation.

Due to a technical problem with the measuring system of the AMPTS II, the biogas was not recorded in any of the experiments. Nonetheless, the decrease of the organic products was observed in both experiments indicating biogas production. The biogas production can be calculated by using equation (4-10) and equation (4-11). As the production of biogas is the final result of the process-cascade of anaerobic digestion, i.e., hydrolysis, acidogenesis and acetogenesis and methanogenesis, the accuracy of the initial value of POM (measured as VSS) becomes a critical parameter of the simulation. The kinetic constant for methane formation (k_{CH4}) was set to 1 1/d for Exp1-ana and 2 1/d for Exp2-ana; von Sperling and Lemos Chernicharo (2005) stated that pH values lower than 6.5 can cause a significant decrease in the methane rate.

$$\frac{dVFA}{dt} = -k_{CH4} * \upsilon_4 * VFA \qquad (4\text{-}10)$$

$$\frac{dCH_4}{dt} = k_{CH4} * \upsilon_4 * VFA \qquad (4\text{-}11)$$

The stoichiometric factor υ_4 was calculated as follows:

$$\upsilon_4 = 0.35 * V * \frac{1}{0.6} \qquad (4\text{-}12)$$

Where, V is the volume of the anaerobic batch reactor, V = 1.8 L, 0.6 was the assumed methane content in the biogas and 0.35 is the relation of L of methane produced per gram of COD consumed at standard conditions (0 °C, 1 atm) (Metcalf and Eddy, 2014). As acetate was found to be the major constituent of the VFA in both experiments (Table 4-2), acetate was converted to COD according to reaction (4-13). The COD of acetate is ≈ 1 g COD/g VFA.

$$\underset{(60\ g/mole)}{C_2H_4O_2} + 2O_2 \rightarrow 2\ CO_2 + \underset{(64\ g/mole)}{2\ H_2O} \qquad (4\text{-}13)$$

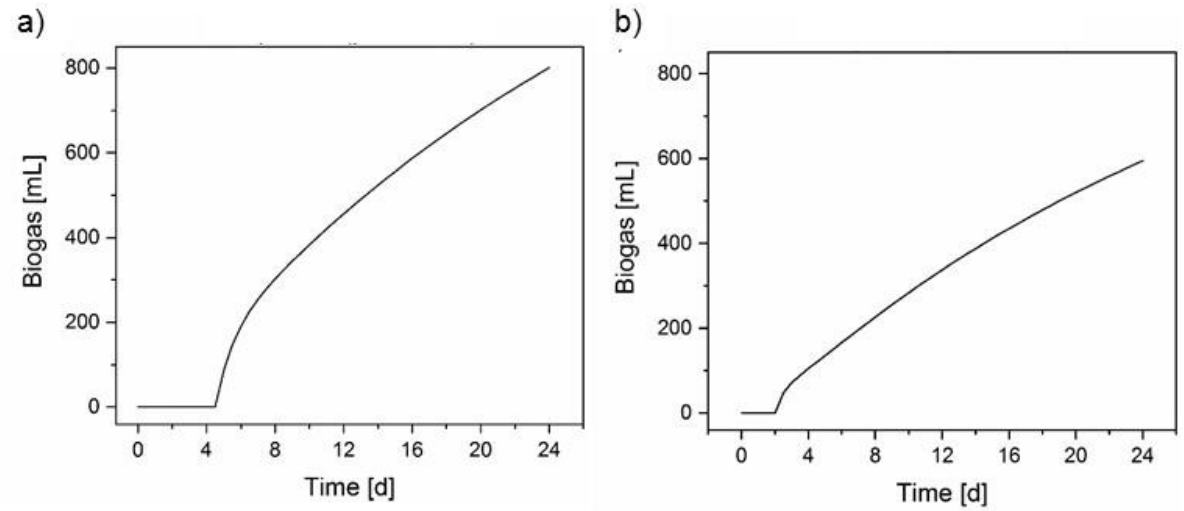

Fig. 4-7: Simulation of biogas production over time in a) Exp1-ana and b) Exp2-ana.

The simulation of biogas in Exp1-ana and Exp2-ana is shown in Fig. 4-7. The main difference found among the experiments was the necessary time for the formation of biogas. Based on the accumulation of F3 (VFA), it was assumed that the full capacity of the methanogenic microorganisms started with the degradation of F3, i.e., t = 4 d in Exp1-ana and t = 2 d in Exp2-ana (Fig. 4-6).

Although the accumulated biogas in Exp2-ana was lower than in Exp1-ana, i.e., 600 mL vs 800 mL of accumulated biogas (Fig. 4-7), the biogas yield of 0.5 L biogas/g VSS_{used} was the same for both experiments. It seems that under optimal pH conditions for the methanogenic group in Exp2-ana the production of methane started 2 days faster (Fig. 4-7b) than with a pH of 6 in Exp1-ana (Fi.4-7a). Moletta et al. (1994) found immediate response to small pH changes (e.g., 6.8 to 6.6) on the gas composition and production because methanogenic bacteria are strongly affected by pH changes (von Sperling and Lemos Chernicharo, 2005). Exp1-ana showed higher accumulation of VFA (Table 4-2) and a consequently accumulation of H_2 causing retardation of the methanogenesis process (Lohani and Havukainen, 2017).

Methanogenic bacteria can still be active at pH 6 but then more days are necessary for the bacteria to adapt to the adverse conditions. Consequently, the methanogenic step may become the limiting factor on the overall anaerobic digestion process.

Table 4-3: Definition of the determined and estimated kinetic parameters used in the simulation of the formation and utilization of the soluble hydrolysis products of particulate organic matter originated from municipal wastewater and treated under anaerobic conditions in Exp1-ana and Exp2-ana.

Parameter	**Definition**	**Unit**	**Value**	
			Exp1-ana	Exp2-ana
X_c	Composite particulate organic matter	g/L	3	2.3
k_{hyd_anaer}	Hydrolysis constant of POM	1/d	0.034	
$k_{hyd\_anaer\ II}$	Hydrolysis constant of $sCOD_{F3}$	1/d	0.55	
k_{CH4}	Constant of methane formation	1/d	1	2
υ_1	Fraction of X_c converted into non-biodegradable and biodegradable organic matter ($sCOD_{F3}$)	-	0.63	
υ_2	Fraction of X_c converted into $sCOD_{F3}$	-	0.6	
υ_3	Fraction of $sCOD_{F3}$ converted into VFA	-	0.8	
υ_4	Amount of methane produced estimating 60 % of the biogas as methane and a volume of 1.8 L	L/d CH_4	1.05	

4.3 EPS and nucleic acids visualization during the anaerobic process

Benneouala et al. (2017) showed the importance of the initial amount of bacteria attached to the particulate matter on the hydrolysis process. In Chapter 3.3, the growth dynamics of the bacteria originally attached to the surface of the particles as well as the production of EPS were studied under aerobic conditions. Correspondingly, the CLSM technique was employed to quantify the bacteria and EPS during the anaerobic treatment of POM from municipal wastewater.

Fig. 4-8 and Fig. 4-9 show the maximum intensity projections of the CLSM stacks in Exp1-ana and Exp2-ana, respectively. The major changes observed during the anaerobic

digestion of POM corresponded to the EPS architecture. Fig. 4-8 and Fig. 4-9 show the structure of the POM at t = 0; the interior of the particles had minimal amounts of fluorescence light, probably because of the self-voids of the particles or to the thickness of the particulate material (Chu et al., 2005; Wilderer et al., 2002). A decrease in the size of the particles after t = 7 d is visualized; the change in the morphology of the EPS was observed in both experiments (Fig. 4-8 and Fig. 4-9). The results match the findings of Chu et al. (2005), who studied the anaerobic digestion rate for flocculated sludge and found a significant reduction of the flocs size in parallel to the anaerobic digestion, that is, a deterioration of the floc´s structure. The same authors found a size decrease of until 55 % during the first 10 d of digestion.

It is known that in the anaerobic digestion the organic matter removal occurs through a series of interconnected processes carried out by the acidogenic, acetogenic and methanogenic microorganisms (see Chapter 1.6 and Chapter 4.2). On the one hand, in Exp1-ana, agglomerations of bacteria onto the surface of the particles (bacteria-particles association) are observed at t = 7 d, most probably, this microbial activity is visible after 7 d because the removal of organic matter in Exp1-ana started after 4 d (see Fig. 4-2 in Chapter 4.1 and Fig. 4-6 in Chapter 4.2) and at t = 6 d only 25 % of the maximum accumulated F3 was removed (see Fig. 4-3 in Chapter 4.1). On the other hand, in Exp2-ana, no significant microbial activity was observed (Fig. 4-9). From t = 2 d to t = 6 d, about 60 % of the maximum accumulated F3 was removed (see Fig. 4-3 in Chapter 4.1). The latter together with the minor signal of nucleic acids detected at t = 7 d (Fig. 4-9 and Fig. 4-10a) leads to conclude that in Exp2-ana, the main microbial activity occurred before 7 d and most probably within the first 2 d (see Fig. 4-2 in Chapter 4.1).

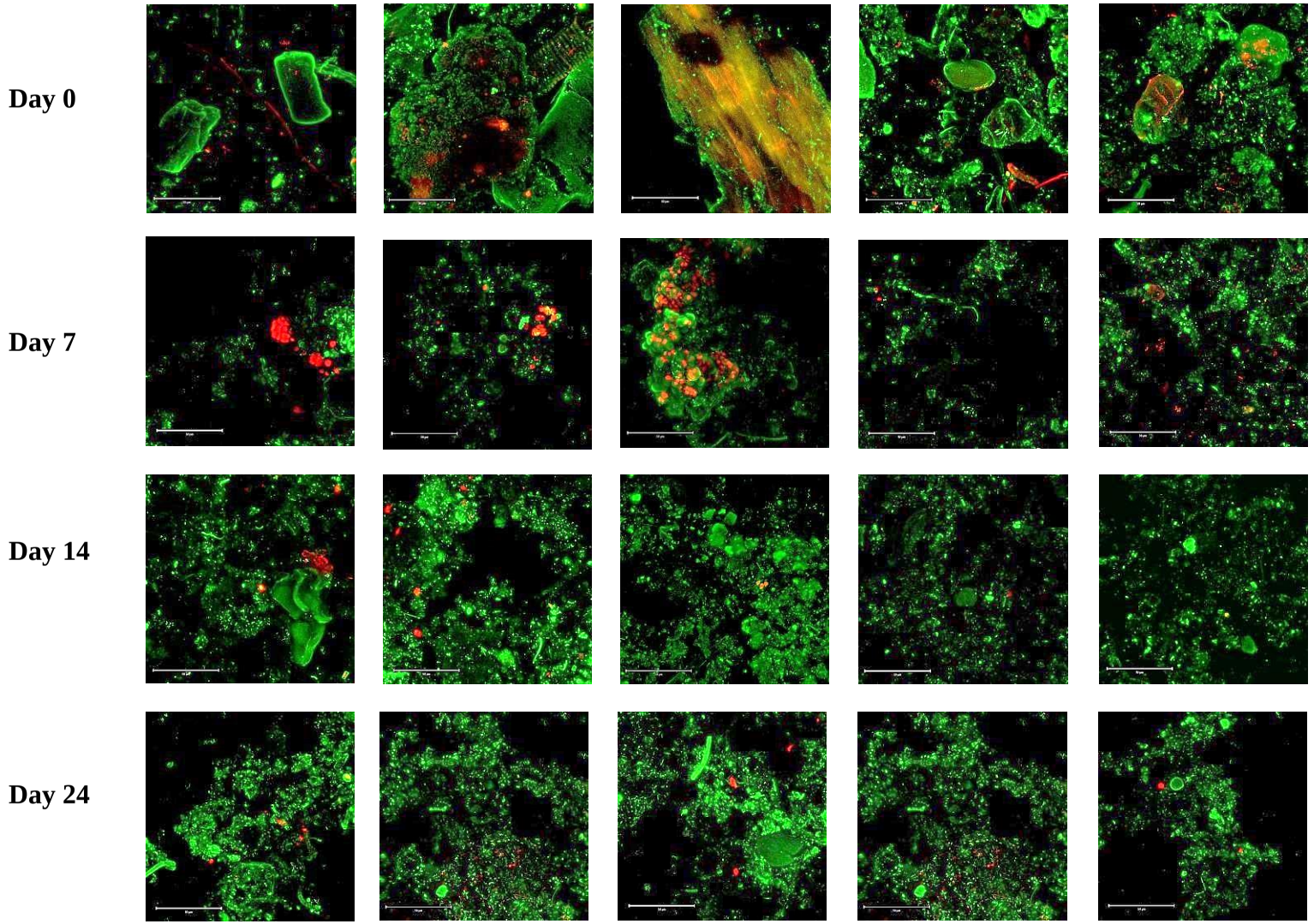

Fig. 4-8: Maximum intensity projections of CLSM images acquired to visualize the hydrolysis process and the bacteria population in Exp1-ana (pH 6 ± 0.2). Stacks at day 0, 7, 14 and 24. Total Stacks per day: 30. EPS: green, nucleic acids: red. Scale bar: 50 µm.

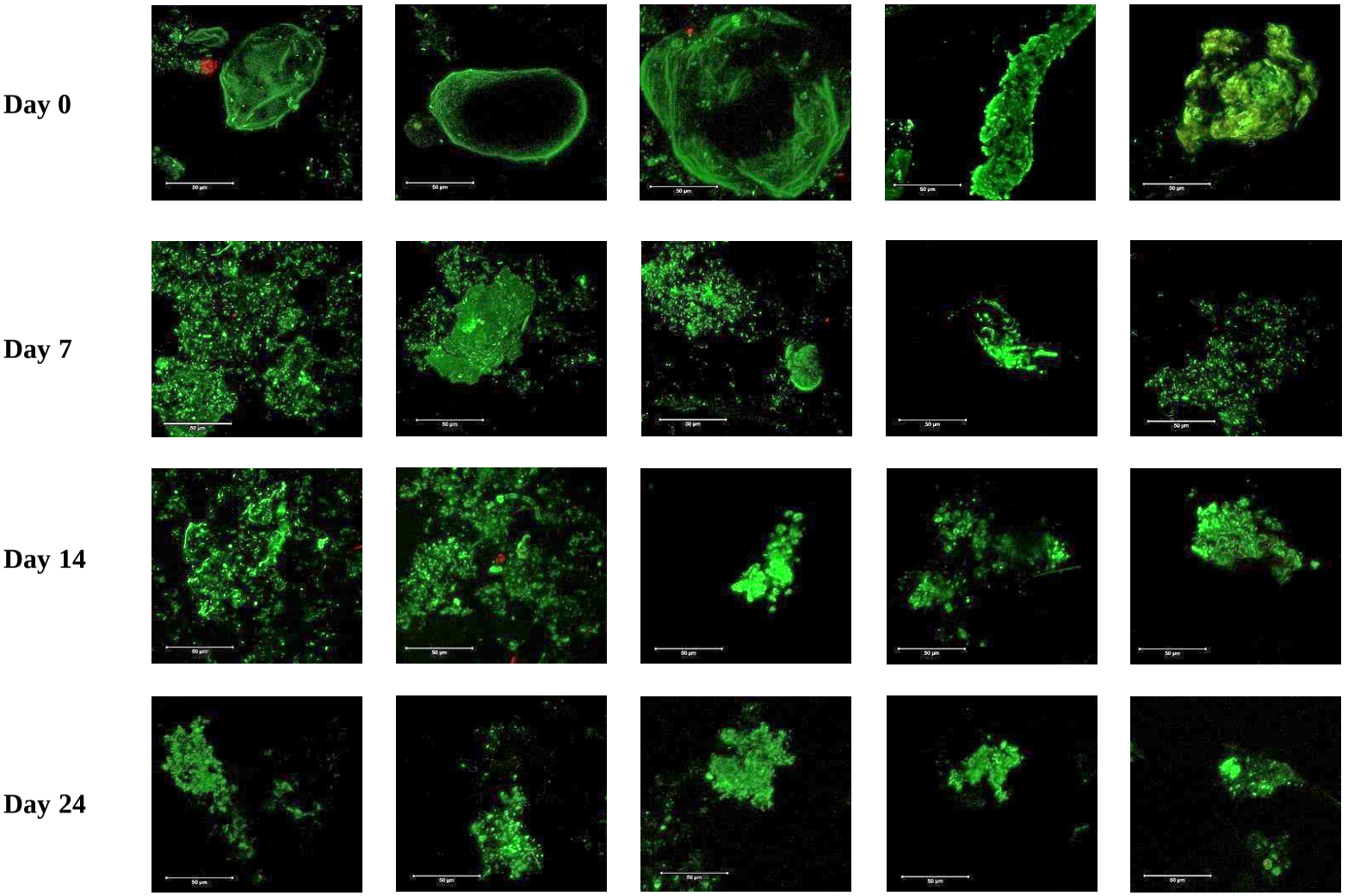

Fig. 4-9: Maximum intensity projections of CLSM images acquired to visualize the hydrolysis process and the bacteria population in Exp2-ana (pH 7 ± 0.2). Stacks at t = 0, 7, 14 and 24 d. Total Stacks per day: 15 - 30. EPS: green, nucleic acids: red. Scale bar: 50 µm.

By reason of the high standard deviation of the EPS coverage (Fig. 4-10b), no major interpretation between Exp1-ana and Exp2-ana can be done. However, the CLSM-images show that both experiments presented comparable EPS structure at t = 0. It is observed that smaller EPS aggregates are formed in Exp2-ana (see Fig. 4-9 and Fig. 4-8). The differences of the EPS agglomerates are evident up to t = 14 d. The EPS aggregates are the result of the microbial activity. The optimal pH for the methanogens in Exp2-ana lead to higher methanogenic activity and therefore, to higher removal performance producing smaller EPS aggregates. In Exp1-ana, the lower methanogenic activity at pH 6 lead to lower removal efficiencies producing bigger aggregates. At t = 14 d, the removal of F3 reached about 85 % in both experiments (Fig. 4-3 in Chapter 4.1). From t = 14 d to t = 24 d the CLSM-images did not show significant changes in none of the experiments (Fig. 4-8 and Fig. 4-9) but the removal of F3 at t = 24 d was about 95 % in both experiments. A minor production of EPS is expected during the anaerobic digestion process in comparison to the aerobic process (Seghezzo, 2004). CLSM-images of both experiments (Fig. 4-8 and Fig. 4-9) show no EPS (biomass) production. A slight decrease of the bacteria population from t = 0 to t = 24 d by reason of substrate depletion was observed in both experiments (Fig. 4-10a) as well as a slight decrease of the NA/EPS ratio (Fig. 4-10c).

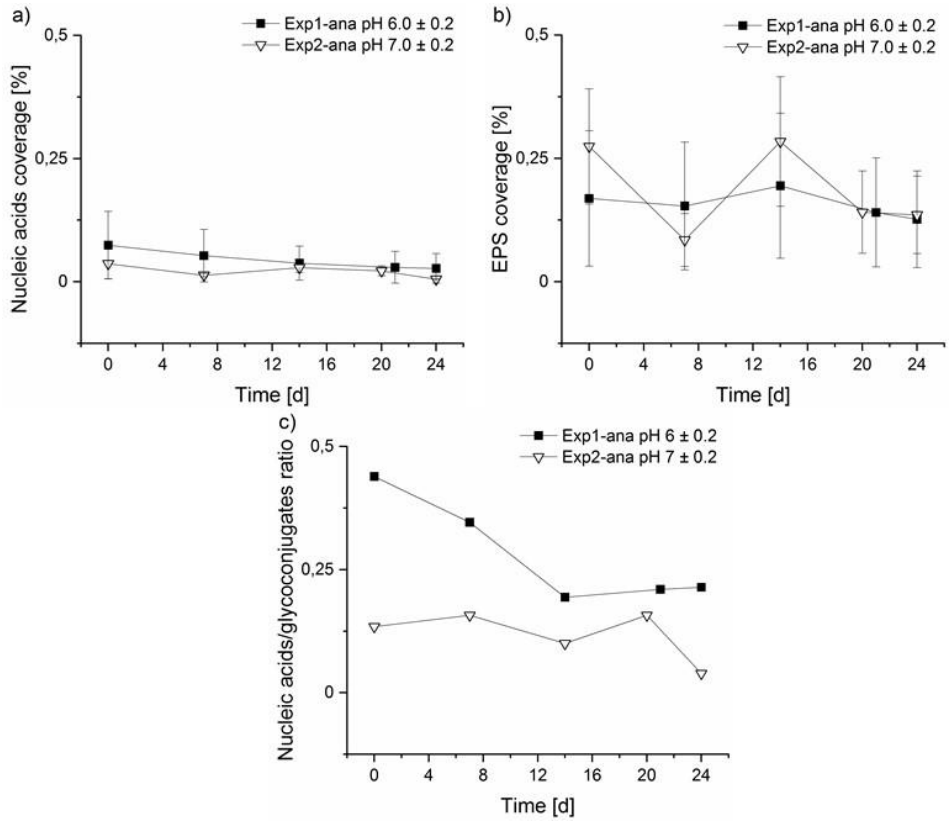

Fig. 4-10: Coverage for nucleic acid (NA) (a) and EPS-glycoconjugates (b) signals. Ratio of NA/EPS (c) at t = 0, 7, 14 and 24 d. 15 - 30 stacks per sample.

4.4 Conclusions of anaerobic digestion of particulate organic matter from municipal wastewater

Although the mechanism of degradation of particulate organic matter (POM) and the limiting factor of the anaerobic digestion, i.e., hydrolysis of solids, have been already identified, the results shown in this work brought new insight into the process by studying the influence of pH on the anaerobic digestion of POM. Optimal pH-values for hydrolytic and acidogenic bacteria (Exp1-ana) and for acetogenic and methanogenic microorganisms (Exp2-ana) were investigated.

By means of size exclusion chromatography coupled with online carbon and UV detection (SEC-OCD-UV), the released hydrolysis products were separated into four molecular weight fractions of DOC (F1 through F4) in the anaerobic batch reactor. These DOC-fractions were evaluated according to their biodegradability during the anaerobic digestion treatment. The results showed that the formation of the low MW fraction, F3, was the main indicator of hydrolysis of POM during the anaerobic digestion process. F3 was related to soluble biodegradable organic matter.

The solubilization of POM into dissolved organic matter was further investigated by following measurements of sCOD, DOC, and VFA throughout the experiments. In addition, a set of differential equations based on first order kinetics was applied in a simulation to determine kinetic parameters and biogas production. The results showed that changes of pH (i.e., 6 and 7) influenced the kind of VFA produced as well as the performance of removal of POM during the first days of anaerobic treatment. At optimal pH conditions for the acetogenic and methanogenic microorganisms, the removal occurred two days faster than at optimal pH conditions for the hydrolytic and acidogenic bacteria. Nevertheless, the overall removal performance of POM after 24 d of anaerobic treatment was comparable at pH 6 and at pH 7. Formation of intermediate MW organic matter after 20 d of anaerobic treatment was only observed at pH 7. The maximum intensity projections of the CLSM images showed a change in the morphology of the wastewater particles structure (decrease of the particles size). No production of biomass was observed.

Chapter 5: Conclusion and consequences for aerobic and anaerobic treatment of municipal wastewater

The hydrolysis of particulate organic matter (POM) from municipal wastewater treated under aerobic and anaerobic conditions has been analyzed along this work. Both types of hydrolysis deliver comparable results with respect to reaction velocity but very different intermediate components before the final products of the entire aerobic (CO_2 and biomass) or anaerobic (CO_2, CH_4 and biomass) process are achieved. The achieved results have to be discussed and compared in relation to the full scale (aerobic and anaerobic) biological treatment of municipal wastewater.

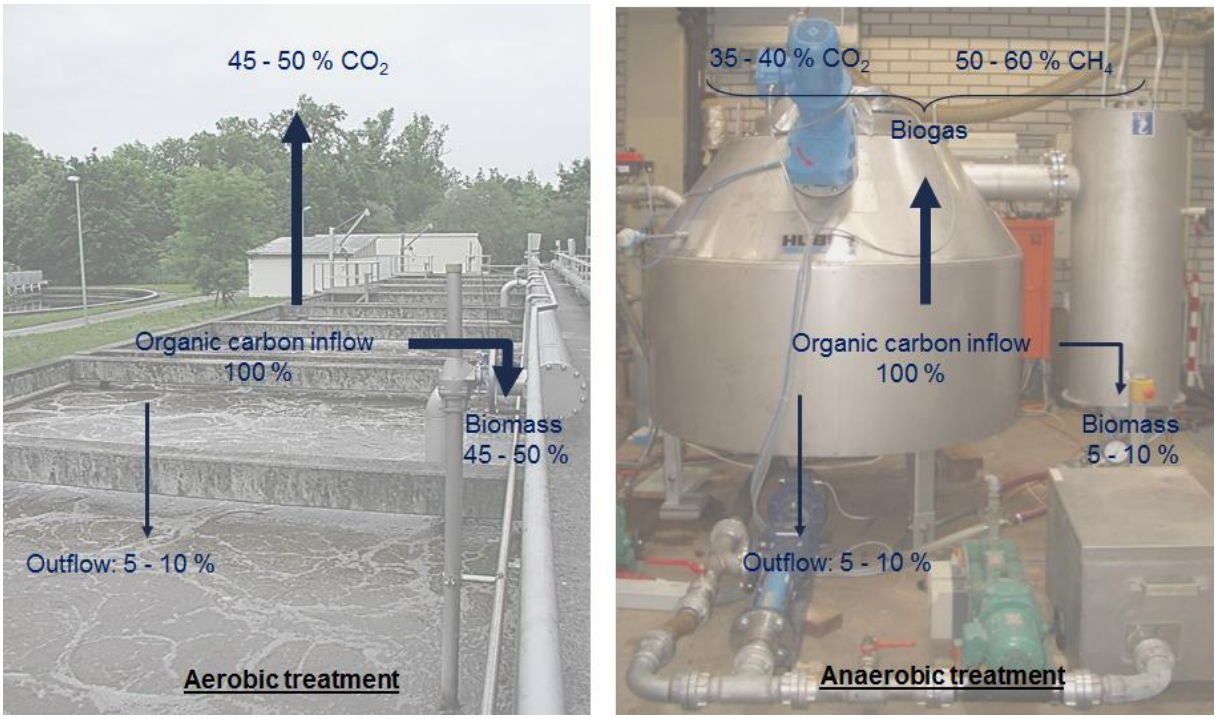

Fig. 5-1: Organic carbon flow during aerobic treatment (activated sludge process) (left) and anaerobic treatment (anaerobic membrane bioreactor- AnMBR) (right) of municipal wastewater. Left image taken from Harald Horn and right image taken from pilot scale AnMBR at TU Munich, BMBF project No. 02WA0854/55.

Fig. 5-1 shows the flow of the organic carbon along an aerobic and anaerobic treatment process for municipal wastewater. During aerobic treatment, around 45 - 50 % of the organic carbon is oxidized to CO_2 and the remaining part (45 - 50 %) is mainly converted into biomass. Especially the latter has to be treated and finally disposed at high costs.

During anaerobic treatment (and if the biomass is retarded by a membrane filtration) most of the organic carbon is converted into CO_2 and CH_4 (35 - 40 % and 50 - 60 %) and only a small

fraction is converted into biomass (i.e.,~5 - 10 %). It seems that the anaerobic treatment does have a clear advantage over the aerobic one. However, the numbers for the anaerobic process shown in Fig. 5-1 can be achieved if the wastewater is treated at T > 25 °C and with an anaerobic membrane bioreactor (AnMBR), this has been shown by Martinez-Sosa et al. (2011).

Independent of which process (aerobic or anaerobic) is chosen, a huge amount of 50 - 70 % of the organic load in wastewater is represented by the POM. Thereby, the question on how quickly these components can be hydrolyzed is essential for the following and final biological degradation by the involved microorganisms. As already stated above, the aerobic and anaerobic kinetic constant for hydrolysis of POM were found to be within the same magnitude. However, the velocity of aerobic hydrolysis found for the conducted experiments is 3 - 4 times higher than the anaerobic one, i.e., aerobic k_{hyd_aer}: 0.12 1/d versus anaerobic k_{hyd_anaer}: 0.034 1/d.

In the end both processes can only be completed if the POM is kept within the biological treatment step for more than 10 days. In an activated sludge system this will be achieved by incorporation of the POM into sludge flocs and a solid retention time (SRT) > 10 d. For anaerobic treatment without sufficient floc formation and very bad settling properties of the biomass the SRT can only be controlled by membrane separation (Martinez-Sosa et al., 2011).

Not only the velocity of the hydrolysis process but also the metabolic pathway and its intermediates must be understood if we want to optimize the processes. Within the experiments it was nicely shown that the DOC formed during the hydrolysis of POM at aerobic and anaerobic conditions presented a certain range of MW products (Fig. 5-2). The size exclusion chromatography coupled with online organic carbon and UV detectors (SEC-OCD-UV) worked out to be an extremely helpful analytical tool. Up to now it was mainly used for characterization of organic carbon in surface water and its value for analyzing processes in wastewater treatment was somehow underestimated.

For aerobic hydrolysis, the HMW products (referring to F1) can be considered the best indicator of the process, since mainly F1 accumulated in the liquid phase. Significant amounts of the other three fractions (F2, F3 and F4) of the organic carbon could not be found within the liquid phase. One can conclude that smaller molecules (F3 and F4) are directly consumed by bacteria and not released to the liquid phase. A link between F1 and the microbial activity was detected; roughly 2 - 3 d were needed by the bacteria originally attached to the particles to grow and develop the required enzymes to start the degradation of F1 (Fig. 5-2, left stack). Therefore, the formation and subsequent degradation of the HMW products was considered the limiting factor

of aerobic hydrolysis. However, it must be considered that no adapted bacteria have been present at the beginning of the experiments. This can be shown with confocal laser microscopy (CLSM), which is able to visualize the formation of bacteria and EPS matrix on the surface of the wastewater particles. The CLSM-images show that during the aerobic digestion of POM after a short formation period for bacteria (first 2 - 3 days) mainly EPS is produced over time. As soon as the available hydrolysis products (F1) are decreasing the number of bacteria is decreasing too (Fig. 5-3, left).

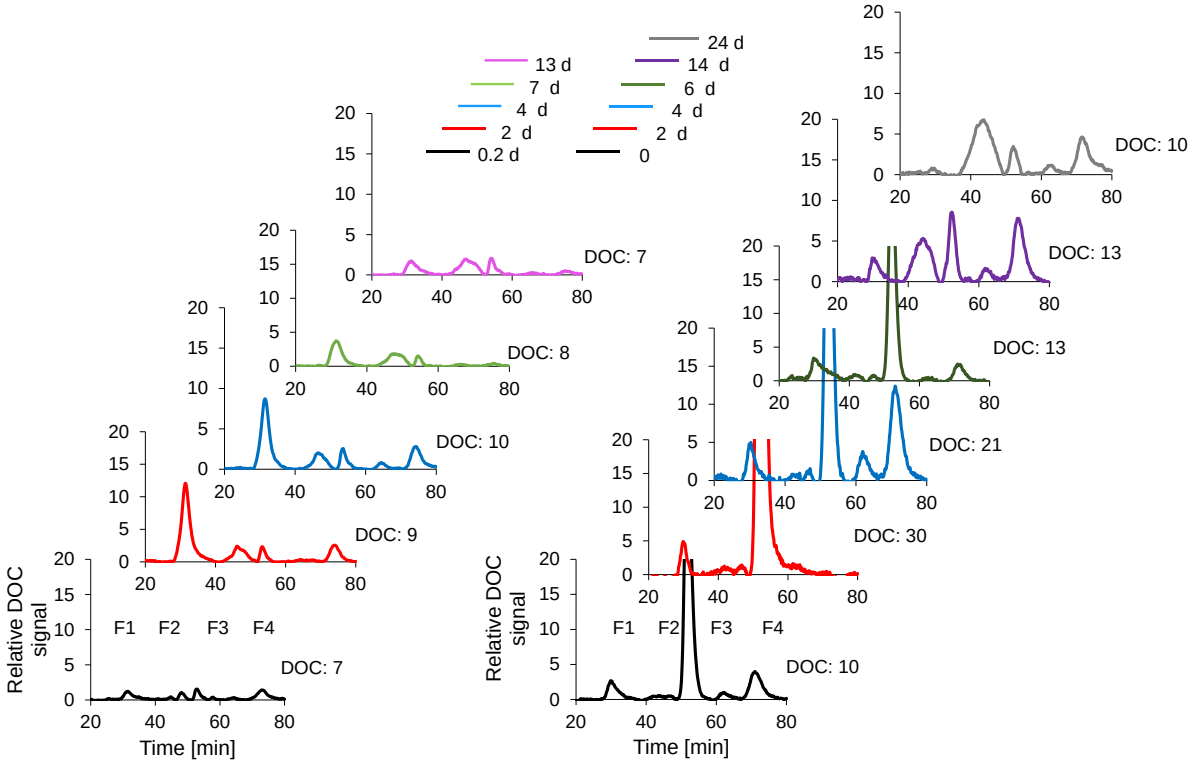

Fig. 5-2: Relative DOC signal in Exp2-aer (left) and in Exp2-ana (right). The dilution factor of all the samples had to be adopted. DOC in mg/g VSS $_{added}$.

The conclusion can be drawn, that the bacteria responsible for hydrolysis and/or the respective enzymes are directly growing or produced on the particles. Biomass (other bacteria in sludge flocs) not directly connected to the particles will not play a role for hydrolysis. With respect to mathematical models this is not easily to solve as we do not know the fraction of bacteria sitting or being directly connected to the particles.

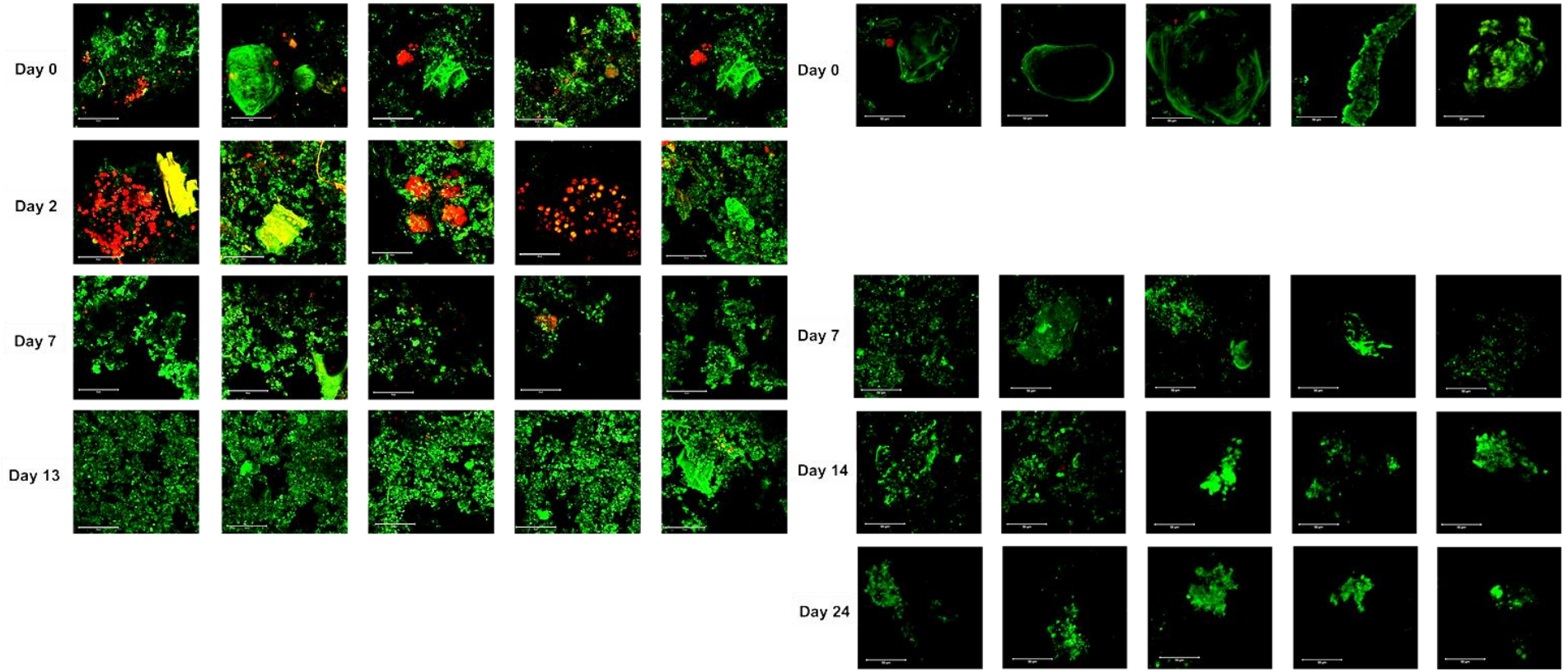

Fig. 5-3: Maximum intensity projections in Exp2-aer (left) and Exp2-ana (right), pH 7 ± 0.2 in both experiments. Left: t = 0, t = 2 d, t = 7 d, t = 13 d. Right: t = 0, t = 7 d, t = 14 d t = 24 d. Stacks per day: 16 in Exp2-aer and 15 - 30 stacks in Exp2-ana. Color: red-nucleic acids; green-EPS glycoconjugates. Scale bar = 40 µm in Exp2-aer and 50 µm in Exp2-ana.

Different from the aerobic hydrolysis, the hydrolysis of POM at anaerobic conditions does mainly show LMW products (F3) in the liquid phase. Only a minor production of other hydrolysis products with different MW range (F1 and F4) are formed (Fig. 5-2, right stack). As it is well known from the process cascade of anaerobic digestions the LMW products were mainly related to VFA. Compared to the aerobic process the anaerobic process chain is represented by different organisms working together. The methanogenic group is responsible for the final step of methane production. Therefore, F3 (produced by acidogenic and acetogenic bacteria) is accumulated in the liquid phase in the beginning as the methanogenic archaea needed more time to develop and thrive to convert the VFA into biogas.

The period where F3 dominated the DOC within the liquid phase was found to be similar to the occurrence of F1 during the aerobic treatment, i.e., 2 to 3 d (see Fig. 5-2, right stack). For the visualization, no significant microbial activity was observed in the CLSM-images (Fig. 5-3, right). Comparing the growth rates of aerobic (μ_{max} is around 6 1/d) and anaerobic microorganisms (μ_{max} is around or even lower than 1 1/d) this result is not surprising. Moreover, in the anaerobic digestion there is minor production of biomass (including EPS). This is related to the yield of biomass, which is lower in the anaerobic digestion. For microbial oxidation of acetate the yield is around 0.4 - 0.6 g VSS/g COD and 0.03 g VSS/g COD by using O_2 and CO_2 as electron acceptor, respectively. Anaerobic reactions in which carbon dioxide acts as an electron acceptor release less energy for microbial growth than aerobic reactions where oxygen is used as electron acceptor leading to less biomass production. However, as already identified for the aerobic hydrolysis the active microorganisms have to be close to the substrate, i.e., the particulate organic matter.

The results presented within this thesis work contribute to both the aerobic and anaerobic hydrolysis process understanding. So far, the DOC produced from the hydrolysis of POM is generally regarded as dissolved organic matter. Nonetheless, efforts have been made to characterize the produced DOC (hydrolysis products), but no detailed information of the hydrolysis products formed and degraded during and along the aerobic and anaerobic treatment of POM was available.

By using the size exclusion chromatography coupled with online carbon detector (SEC-OCD), the hydrolysis products (DOC) were characterized based on their MW and thus, it could be identified at which time these organic carbon fractions were formed and further degraded. The aerobic microorganisms are able to conduct both hydrolyze POM and then oxidize the dissolved large molecules (fraction F1) to carbon dioxide. The identification/quantification of this

fraction (F1) is a major finding of the work presented. Here the combination of SEC-OCD (for identification of intermediates) and parallel respirometric measurements (for calculation of OUR) worked out to be extremely helpful.

On the other side the large molecular fraction (F1) cannot be seen (or analyzed) in the liquid phase for the experiments with anaerobic organisms. Here the pathway can be identified in the liquid phase by smaller molecules (fraction F3, referring to VFA). That is not surprising as (compared to the aerobic pathway) the anerobic degradation is done by a cascade of microorganisms. Important intermediates are VFA (especially acetate) whereas the end product is methane and carbon dioxide. A huge difference between pH 6 or 7 could not be seen.

With respect to process optimization, it has become clear, that the acting microorganisms are fixed to the particles, that was nicely shown by the imaging with CLSM. As mentioned above the time needed for complete aerobic and anaerobic hydrolysis of POM is larger than 10 and 20 days, respectively.

However, one can think whether we want to optimize the conversion of POM during aerobic treatment to climate-damaging carbon dioxide and biomass or generate a benefit if we can produce chemicals (acetate and propionate) by an anaerobic treatment step. Especially propionate is a chemical, which does have a higher value compared to methane.

Therefore, a partial reorganization of municipal wastewater treatment would be necessary. First of all, the huge load of POM has to be separated (micro sieve) before the aerobic biological treatment step. By running an optimized hydrolysis reactor, one could generate larger amounts of propionate and use membranes for down streaming. Necessarily, the second task is to provide enough organic carbon for denitrification. Both can only be done if we understand the processes before designing the reactors.

References

Alvarado, A., West, S., Abbt-Braun, G., Horn, H., 2021. Hydrolysis of particulate organic matter from municipal wastewater under aerobic treatment. Chemosphere 263, 128329. https://doi.org/10.1016/j.chemosphere.2020.128329

An, W., Guo, F., Song, Y., Gao, N., Bai, S., Dai, J., Wei, H., Zhang, L., Yu, D., Xia, M., Yu, Y., Qi, M., Tian, C., Chen, H., Wu, Z., Zhang, T., Qiu, D., 2016. Comparative genomics analyses on EPS biosynthesis genes required for floc formation of Zoogloea resiniphila and other activated sludge bacteria. Water Res. 102, 494–504. https://doi.org/10.1016/j.watres.2016.06.058

Anukam, A., Mohammadi, A., Naqvi, M., Granström, K., 2019. A review of the chemistry of anaerobic digestion : methods of accelerating and optimizing process efficiency. Processes 7, 1–19. https://doi.org/10.3390/pr7080504

APHA, AWWA, WEF, 2005. Standard methods for the examination of water and wastewater, twentyfirs. ed. American Public Health Association (APHA), American Water Works Association (AWWA), Water Environmental Federation (WEF), Washington, DC.

Argaman, Y., 1995. A steady-state model for the single sludge activated sludge system - I. Model description. Water Sci. Technol. 29, 137–145.

Bajpai, P., 2017. Anaerobic technology in pulp and paper industry. SpringerBriefs in Applied Sciences and Technology. Springer, Singapore. https://doi.org/10.1007/978-981-10-4130-3

Batstone, D.J., Keller, J., Angelidaki, I., Kalyuzhnyi, S.V., Pavlostathis, S.G., Rozzi, A., Sanders, W.T.M., Siegrist, H., Vavilin, V.A., 2002. Anaerobic digestion model no. 1. IWA Publishing, Alliance House, 12 Caxton Street, London SW1H 0QS, UK, London. https://doi.org/https://doi.org/10.2166/9781780403052

Behle, C., 2011. Sonnenlichtabhängige Inaktivierung und Akkumulation fäkaler Indikatorbakterien in Fließgewässern. Dissertation. Technische Universität München.

Benneouala, M., Younes, B., Mengelle, E., Bounouba, M., Sperandio, M., Bessiere, Y., Etienne, P., 2017. Hydrolysis of particulate settleable solids (PSS) in activated sludge is determined by the bacteria initially adsorbed in the sewage. Water Res. 125, 400–409. https://doi.org/10.1016/j.watres.2017.08.058

Boczar, B.A., Begley, W.M., Larson, R.J., 1992. Characterization of enzyme activity in activated sludge using rapid analyses for specific hydrolases. Water Environ. Res. 64, 792–797. https://doi.org/10.2175/wer.64.6.6

Bridié, A.L.A.M., 1969. Determination of biochemical oxygen demand with continuous recording of oxygen uptake. Water Res. 3, 157–165. https://doi.org/10.1016/0043-1354(69)90034-7

Brown, P., 2019. Impact of antibiotics and particulate matter from wastewater discharges on the abundance of antibiotic resistance genes in river sediments. Ph.D. Thesis. Karlsruher Institut für Technologie.

Butler, D., Friedler, E., Gatt, K., 1995. Characterising the quantity and quality of domestic wastewater inflows. Water Sci. Technol. 31, 13–24. https://doi.org/10.2166/wst.1995.0190

Cadoret, A., Conrad, A., Block, J.C., 2002. Availability of low and high molecular weight substrates to extracellular enzymes in whole and dispersed activated sludges. Enzyme Microb. Technol. 31, 179–186. https://doi.org/10.1016/S0141-0229(02)00097-2

Chen, R., Nie, Y., Kato, H., Wu, J., Utashiro, T., Lu, J., Yue, S., Jiang, H., Zhang, L., Li, Y.Y., 2017. Methanogenic degradation of toilet-paper cellulose upon sewage treatment in an anaerobic membrane bioreactor at room temperature. Bioresour. Technol. 228, 69–76. https://doi.org/10.1016/j.biortech.2016.12.089

Chen, X., Ma, R., Yang, Y., Jiao, N., Zhang, R., 2019. Viral Regulation on Bacterial Community Impacted by Lysis-Lysogeny Switch: A Microcosm Experiment in Eutrophic Coastal Waters. Front. Microbiol. 10. https://doi.org/10.3389/fmicb.2019.01763

Chisti, Y., 2014. Fermentation (industrial): basic considerations, Second Edi. ed, Encyclopedia of food microbiology. Elsevier. https://doi.org/10.1016/B978-0-12-384730-0.00106-3

Christofi, N., 2004. Bioassays - microbial tests, in: Encyclopedia of Analytical Science: Second Edition. Elsevier Inc., pp. 265–271. https://doi.org/10.1016/B0-12-369397-7/00044-3

Chróst, R.J., 1991. Environmental Control of the Synthesis and Activity of Aquatic Microbial Ectoenzymes. https://doi.org/10.1007/978-1-4612-3090-8_3

Chu, C.P., Tsai, D.G., Lee, D.J., Tay, J.H., 2005. Size-dependent anaerobic digestion rates of flocculated activated sludge : Role of intrafloc mass transfer resistance. J. Environ. Manage. 76, 239–244. https://doi.org/10.1016/j.jenvman.2005.01.022

Clara, M., Kreuzinger, N., Strenn, B., Gans, O., Kroiss, H., 2005. The solids retention time — a suitable design parameter to evaluate the capacity of wastewater treatment plants to remove micropollutants 39, 97–106. https://doi.org/10.1016/j.watres.2004.08.036

Confer, D.R., Logan, B.E., 1998. Location of protein and polysaccharide hydrolytic activity in suspended and biofilm wastewater cultures. Water Res. 32, 31–38. https://doi.org/10.1016/S0043-1354(97)00194-2

Confer, D.R., Logan, B.E., 1997. Molecular weight distribution of hydrolysis products during biodegradation of model macromolecules in suspended and biofilm cultures I. Bovine serum albumin. Water Res. 31, 2127–2136. https://doi.org/10.1016/S0043-1354(97)00049-3

de Beer, D., Huisman, J.W., Van den Heuvel, J.C., Ottengraf, S.P.P., 1992. The effect of pH profiles in methanogenic aggregates on the kinetics of acetate conversion. Water Res. 26, 1329–1336. https://doi.org/10.1016/0043-1354(92)90127-P

de Lemos Chernicharo, C.A., 2005. Biological wastewater treatment series, volume four: Anaerobic reactors, in: Biological Wastewater Treatment in Warm Climate Regions. IWA Publishing, London, UK., pp. 657–829.

Derlon, N., Wagner, J., da Costa, R.H.R., Morgenroth, E., 2016. Formation of aerobic granules for the treatment of real and low-strength municipal wastewater using a sequencing batch reactor operated at constant volume. Water Res. 105, 341–350. https://doi.org/10.1016/j.watres.2016.09.007

Dimock, R., Morgenroth, E., 2006. The influence of particle size on microbial hydrolysis of protein particles in activated sludge. Water Res. 40, 2064–2074. https://doi.org/10.1016/j.watres.2006.03.011

Drewnowski, J., 2014. The impact of slowly biodegradable organic compounds on the oxygen uptake rate in activated sludge systems. Water Sci. Technol. 69, 1136–1144. https://doi.org/10.2166/wst.2013.771

Droppo, I.G., Liss, S.N., Williams, D., Nelson, T., Jaskot, C., Trapp, B., 2009. Dynamic existence of waterborne pathogens within river sediment compartments. Implications for water quality regulatory affairs. Environ. Sci. Technol. 43, 1737–1743. https://doi.org/10.1021/es802321w

Dyk, J.S. Van, Pletschke, B.I., 2012. A review of lignocellulose bioconversion using enzymatic hydrolysis and synergistic cooperation between enzymes — Factors affecting enzymes , conversion and synergy. Biotechnol. Adv. 30, 1458–1480. https://doi.org/10.1016/j.biotechadv.2012.03.002

Eastman, J.A., Ferguson, J.F., 1981. Solubilization organic phase of carbon anaerobic particulate during the acid phase of anaerobic digestion. J. (Water Pollut. Control Fed. 53, 352–366.

Esparza-Soto, M., Fox, P., Westerhoff, P., 2006. Transformation of molecular weight distributions of dissolved organic carbon and UV-absorbing compounds at full-scale wastewater-treatment plants. Water Environ. Res. 78, 253–262. https://doi.org/10.2175/106143005x90083

Fatoorehchi, E., West, S., Abbt-Braun, G., Horn, H., 2018. The molecular weight distribution of dissolved organic carbon after application off different sludge disintegration techniques. Sep. Purif. Technol. 194, 338–345. https://doi.org/10.1016/j.seppur.2017.11.047

Felder, R.M., Rousseau, R.W., 2004. Principios elementales de los procesos químicos, 3a edición. ed, Termodinamica. Limusa Wiley.

Friedler, E., Butler, D., 1996. Quantifying the inherent uncertainty in the quantity and quality of domestic wastewater. Water Sci. Technol. 33, 65–78. https://doi.org/10.2166/wst.1996.0038

Friedrich, M., 2016. Adaptation of growth kinetics and degradation potential of organic material in activated sludge. Ph.D. Thesis. Universität Rostock. https://doi.org/10.13140/RG.2.2.18760.72960

Friedrich, M., Takács, I., 2013. A new interpretation of endogenous respiration profiles for the evaluation of the endogenous decay rate of heterotrophic biomass in activated sludge. Water Res. 47, 5639–5646. https://doi.org/10.1016/j.watres.2013.06.043

Frimmel, F.H., Abbt-Braun, G., 2011. Sum parameters: potential and limitations, In: Peter. ed,

Treatise on Water Science. vol. 3, pp. 3-29, Oxford: Academic Press. https://doi.org/10.1021/jp037247d

Gatti, M.N., García-Usach, F., Seco, A., Ferrer, J., 2010. Wastewater COD characterization: analysis of respirometric and physical-chemical methods for determining biodegradable organic matter fractions. J. Chem. Technol. Biotechnol. 85, 536–544. https://doi.org/10.1002/jctb.2325

Goel, R., Mino, T., Satoh, H., Matsuo, T., 1998. Comparison of hydrolytic enzyme systems in pure culture and activated slugde under different electron acceptor conditions. Water Sci. Technol. 37, 335–343.

Goel, R., Mino, T., Satoh, H., Matsuo, T., 1997. Effect of electron acceptor: conditions on hydrolytic enzyme synthesis in bacterial cultures. Water Res. 31, 2597–2603. https://doi.org/10.1016/S0043-1354(97)00100-0

González, O., Justo, A., Bacardit, J., Ferrero, E., Malfeito, J.J., Sans, C., 2013. Characterization and fate of effluent organic matter treated with UV/H2O2 and ozonation. Chem. Eng. J. 226, 402–408. https://doi.org/10.1016/j.cej.2013.04.066

Grabber, J.H., Mertens, D.R., Kim, H., Funk, C., Lu, F., Ralph, J., 2009. Cell wall fermentation kinetics are impacted more by lignin content and ferulate cross-linking than by lignin composition. J. Sci. Food Agric. 89, 122–129. https://doi.org/10.1002/jsfa.3418

Guellil, A., Boualam, M., Quiquampoix, H., Ginestet, P., Audic, J.M., Block, J.C., 2001. Hydrolysis of wastewater colloidal organic matter by extracellular enzymes extracted from activated sludge flocs. Water Sci. Technol. 43, 33–40. https://doi.org/10.2166/wst.2001.0334

Hao, X., Wang, Q., Cao, Y., Loosdrecht, M.C.M. Van, 2011. Evaluating sludge minimization caused by predation and viral infection based on the extended activated sludge model No . 2d. Water Res. 45, 5130–5140. https://doi.org/10.1016/j.watres.2011.07.013

Hatoum, R., Potier, O., Roques-carmes, T., Lemaitre, C., Hamieh, T., Toufaily, J., Horn, H., Borowska, E., 2019. Elimination of micropollutants in activated sludge reactors with a special focus on the effect of biomass concentration. Water 11, 1–21. https://doi.org/10.3390/w11112217

Hayet, C., Hédi, S., Sami, A., Ghada, J., Mariem, M., 2010. Temperature effect on settling velocity of activated sludge. ICBEE 2010 - 2010 2nd Int. Conf. Chem. Biol. Environ. Eng. Proc. 290–292. https://doi.org/10.1109/ICBEE.2010.5650190

Henze, M., Grady Jr., C.P., Gujer, W., Marais, G.V.R., Matsuo, T., 1987. A general model for single-sludge wastewater treatment systems. Water Res. 21, 505–515. https://doi.org/https://doi.org/10.1016/0043-1354(87)90058-3

Henze, M., Mladenovski, C., 1991. Hydrolysis of particulate substrate by activated sludge under aerobic, anoxic and anaerobic conditions. Water Res. 25, 61–64. https://doi.org/10.1016/0043-1354(91)90099-C

Himmel, M.E., Ding, S., Johnson, D.K., Adney, W.S., Nimlos, M.R., Brady, J.W., Foust, T.D., 2007. Biomass recalcitrance: Engineering plants and enzymes for biofuels production. Science (80-.). 315, 804–808.

Horan, N.J., 1990. Biological wastewater treatment systems. Theory and operation. John Wiley & Sons, Chichester., Chichester.

Huber, S., Balz, A., Frimmel, F.H., 1994. Identification of diffuse and point sources of dissolved organic carbon (DOC) in a small stream (Alb, Southwest Germany), using gel filtration chromatography with high-sensitivity DOC-detection. Fresenius J. Anal Chem 350, 496–503.

Huber, S.A., Balz, A., Abert, M., 2011a. New method for urea analysis in surface and tap waters with LC-OCD-OND (liquid chromatography-organic carbon detection-organic nitrogen detection). J. Water Supply Res. Technol. - AQUA 60, 159–166. https://doi.org/10.2166/aqua.2011.016

Huber, S.A., Balz, A., Abert, M., Pronk, W., 2011b. Characterisation of aquatic humic and non-humic matter with size-exclusion chromatography - organic carbon detection - organic nitrogen detection (LC-OCD-OND). Water Res. 45, 879–885. https://doi.org/10.1016/j.watres.2010.09.023

Huber, S.A., Balz, A., Abert, M., Pronk, W., 2011c. Characterisation of aquatic humic and non-humic matter with size-exclusion chromatography – organic carbon detection – organic nitrogen detection (LC-OCD-OND). Water Res. 45, 879–885. https://doi.org/10.1016/j.watres.2010.09.023

Huber, S.A., Frimmel, F.H., 1994. Direct gel chromatographic characterization and quantification of marine dissolved organic carbon using high-sensitivity DOC detection. Environ. Sci. Technol. 28, 1194–1197. https://doi.org/10.1021/es00055a035

Huber, S.A., Frimmel, F.H., 1991. Flow injection analysis of organic and inorganic carbon in the low-ppb range. Anal.Chem. 63, 2122–2130. https://doi.org/https://doi.org/10.1021/ac00019a011

Insel, G., Karahan Gül, Ö., Orhon, D., Vanrolleghem, P.A., Henze, M., 2002. Important limitations in the modeling of activated sludge: Biased calibration of the hydrolysis process. Water Sci. Technol. 45, 23–36. https://doi.org/10.2166/wst.2002.0406

Jin, G., Yongzhen, P., Jianhua, G., Juan, M., Wei, W., Baogui, W., 2011. Dissolved organic matter in biologically treated sewage effluent (BTSE): Characteristics and comparison. Desalination 278, 365–372. https://doi.org/10.1016/j.desal.2011.05.057

Kapoor, M., Semwal, S., Satlewal, A., Christopher, J., Gupta, R.P., Kumar, R., Puri, S.K., Ramakumar, S.S.V., 2019. The impact of particle size of cellulosic residue and solid loadings on enzymatic hydrolysis with a mass balance. Fuel 245, 514–520. https://doi.org/10.1016/j.fuel.2019.02.094

Kappeler, J., Gujer, W., 1992. Estimation of kinetic parameters of heterotrophic biomass under aerobic conditions and characterization of wastewater for activated sludge modelling. Water Sci. Technol. 25, 125–139.

Koch, K., Wichern, M., Lübken, M., Horn, H., 2009. Mono fermentation of grass silage by means of loop reactors. Bioresour. Technol. 100, 5934–5940. https://doi.org/10.1016/j.biortech.2009.06.020

Kommedal, R., 2003. Degradation of polymeric and particulate organic carbon in biofilms.

Sci. Technol. 1–181.

Kuo, W.-C., Parkin, G.F., 1996. Characterization of soluble microbial products from anaerobic treatment by molecular weight distribution and nickel-chelating properties. Water Res. 30, 915–922.

Lackner, S., 2015. Grundlagen der Abwasserreinigung. SS 2015, 26.04.2015. Karlsruhe Institute of Technology. Lecture.

Lamarre, D., Gadbois, A., Ramdani, A., Dold, P., Comeau, Y., 2010. Biodegradation of the endogenous residue of activated sludge 44, 2179–2188. https://doi.org/10.1016/j.watres.2009.12.037

Leitão, R.C., Haandel, A.C. Van, Zeeman, G., Lettinga, G., 2006. The effects of operational and environmental variations on anaerobic wastewater treatment systems : A review. Bioresour. Technol. 97, 1105–1118. https://doi.org/10.1016/j.biortech.2004.12.007

Levine, A.D., Tchobanoglous, G., Asano, T., 1991. Size distributions of particulate contaminants in wastewater and their impact on treatability. Water Res. 25, 911–922. https://doi.org/https://doi.org/10.1016/0043-1354(91)90138-G

Li, Chunyan, Brunner, F., Wagner, M., Lackner, S., Horn, H., 2018. Quantification of particulate matter attached to the bulk-biofilm interface and its influence on local mass transfer. Sep. Purif. Technol. 197, 86–94. https://doi.org/10.1016/j.seppur.2017.12.044

Li, Chunying, Zhao, Y., Ouyang, J., Wei, D., Wei, L., Chang, C.-C., 2018. Activated Sludge and other Aerobic Suspended Culture Processes. Water Environ. Res. 90, 1439–1457. https://doi.org/10.2175/106143018x15289915807470

Li, S., Wu, Z., Liu, G., 2019. Degradation kinetics of toilet paper fiber during wastewater treatment: Effects of solid retention time and microbial community. Chemosphere 225, 915–926. https://doi.org/10.1016/j.chemosphere.2019.03.097

Li, X., Li, J., 2015. Cutoff Membrane, in: Drioli, E., Giorno, L. (Eds.), Encyclopedia of Membranes. Springer Berlin Heidelberg, Berlin, Heidelberg, pp. 1–2. https://doi.org/10.1007/978-3-642-40872-4_2195-1

Li, Y., Chróst, R.J., 2006. Microbial enzymatic activities in aerobic activated sludge model reactors. Enzyme Microb. Technol. 39, 568–572. https://doi.org/10.1016/j.enzmictec.2005.10.028

Liu, X., Chen, Q., Zhu, L., 2016. Improving biodegradation potential of domestic wastewater by manipulating the size distribution of organic matter. J. Environ. Sci. (China) 47, 174–182. https://doi.org/10.1016/j.jes.2016.02.004

Lohani, S.P., Havukainen, J., 2017. Anaerobic digestion: factors affecting anaerobic digestion process. Chapter 18, in: S. J. Varjani et al. (eds.) (Ed.), Waste Bioremediation, Energy, Environment, and Sustainability. Springer Nature Singapore Pte Ltd. 2018, pp. 343–359. https://doi.org/10.1007/978-981-10-7413-4_18

Lübken, M., 2009. Mathematical modeling of anaerobic digestion processes. PhD. Thesis. Technischen Universität München.

Luo, Y., Nghiem, L.D., Hai, F.I., 2014. A review on the occurrence of micropollutants in the aquatic environment and their fate and removal during wastewater treatment. https://doi.org/10.1016/j.scitotenv.2013.12.065

Martinez-Sosa, D., Helmreich, B., Netter, T., Paris, S., Bischof, F., Horn, H., 2011. Anaerobic submerged membrane bioreactor (AnSMBR) for municipal wastewater treatment under mesophilic and psychrophilic temperature conditions. Bioresour. Technol. 102, 10377–10385. https://doi.org/10.1016/j.biortech.2011.09.012

Maximova, N., Dahl, O., 2006. Environmental implications of aggregation phenomena: current understanding. Curr. Opin. Colloid Interface Sci. 11, 246–266. https://doi.org/10.1016/j.cocis.2006.06.001

McCarty, P., 1964. Anaerobic waste treatment fundamentals. Public Work. 95, 91–94.

Meegoda, J.N., Li, B., Patel, K., Wang, L.B., 2018. A review of the processes, parameters, and optimization of anaerobic digestion. Int. J. Environ. Res. Public Health 15. https://doi.org/10.3390/ijerph15102224

Metcalf and Eddy, 2014. Wastewater engineering -treatment and resource recovery, Fifth. ed. McGraw-Hill Education, New York.

Moletta, R., Escoffier, Y., Ehlinger, F., Coudert, J.-P., Leyris, J.-P., 1994. On-line automatic control system for monitoring an anaerobic fluidized-bed reactor: response to organic overload. Water Sci. Technol. 30, 11–20. https://doi.org/10.2166/wst.1994.0572

Moore, H.R., 1970. The effects of pH on aerobic sludge digestion. Master thesis. Virginia Polytechnic Institute and State University.

Morgenroth, E., Kommedal, R., Harremoës, P., 2002. Processes and modeling of hydrolysis of particulate organic matter in aerobic wastewater treatment - a review. Water Sci. Technol. 45, 25–40. https://doi.org/10.2166/wst.2002.0091

Müller, M.B., Frimmel, F.H., 2002. A new concept for the fractionation of DOM as a basis for its combined chemical and biological characterization. Water Res. 36, 2643–2655. https://doi.org/10.1016/S0043-1354(01)00488-2

Müller, M.B., Schmitt, D., Frimmel, F.H., 2000. Fractionation of natural organic matter by size exclusion chromatography - properties and stability of Fractions. Environ. Sci. Technol. 34, 4867–4872. https://doi.org/10.1021/es000076v

Nielsen, P.H., Saunders, A.M., Hansen, A.A., Larsen, P., Nielsen, J.L., 2012. Microbial communities involved in enhanced biological phosphorus removal from wastewater - a model system in environmental biotechnology. Curr. Opin. Biotechnol. 23, 452–459. https://doi.org/10.1016/j.copbio.2011.11.027

Nybroe, O., Jørgensen, P.E., Henze, M., 1992. Enzyme activities in waste water and activated sludge. Water Res. 26, 579–584. https://doi.org/10.1016/0043-1354(92)90230-2

Ødegaard, H., 1999. The influence of wastewater characteristics on choice of wastewater treatment method, in: Nitrogen Removal and Biological Phosphate Removal, Oslo. Norway 2.-4. p. 16.

Pavlostathis, S.G., Giraldo-Gomez, E., 1991. Kinetics of anaerobic treatment. Water Sci. Technol. 24, 35–59.

Perminova, I.V., Frimmel, F.H., Kovalevskii, D.V., Abbt-Braun, G., Kudryavtsev, A.V., Hesse, S., 1998. Development of a predictive model for calculation of molecular weight of humic substances. Water Res. 32, 872–881. https://doi.org/https://doi.org/10.1016/S0043-1354(97)00283-2

Petrie, B., Kasprzyk-hordern, B., Petrie, B., Barden, R., Kasprzyk-hordern, B., 2015. A review on emerging contaminants in wastewaters and the environment : current knowledge, understudied areas and recommendations for future monitoring. Water Res. 72, 3–27. https://doi.org/10.1016/j.watres.2014.08.053

Proia, L., Anzil, A., Subirats, J., Borrego, C., Farrè, M., Llorca, M., Balcázar, J.L., Servais, P., 2018. Antibiotic resistance along an urban river impacted by treated wastewaters. Sci. Total Environ. 628–629, 453–466. https://doi.org/10.1016/j.scitotenv.2018.02.083

Ramdani, A., Dold, P., Gadbois, A., Déléris, S., Houweling, D., Comeau, Y., 2012. Characterization of the heterotrophic biomass and the endogenous residue of activated sludge. Water Res. 46, 653–668. https://doi.org/10.1016/j.watres.2011.11.030

Reichert, P., 1998. Aquasim 2.0 - User manual. Computer program for the identification and simulation of aquatic systems. Swiss Fed. Inst. Environ. Sci. Technol. https://doi.org/10.2166/wst.1994.0025

Rodriguez-Mozaz, S., Vaz-Moreira, I., Varela Della Giustina, S., Llorca, M., Barceló, D., Schubert, S., Berendonk, T.U., Michael-Kordatou, I., Fatta-Kassinos, D., Martinez, J.L., Elpers, C., Henriques, I., Jaeger, T., Schwartz, T., Paulshus, E., O'Sullivan, K., Pärnänen, K.M.M., Virta, M., Do, T.T., Walsh, F., Manaia, C.M., 2020. Antibiotic residues in final effluents of European wastewater treatment plants and their impact on the aquatic environment. Environ. Int. 140, 105733. https://doi.org/10.1016/j.envint.2020.105733

Rogowska, J., Cieszynska-Semenowicz, M., Ratajczyk, W., Wolska, L., 2019. Micropollutants in treated wastewater. Ambio 49, 487–503. https://doi.org/10.1007/s13280-019-01219-5

Ruiken, C.J., Breuer, G., Klaversma, E., Santiago, T., van Loosdrecht, M.C.M., 2013. Sieving wastewater - cellulose recovery, economic and energy evaluation. Water Res. 47, 43–48. https://doi.org/10.1016/j.watres.2012.08.023

Rusanowska, P., Cydzik-Kwiatkowska, A., Świątczak, P., Wojnowska-Baryła, I., 2019. Changes in extracellular polymeric substances (EPS) content and composition in aerobic granule size-fractions during reactor cycles at different organic loads. Bioresour. Technol. 272, 188–193. https://doi.org/10.1016/j.biortech.2018.10.022

Salt, G.W., 1987. The components of feeding behavior in rotifers. Hydrobiologia 147, 271–281. https://doi.org/10.1007/BF00025754

Samer, M., 2015. Wastewater treatment engineering. Chapter 1: Biological and chemical wastewater treatment processes. Licensee InTech open science, p. 13. https://doi.org/http://dx.doi.org/10.5772/61250

San Pedro, D.C., Mino, T., Matsuo, T., 1994. Evaluation of the rate of hydrolysis of slowly

biodegradable COD (SBCOD) using starch as substrate under anarobic, anoxic and aerobic conditions. Water Sci. Technol. 30, 191–199.

Schlafer, S., Meyer, R.L., 2017. Confocal microscopy imaging of the biofilm matrix. J. Microbiol. Methods 138, 50–59. https://doi.org/10.1016/j.mimet.2016.03.002

Schmid, M., Thill, A., Purkhold, U., Walcher, M., Bottero, J.Y., Ginestet, P., Nielsen, P.H., Wuertz, S., Wagner, M., 2003. Characterization of activated sludge flocs by confocal laser scanning microscopy and image analysis. Water Res. 37, 2043–2052. https://doi.org/10.1016/S0043-1354(02)00616-4

Seghezzo, L., 2004. Anaerobic treatment of domestic wastewater in subtropical regions. Ph.D. Thesis. Wageningen University, Wageningen, the Netherlands.

Seviour, T., Derlon, N., Dueholm, M.S., Flemming, H.C., Girbal-Neuhauser, E., Horn, H., Kjelleberg, S., van Loosdrecht, M.C.M., Lotti, T., Malpei, M.F., Nerenberg, R., Neu, T.R., Paul, E., Yu, H., Lin, Y., 2019. Extracellular polymeric substances of biofilms: suffering from an identity crisis. Water Res. 151, 1–7. https://doi.org/10.1016/j.watres.2018.11.020

Song, H., Clarke, W.P., 2009. Cellulose hydrolysis by a methanogenic culture enriched from landfill waste in a semi-continuous reactor. Bioresour. Technol. 100, 1268–1273. https://doi.org/10.1016/j.biortech.2008.08.029

Sophonsiri, C., Morgenroth, E., 2004. Chemical composition associated with different particle size fractions in municipal, industrial, and agricultural wastewaters. Chemosphere 55, 691–703. https://doi.org/10.1016/j.chemosphere.2003.11.032

Specht, C., Frimmel, F., 2000. Specific interactions of organic substances in size-exclusion chromatography. Environ. Sci. Technol. 34, 2361–2366. https://doi.org/10.1021/es991034d

Stallman, D.D., Nelsen, D., Amador, J., Evans, P., Parry, D., H. D., S., 2012. Use of ADM1 to evaluate anaerobic digestion of food waste, in: Proceedings of the Water Environment Federation Residuals and Biosolids Conference 2012. Raleigh. N.C.

Staudt, C., Horn, H., Hempel, D.C., Neu, T.R., 2003. Biofilms in medicine, industry and environmental biotechnology: characteristics , analysis and control. IWA Publishing, London, UK.

Stover, E.L., Campana, C.K., 2003. Effluents from food processing: microbiology of treatment processes, in: Encyclopedia of Food Sciences and Nutrition. Elsevier, pp. 1976–1985. https://doi.org/10.1016/b0-12-227055-x/00382-5

Suttle, C.A., 1994. The significance of viruses to mortality in aquatic microbial communities. Microb. Ecol. 28, 237–243. https://doi.org/10.1007/BF00166813

Swerhone, G.D.W., Lawrence, J.R., Neu, T.R., 2015. Assessment of lectin-binding analysis for in situ detection of glycoconjugates in biofilm systems. Microbiology 147, 299–313. https://doi.org/10.1099/00221287-147-2-299

Tran, N.H., Hao, H., Urase, T., Gin, K.Y., 2015. A critical review on characterization strategies of organic matter for wastewater and water treatment processes. Bioresour.

Technol. 193, 523–533. https://doi.org/10.1016/j.biortech.2015.06.091

Tran, N.H., Nguyen, V.T., Urase, T., Ngo, H.H., 2014. Role of nitrification in the biodegradation of selected artificial sweetening agents in biological wastewater treatment process. Bioresour. Technol. 161, 40–46. https://doi.org/10.1016/j.biortech.2014.02.116

Vavilin, V.A., Fernandez, B., Palatsi, J., Flotats, X., 2008. Hydrolysis kinetics in anaerobic degradation of particulate organic material: An overview. Waste Manag. 28, 939–951. https://doi.org/10.1016/j.wasman.2007.03.028

Vavilin, V.A., Rytov, S. V., Lokshina, L.Y., 1996. A description of hydrolysis kinetics in anaerobic degradation of particulate organic matter. Bioresour. Technol. 56, 229–237. https://doi.org/10.1016/0960-8524(96)00034-X

von Sperling, M., 2007. Biological wastewater treatment series, volume one: wastewater charactristics, treatment and disposal. IWA Publishing, Alliance House, 12 Caxton Street, London SW1H 0QS, UK.

von Sperling, M., Lemos Chernicharo, C.A., 2005. Biological wastewater treatment in warm climate regions, TechBooks,. ed, IWA Publishing. IWA Publishing, Alliance House, 12 Caxton Street, London SW1H 0QS, UK.

von Sperling, M., Verbyla, M.E., Oliveira, S.M.A.C., 2020. Assessment of treatment plant performance and water quality data: a guide for students, researchers and practitioners. https://doi.org/10.2166/9781780409320

Wagner, J., Weissbrodt, D.G., Manguin, V., Ribeiro da Costa, R.H., Morgenroth, E., Derlon, N., 2015. Effect of particulate organic substrate on aerobic granulation and operating conditions of sequencing batch reactors. Water Res. 85, 158–166. https://doi.org/10.1016/j.watres.2015.08.030

Walters, E., Graml, M., Behle, C., Müller, E., Horn, H., 2014. Influence of particle association and suspended solids on UV inactivation of fecal indicator bacteria in an urban river. Water. Air. Soil Pollut. 225. https://doi.org/10.1007/s11270-013-1822-8

Walters, Evelyn, Kätzl, K., Schwarzwälder, K., Rutschmann, P., Müller, E., Horn, H., 2014. Persistence of fecal indicator bacteria in sediment of an oligotrophic river: Comparing large and lab-scale flume systems. Water Res. 61, 276–287. https://doi.org/10.1016/j.watres.2014.05.007

Wang, N.X., Lu, X.Y., Tsang, Y.F., Mao, Y., Tsang, C.W., Yueng, V.A., 2019. A comprehensive review of anaerobic digestion of organic solid wastes in relation to microbial community and enhancement process. J. Sci. Food Agric. 99, 507–516. https://doi.org/10.1002/jsfa.9315

Wang, S., Bakke, R., 2014. Modeling and simulation of anaerobic diestion in ADM1 usign Aquasim. ASIN : B08C4Q1757, Telemark University College, Norway. https://doi.org/10.1007/978-1-4419-6996-5_270

Ward, A.J., Hobbs, P.J., Holliman, P.J., Jones, D.L., 2008. Optimisation of the anaerobic digestion of agricultural resources. Bioresour. Technol. 99, 7928–7940. https://doi.org/10.1016/j.biortech.2008.02.044

Wilderer, P.A., Bungartz, H.J., Lemmer, H., Wagner, M., Keller, J., Wuertz, S., 2002. Modern scientific methods and their potential in wastewater science and technology. Water Res. 36, 370–393. https://doi.org/10.1016/S0043-1354(01)00220-2

Wilhelm, S.W., Suttle, C. a, 1999. Viruses and nutrient cycles in the sea aquatic food webs. Bioscience 49, 781–788.

Xia, Y., Kong, Y., Nielsen, P.H., 2008. In situ detection of starch-hydrolyzing microorganisms in activated sludge. FEMS Microbiol. Ecol. 66, 462–471. https://doi.org/10.1111/j.1574-6941.2008.00559.x

Xiao, K., Abbt-Braun, G., Horn, H., 2020. Changes in the characteristics of dissolved organic matter during sludge treatment: A critical review. Water Res. 187. https://doi.org/10.1016/j.watres.2020.116441

Yang, Q., Zhao, H., Du, B., 2017. Bacteria and bacteriophage communities in bulking and non-bulking activated sludge in full-scale municipal wastewater treatment systems 119, 101–111.

Yu, G.H., He, P.J., Shao, L.M., He, P.P., 2008. Stratification structure of sludge flocs with implications to dewaterability. Environ. Sci. Technol. 42, 7944–7949. https://doi.org/10.1021/es8016717

Zheng, M., Liu, Y., Wang, C., Xu, K., 2013. Study on enhanced denitrification using particulate organic matter in membrane bioreactor by mechanism modeling. Chemosphere 93, 2669–2674. https://doi.org/10.1016/j.chemosphere.2013.08.045